

Characterisation of Mitochondrial Complex I Assembly Factors in Biogenesis and Disease

Submitted by

Luke Formosa

B. Med. Sc. (Hons)/ B. Sc.

A thesis submitted in total fulfilment
of the requirements for the degree of
Doctor of Philosophy

Department of Biochemistry and Genetics
La Trobe Institute for Molecular Science
College of Science, Health and Engineering

La Trobe University

Bundoora, Victoria 3086

Australia

February 2016

Table of Contents

Table of contents.....	I
List of abbreviations.....	VI
Summary.....	IX
Statement of authorship.....	X
Acknowledgments.....	XI
List of Publications.....	XIII

Chapter 1: Introduction..... 1

1.1 Mitochondria- Structure, Function and Evolution.....	2
1.2 Oxidative Phosphorylation.....	2
1.2.1 Complex I- NADH: ubiquinone Oxidoreductase.....	3
1.2.2 Complex II- Succinate: ubiquinone Oxidoreductase.....	3
1.2.3 Complex III- Ubiquinol: cytochrome <i>c</i> Oxidoreductase.....	3
1.2.4 Complex IV- Cytochrome <i>c</i> Oxidase.....	4
1.2.5 Complex V- F ₀ F ₁ ATP synthase.....	4
1.3 Complex I- Structure, Function, Evolution and Assembly.....	6
1.4 Mitochondrial Disease and Complex I deficiency.....	11
1.4.1 Identification and molecular diagnosis of mitochondrial disease.....	11
1.4.2 Inheritance of mitochondrial disease.....	13
1.4.3 Clinical presentation of Complex I deficiency.....	14
1.4.4 Neurological defects associated with Complex I deficiency.....	15
1.5 The Complex I assembly machinery- assembly factors required for biogenesis.....	15
1.5.1 Early stage assembly factors.....	15
1.5.1.1 NDUFAF3 (C3ORF60) and NDUFAF4 (C6ORF66).....	15
1.5.1.2 NDUFAF5 (C20ORF7).....	16
1.5.1.3 NDUFAF6 (C8ORF38).....	17
1.5.1.4 NDUFAF7 (MidA).....	17
1.5.1.5 NUBPL (hInd1).....	18
1.5.2 Mid-stage assembly factors-The MCIA complex.....	18
1.5.2.1 NDUFAF1 (CIA30).....	18
1.5.2.2 Ecsit.....	19
1.5.2.3 ACAD9.....	20

1.5.2.4	TMEM126B.....	23
1.5.2.5	TIMMDC1 (C3ORF1).....	23
1.5.3	Late stage assembly factors.....	23
1.5.3.1	NDUFAF2 (B17.2L).....	23
1.5.4	Putative assembly factors.....	24
1.5.4.1	Apoptosis inducing Factor.....	24
1.5.4.2	FOXRED1.....	25
1.5.4.3	LactB and LYRM5.....	26
1.6	Aims of the study.....	27
Chapter 2: Materials and Methods.....		28
2.1	Chemical Reagents.....	29
2.2	Cloning and Molecular Biology.....	29
2.2.1	Plasmid Purification.....	29
2.2.2	Polymerase Chain Reaction (PCR).....	29
2.2.2.1	PCR from a plasmid as template.....	29
2.2.2.2	PCR from genomic DNA.....	29
2.2.2.3	PCR from a human cDNA library.....	30
2.2.2.4	Mutagenesis using inverse PCR.....	30
2.2.3	Restriction enzyme digestion and DNA ligation.....	30
2.2.4	Bacterial Transformation.....	30
2.2.5	Dideoxynucleotide Sequencing.....	31
2.3	Genome Editing.....	31
2.3.1	TALEN design and construction.....	31
2.3.2	CRISPR-Cas9 design and construction.....	31
2.4	Tissue Culture.....	31
2.4.1	Cell Culture.....	31
2.4.2	Transient transfection of cultured cells.....	31
2.4.3	Cell sorting, screening and validation of disruptions.....	32
2.4.4	Generation of pseudotyped pantropic retrovirus for stable protein expression.....	32
2.4.5	Oxygen consumption and enzyme activity measurements.....	32
2.4.6	[³⁵ S]-Met pulse-chase labelling of mtDNA encoded subunits.....	33
2.4.7	Mitochondrial isolation.....	33

2.4.8	Trichloroacetic acid precipitation.....	33
2.5	Analysis of interacting proteins.....	33
2.5.1	Co-immunoprecipitation of exogenously expressed FLAG-tagged protein.....	33
2.5.2	Streptavidin-mediated pulldown of BirA* biotinylated proteins.....	34
2.6	Proteomics and data analysis.....	34
2.7	Polyacrylamide Gel Electrophoresis.....	34
2.7.1	Tris-Tricine SDS-PAGE.....	34
2.7.2	Blue Native PAGE.....	35
2.8	Protein detection.....	35
2.8.1	Antibodies.....	35
2.8.2	Western Blot analysis.....	36
2.8.2.1	Western Transfer.....	36
2.8.2.2	Immunoblot analysis.....	36
2.8.3	Autoradiography of [³⁵ S]-labelled proteins.....	36
2.9	Fluorescence Microscopy.....	37
2.9.1	Immunofluorescence assay.....	37
2.9.2	Confocal Microscopy.....	37
Chapter 3:	Characterisation of FOXRED1 in Complex I assembly.....	38
3.1	Introduction.....	39
3.2	A TALEN pair targeting the <i>FOXRED1</i> gene can result in disruption.....	40
3.3	Δ FOXRED1 cells harbour a specific Complex I defect.....	42
3.4	The ~815 kDa intermediate is still produced in the Δ FOXRED1 cell line.....	44
3.5	Global proteomic analysis of Δ FOXRED1 cells suggests an isolated Complex I deficiency.....	45
3.6	Δ FOXRED1 cells have a reduced respiratory capacity.....	47
3.7	Complementation analysis of Δ FOXRED1 cells.....	49
3.8	FOXRED1 may not associate with the ~815 kDa subcomplex.....	52
3.9	FOXRED1 can associate with a subset of Complex I subunits.....	54
3.10	Discussion.....	57
3.10.1	Loss of FOXRED1 leads to impaired Complex I assembly and the presence of a crippled subassembly.....	57
3.10.2	FOXRED1 is found in association with Complex I subunits.....	57
3.10.3	FOXRED1 patient mutations remain partially functional.....	58

Chapter 4: Functional analysis of the Mitochondrial Complex I Assembly (MCIA) Complex..... 60

4.1 Introduction.....	61
4.2 Design and validation of MCIA complex gene disruptions.....	62
4.3 Steady state levels of MCIA complex proteins differ in the absence of various proteins..	65
4.4 Loss of any MCIA complex component results in a strong Complex I defect.....	67
4.5 Complex I subunits are reduced in MCIA complex disruption.....	68
4.6 Complementation of MCIA complex disruption cell lines with the missing protein is sufficient for Complex I biogenesis.....	70
4.7 ACAD9 fails to assemble into higher order complexes in the absence of CIA30 and Ecsit.....	71
4.8 Pathogenic mutations in CIA30 deficient patients are either hypomorphic in nature or result in a total loss of function.....	73
4.9 TIMMDC1 accumulates in a ~440 kDa intermediate independent of other MCIA complex proteins.....	76
4.10 NDUFS3 also accumulates in a ~440 kDa intermediate in the absence of MCIA complex proteins.....	78
4.11 Identification of a unique loop in TIMMDC1 important for function in Complex I assembly.....	80
4.12 The loss of TIMMDC1 affects the translation/stability of mt-ND1, while the loss of CIA30 affects the mt-ND2 protein.....	82
4.13 TIMMDC1 interacts with newly synthesised mt-ND1, while CIA30 interacts with mt-ND2.....	84
4.14 Loss of TIMMDC1 more closely resembles the disruption of Complex I assembly at an early stage.....	86
4.15 Global Complex I levels suggest TIMMDC1 behaves in a similar fashion to the other MCIA complex proteins.....	89
4.16 Discussion.....	91
4.16.1 TIMMDC1 functions at the nexus of the mt-ND1 and mt-ND2 assembly modules.....	91
4.16.2 The subunits NDUFS5 and NDUF6 behave in a similar fashion if early or mid-stage assembly is disrupted.....	94
4.16.3 Mutagenesis of CIA30 and TIMMDC1 provides insights into their role in Complex I biogenesis and disease.....	96

Chapter 5: Identification of CIA30-interacting proteins using proximity based biotin labelling.....	97
5.1 Introduction.....	98
5.2 Generation of CIA30-BirA*-HA expressing cells in the Δ CIA30 cell line background.....	100
5.3 Identification of proteins enriched in proximity to CIA30.....	102
5.4 Identification of TMEM186- A potential Complex I assembly factor.....	105
5.5 TMEM186-FLAG localises to mitochondria.....	107
5.6 Depletion of TMEM186 reduces the levels of mature Complex I.....	108
5.7 Discussion.....	112
5.7.1 CIA30 can act as a bait for the identification of new Complex I assembly factors.....	112
5.7.2 Complex I intermediates that assemble into super-complexes may still contain CIA30.....	112
5.7.3 TMEM186 plays a role in the biogenesis of Complex I.....	112
 Chapter 6: Concluding remarks and future directions.....	 114
6.1 Determining the molecular function of assembly factors will increase the understanding of Complex I biogenesis.....	115
6.2 Structural determination of components of the MCIA complex may uncover their molecular mechanism of action in the assembly of Complex I.....	117
6.3 Assembling the mt-ND4/mt-ND5 module- Undiscovered assembly factors for the membrane arm of Complex I?.....	117
6.4 TMEM186- A novel assembly factor for Complex I.....	118
6.5 Assembly factors to the end- Required for the stability of the ~815 kDa intermediate?	119
6.6 Assembly factors, mtDNA translation, the membrane insertion machinery and protein quality control- Functionally connected for functional mitochondria?.....	120
 References.....	 122
 Publications.....	 139

List of Abbreviations

Å	Angstrom
ACAD9	Acyl-CoA Dehydrogenase type 9
APS	Ammonium persulphate
<i>A. thaliana</i>	<i>Arabidopsis thaliana</i>
ADP	Adenosine Diphosphate
ATP	Adenosine Triphosphate
BN-PAGE	Blue Native polyacrylamide gel electrophoresis
BSA	Bovine serum albumin
<i>B. taurus</i>	<i>Bos taurus</i>
cDNA	Complementary DNA
<i>C. elegans</i>	<i>Caenorhabditis elegans</i>
CIA30	Complex I intermediate associated protein of 30kDa
Co-IP	Co-immunoprecipitation
COXII	Cytochrome <i>c</i> Oxidase subunit II
COX5A	Cytochrome <i>c</i> Oxidase subunit 5A
<i>C. reinhardtii</i>	<i>Chlamydomonas reinhardtii</i>
CRISPR	Clustered Regularly Interspaced Short Palindromic Repeats
Da	Dalton
<i>D. hansenii</i>	<i>Debaryomyces hansenii</i>
Dig	Digitonin
<i>D. melanogaster</i>	<i>Drosophila melanogaster</i>
dNTPs	deoxyribonucleotide triphosphates
DSB	Double strand break
DTT	Dithiothreitol
<i>E. coli</i>	<i>Escherichia coli</i>
Ecsit	Evolutionarily conserved intermediate in toll pathways
FAD	Flavin Adenine Dinucleotide (Oxidised form)

FADH ₂	Flavin Adenine Dinucleotide (Reduced Form)
Fe-S	Iron-Sulphur cluster
FILA	Fatal infantile lactic acidosis
FMN	Flavin Mononucleotide
FOXRED1	Flavin-dependant Oxidoreductase 1
<i>g</i>	Gravitational force
HA	Hemagglutinin
HEK293T	Human embryonic kidney 293 cells, large T antigen
HRP	Horse radish peroxidase
<i>H. sapiens</i>	<i>Homo sapiens</i>
IMS	Intermembrane Space
LHON	Leber hereditary optic neuropathy
MELAS	Mitochondrial encephalomyopathy with lactic acidosis and stroke-like episodes
MIM	Mitochondrial inner membrane
<i>M. musculus</i>	<i>Mus musculus</i>
mtDNA	Mitochondrial DNA
mt-NDX	mtDNA encoded-NADH dehydrogenase subunit X
NAD ⁺	Nicotinamide Adenine Dinucleotide (Oxidised form)
NADH	Nicotinamide Adenine Dinucleotide (Reduced form)
<i>N. crassa</i>	<i>Neurospora crassa</i>
nDNA	Nuclear DNA
NDUFAX	NADH Dehydrogenase (Ubiquinone) 1 Alpha Subcomplex X
NDUFAFX	NADH Dehydrogenase (Ubiquinone) 1 Alpha Subcomplex, Assembly Factor X
NDUFBX	NADH Dehydrogenase (Ubiquinone) 1 Beta Subcomplex X
NDUFSX	NADH Dehydrogenase (Ubiquinone) Iron-sulphur protein X
NDUFVX	NADH Dehydrogenase (Ubiquinone) flavoprotein X
NHEJ	Non-homologous end joining
<i>O. sativa</i>	<i>Oryza sativa</i>

OXPHOS	Oxidative Phosphorylation
PAGE	Polyacrylamide-gel electrophoresis
PBS	Phosphate buffered saline
PCR	Polymerase Chain Reaction
PK	Proteinase K
PMSF	Phenyl methyl sulphonyl fluoride
PVDF	Polyvinylidene Fluoride
Q	Ubiquinone
QH ₂	Ubiquinol
<i>S. cerevisiae</i>	<i>Saccharomyces cerevisiae</i>
SDS	Sodium dodecyl sulphate
TALEN	Transcription Activator-like Effector Nucleases
TAP	Tandem affinity purification
TCA	Trichloroacetic Acid
TEMED	1, 2-Bis(dimethylamino)ethane
TMD	Transmembrane Domain
TMEM	Transmembrane protein
TIMMDC1	TIMM domain-containing protein 1
Tris-HCl	Tris(hydroxymethyl)aminomethane-hydrochloric acid
<i>T. thermophilus</i>	<i>Thermus thermophilus</i>
TX-100	Triton X-100
U	Enzyme unit
VLCAD	Very-long chain acyl CoA dehydrogenase
<i>Y. lipolytica</i>	<i>Yarrowia lipolytica</i>

Summary

Mitochondria play a critical role in most eukaryotic cells as they contribute to a number of different processes, including ATP generation. The mitochondrial inner membrane houses 5 multi-subunit complexes, which together are known as the Oxidative Phosphorylation System and together generate a membrane potential that powers ATP production. The first enzyme in this process is known as NADH:Ubiquinone Oxidoreductase (Complex I) that is composed of 45 subunits and is approximately 1 MDa in size. This enzyme transfers electrons from NADH to ubiquinone, which is coupled to the translocation of protons across the membrane and so contributes to the mitochondrial membrane potential. Mitochondrial disease affects approximately 1 in 5000 live births and one third of these are diagnosed with an isolated Complex I deficiency, making this the most common cause of mitochondrial dysfunction. Defects in Complex I can be caused by mutations in the structural subunits of the enzyme as well as assembly factors involved in Complex I biogenesis.

The work presented in this thesis has utilised genome editing techniques coupled to Blue-Native PAGE, proteomics and other biochemical techniques to characterise the role of assembly factors in the Complex I assembly process. The role of the putative Complex I assembly factor FOXRED1 was investigated and was shown to be required for efficient Complex I biogenesis at a late stage of the assembly pathway. Also, biochemical and cellular approaches were employed to provide new insights into the individual roles played by various members of the Mitochondrial Complex I Assembly (MCIA) complex. From this, additional components of the Complex I assembly machinery were postulated. This serves to increase our understanding of Complex I biogenesis and defects in disease.

Statement of authorship

Except where reference is made in the text of this thesis, this thesis contains no material published elsewhere or extracted in whole or part from a thesis submitted for the award of any other degree or diploma.

No other persons work has been used without due acknowledgment in the main text of this thesis.

This thesis has not been submitted for the award of any other degree or diploma at any other tertiary institution.

11/2/2016

Luke Formosa

Acknowledgments

The research presented in this thesis would not have been possible without a number of people, to which I owe a great deal of gratitude.

Firstly, I would like to thank my supervisor Professor Mike Ryan. I cannot express the gratitude I have for letting me stay and be a part of your team over the course of my PhD research. You have helped me every step of the way from my first presentation to my first publication. I have learned so much from you and I will carry this knowledge and experience I have gained with me for the rest of my career. Thank you so much for the opportunities to learn something new, to try something different and letting me explore my scientific ideas and endeavours. I could not have asked for a more enthusiastic supervisor to guide me through this journey. Thank you for being an amazing supervisor, a mentor and a friend.

To the MTR lab members, past and present. Having you all around has been one of the best parts of my time in the lab. I would especially like to thank Dr David Stroud. Thank you for your hard work in this lab and setting up so many techniques. The first time anything gets done it can be a challenge and there have been many firsts in this lab thanks to you. Thank you for your help with my research, for discussions, for your encouragement and your impeccable taste in beer! Dr Laura Osellame, thank you for being there when it was getting hard, chatting with you made science so much easier. Thank you for your insights, for your chats, the stories and the laughs we have shared working side-by-side at the bench. Though not technically an MTR member anymore, I would also like to thank Dr Michael Lazarou, for his insights and a different perspective, to be serious when you need to be but also know how to have a laugh. To the past postdocs of the lab, especially Dr Masa Mimaki for starting the FOXRED1 project, Dr Catherine Palmer, Dr Diana Stojanovski and Dr Kirsty Elgass. Thank you for your time in the lab, you have each helped me in one way or another and I truly appreciate that.

To the past and present students and members of the MTR lab. Abeer Singh, the partner-in-crime that started the journey with me all those years ago. Looking back we had some great times especially at conferences when someone's having too much of a good time! Thanks for being there and being an amazing friend. I know you will do amazing things in the future. I would also like to thank in a special way Viviane Richter, Boris Reljic, Christina Nedeva, Elliot Surgenor, Laura Twigg, Matteo Bonas, Marris Dibley, Thanh (Tango) Nguyen and Jo Usher. Thanks for making the Ryan lab the great place it has been over the course of my PhD, it has been a pleasure to work with all of you.

To the Biochemistry department at La Trobe University, it was amazing to learn and teach in your rooms, to talk about science with the academics and to enjoy the strong family atmosphere we have there. In particular I would like to thank Nick and Joan Hoogenraad, Julian Pakay, Mark Hulett, Matt Perugini and Hendrika Duivenvoorden. I would also like to thank the Department of Biochemistry and Molecular Biology at Monash University for welcoming us and making the entire group feel welcome.

To my friends who have been there for talks, dinners, dancing and the rest. Tony, Tracey, Andrea, Ashika, Shainie, Lynnette, Rose, Anthony, thanks for being great friends along the journey and making sure that the PhD didn't get the better of me!

Last, but certainly not least, I would like to thank my family for the unwavering support over the last 9 years. To my parents Rita and George, I would never be able to repay what you have done for me, nor describe the gratitude I have to you both. Thank you for your sacrifices, your love, your support and your kindness you shower on me I am very lucky to have parents like you. I love you both so much and I wouldn't be here today without you. To my Nanna Teresa and Nannu Wigi, thank you for all you have done for me. I appreciate all that you have done for me in any way that you could. Thank you for your love and support and the many many things you have done for me. I love both very much. My brothers Paul and Andrew, for making sure I didn't forget I'm not a doctor yet, for being pretty amazing brothers and for always having a laugh or a fight. To my Aunt Roslyn, Uncle Joe and cousins Daniel, Jordan and Matthew. You guys are amazing and I'm so lucky to have you as my family. Thank you for the encouragement and the support over the years, I appreciate it so much.

List of Publications

Formosa LE., Mimaki M., Fraizer AE., McKenzie M., Stait TL., Thorburn DR., Stroud DA., Ryan MT. (2015) Characterization of mitochondrial FOXRED1 in the assembly of respiratory chain complex I, **Human Molecular Genetics**, 24 (10): 2952-2956.

Formosa LE., Hofer A., Tischner C., Wenz T., Ryan MT. (2016), Translation and assembly of radiolabelled mitochondrial DNA-encoded protein subunits from cultured cells and isolated mitochondria, **Methods in Molecular Biology (Clifton, NJ)**, 1351: 115-129

Yeo JH., Skinner JP., Bird MJ., Formosa LE., Zhang JG., Kluck RM., Belz GT., Chong MMW (2015) A role for the Mitochondrial protein Mrpl44 in maintaining OXPHOS capacity, **PLoS ONE**, 10(7): e0134326. doi: 10.1371/ journal.pone.0134326

Stroud DA., Formosa LE., Wijeyeratne XW., Nguyen TN., Ryan MT. (2013), Gene Knockout Using Transcription Activator-like Effector Nucleases (TALENs) Reveals That Human NDUFA9 Protein Is Essential for Stabilizing the Junction between Membrane and Matrix Arms of Complex I, **The Journal of Biological Chemistry**, 288(3): 1685-1690.

Chapter 1
Introduction

1.1 Mitochondria- Structure, Function and Evolution

In its simplest form, life can be considered the interplay of two complementary processes; the flow of genetic information and the ability to extract energy from the environment to perform cellular work. Mitochondria play a crucial role in the latter process and are essential organelles for the function of most eukaryotic cells. While first appreciated as the sites of energy generation, further studies have revealed a myriad of other roles including steroid and iron-sulphur cluster biosynthesis, β -oxidation of fatty acids, antiviral and innate immune signalling, calcium homeostasis and apoptosis (Kim & Simon, 2004; Liu et al, 1996; Rouault & Tong, 2005; Seth et al, 2005). Mitochondria are hypothesised to have evolved from a single endosymbiotic event where an α -proteobacterium was engulfed by and resided within a proto-eukaryotic host at least one billion years ago, followed by horizontal gene transfer of bacterial genes to the host nucleus (Lang et al, 1999). Providing evidence to the symbiotic theory, mitochondria harbour a small circular genome within the organelle, reminiscent of its bacterial ancestor. The mitochondrial DNA (mtDNA) in humans is much smaller than the ancestral α -proteobacterial genome, encoding only 13 proteins required for energy generation, as well as components of the protein translation machinery (2 ribosomal RNAs and 22 tRNAs) (Anderson et al, 1981). Residing in the milieu of the cell cytoplasm, mitochondria are composed of a permeable outer membrane and a highly folded, impermeable inner membrane that forms structures known as cristae (Palade, 1952). These membranes enclose two aqueous compartments, the intermembrane space and the mitochondrial matrix. Proper function of each compartment is dependent on the correct complement of proteins and so sophisticated protein import and sorting machineries have evolved to localise proteins to their correct destination (Hoogenraad et al, 2002). In conjunction with proteins that are synthesised in the cytosol, the mtDNA-encoded proteins assemble into 4 multi-subunit complexes that convert energy rich compounds into ATP, the cellular currency of the cell.

1.2 Oxidative Phosphorylation

Mitochondria are synonymous with energy production as Albert Einstein is known for his famous 'E=mc²' equation. Mitochondria execute this vital function through the generation of stored energy via a proton gradient and the controlled flow of protons through ATP synthase to a state of quasi-equilibrium that is coupled to ATP generation. This phenomenon is known as chemiosmotic coupling (Mitchell, 2011). As Rich (2003) elegantly demonstrated, at rest an average person requires 420 kJ per hour, akin to a household light globe, for normal cellular function. While this may sound trivial for a light globe, for mitochondria this is the start of a mammoth task. The free energy released from ATP hydrolysis is $\Delta G = -50$ kJ/mol under physiological conditions, and so

the amount of ATP required is in the order of 125 moles per day. This energy production is equivalent to a turnover of 65 kg of ATP per day. If the generation of 3 ATP molecules requires the translocation of 10 protons across the mitochondrial membrane (based on the crystal structure of ATP synthase from the yeast *Saccharomyces cerevisiae*), 2.7×10^{21} protons need to pass through ATP synthase per second to sustain basal energy requirements. This gradient is produced through a number of multi-subunit oxidoreductases that constitute the electron transport chain, that couple electron flow with proton pumping across the membrane from the matrix into the intermembrane space, and together with ATP synthase, sustain the high energy demand for life.

1.2.1 Complex I- NADH: ubiquinone Oxidoreductase

Complex I is the largest complex of the electron transport chain. This enzyme catalyses the oxidation of NADH produced during various metabolic pathways, transferring two electrons to the lipophilic electron carrier ubiquinone (Schultz & Chan, 2001). The binding and unbinding of ubiquinone is thought to be coupled to conformational changes resulting in the translocation of four protons across the inner membrane into the intermembrane space (Schultz & Chan, 2001).

1.2.2 Complex II- Succinate: ubiquinone Oxidoreductase

Complex II is composed of four subunits, which all are encoded by the nuclear genome. It is responsible for the conversion of succinate to fumarate as part of the citric acid cycle and also contributes electrons through the reduction of ubiquinone. This process liberates two electrons that pass through a covalently bound FAD cofactor and subsequently through a number of iron-sulphur clusters before finally reducing ubiquinone (Schultz & Chan, 2001). The transfer of electrons to ubiquinone in Complex II does not release sufficient energy for proton translocation and so this complex does not contribute to the proton motive force (Schultz & Chan, 2001).

1.2.3 Complex III- Ubiquinol: cytochrome *c* Oxidoreductase

Complex III is a dimer consisting of at least eleven subunits, with one being encoded by mtDNA (Iwata et al, 1998). This complex is responsible for oxidation of the ubiquinol and the transfer of electrons to cytochrome *c*, a hydrophilic electron carrier located in the intermembrane space (Crofts, 2004). One electron is passed to cytochrome *c* via an Fe_2S_2 cluster and cytochrome c_1 (Crofts, 2004). The remaining electron is transferred via a Q-cycle that utilises semiubiquinone (Q^\bullet) and two *b*-type cytochromes b_L and b_H (Crofts, 2004). The energy released by the transfer of electrons results in the translocation of 4 protons, two from the matrix and two from ubiquinol (Crofts, 2004).

1.2.4 Complex IV- Cytochrome *c* Oxidase

The terminal electron acceptor is Complex IV, which accepts electrons from cytochrome *c* through a system of copper atoms and cytochromes that reduce molecular oxygen to water. Electrons first pass through a copper ion (Cu_A^{2+}) then to cytochrome *a* (Yoshikawa et al, 2011). Following this, the electron is then transferred to another copper ion (Cu_B^{2+}) and a haem moiety in cytochrome *a*₃. From here, the electrons are transferred to molecular oxygen, which is reduced to water. The energy released by this process is coupled to the translocation of four protons cross the membrane (Yoshikawa et al, 2011).

1.2.5 Complex V- F_0F_1 ATP Synthase

Using the membrane potential generated by Complexes I-IV, Complex V catalyses the generation of ATP from ADP and inorganic phosphate. This complex is composed of a catalytic domain composed of an $\alpha_3\beta_3$ hexamer and a peripheral stalk that protrudes into the mitochondrial matrix forming a stator (Walker, 2013). The rotor is composed of fourteen identical transmembrane subunits and an asymmetric stalk (known as the γ subunit) that extends deep into the catalytic domain (Walker, 2013). Movement of protons from the intermembrane space into the matrix through the rotor via interaction with ionisable sidechain residues in the membrane in turn rotates the γ subunit. This rotational energy is then transmitted through conformational changes in the catalytic domain that result in binding of precursor ADP and inorganic phosphate, followed by formation of a high energy phosphoanhydride bond and finally release of the ATP (Walker, 2013).

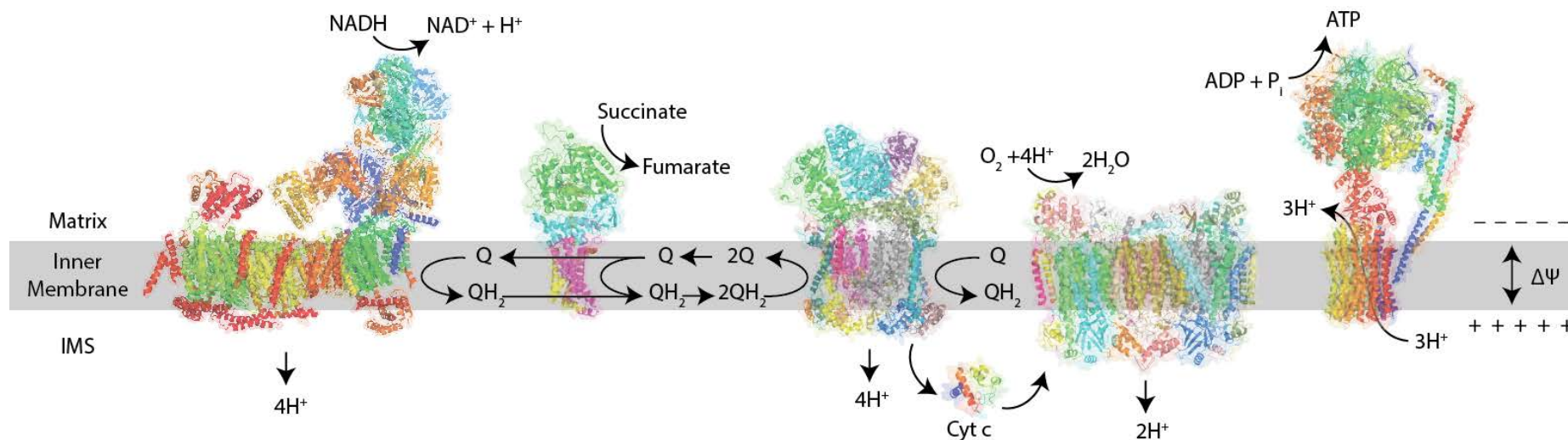


Figure 1.1: Structural representation of the mitochondrial electron transport chain. Oxidation of NADH to NAD⁺ occurs through Complex I resulting in the reduction of ubiquinone (Q) to ubiquinol (QH₂). This transfer is coupled to proton translocation across the inner membrane. Succinate is oxidised to Fumarate in Complex II with electrons also transferred to Q though an FAD moiety. The generated pool of QH₂ is oxidised by Complex III, and electrons are then transferred to cytochrome *c*. Complex IV then transfers electrons from cytochrome *c* to oxygen (O₂) to form water. Electron transport through complexes III and IV also translocates protons across the inner membrane. ATP synthase then uses the proton gradient to generate ATP from ADP and inorganic phosphate. The matrix, inner membrane and intermembrane space (IMS) are indicated. The direction of the mitochondrial membrane potential ($\Delta\Psi$) is also shown. The structure of each complex is shown: Complex I from *Bos taurus* (Protein databank (PDB) identifier 4UQ8), Complex II from *Sus scrofa* (PDB identifier 1ZOY), Complex III from *Bos taurus* (PDB identifier 1BGY), Complex IV from *Bos taurus* (PDB identifier 1OCC) and Complex V (composite of PDB identifiers F₁: 4YXW, stalk: 2CLY and F₀: 4BEM), cytochrome *c* (PDB identifier 3ZCF). Figure adapted from Sazanov (2015).

1.3 Complex I- Structure, Function, Evolution and Assembly

Mitochondrial Complex I is an 'L' shaped enzyme composed of a hydrophilic arm that protrudes into the matrix, and a hydrophobic arm that lies within the inner membrane (Vinothkumar et al, 2014). The matrix arm contains 7 core subunits encoded by nuclear genes that are involved in NADH oxidation, electron transport and the reduction of ubiquinone to ubiquinol (Brandt, 2006). Hydride transfer occurs from NADH to Flavin mononucleotide (FMN) located in the subunit NADH dehydrogenase (ubiquinone) flavoprotein 1(NDUFV1; homologue of Nqo1 in bacteria) of the NADH dehydrogenase module followed by 7 conductive Fe-S clusters that shuttle electrons to the lipophilic electron acceptor ubiquinone (Berrisford & Sazanov, 2009). The membrane arm contains the 7 highly hydrophobic core subunits (mt-ND1-6 and mt-ND4L) that are encoded by the mitochondrial genome and are involved in proton translocation from the matrix to the intermembrane space. It is thought that the binding and release of ubiquinone/ubiquinol in the ubiquinone binding site is coupled to conformational changes in the membrane arm (Baradaran et al, 2013). Conformational coupling of protons may be mediated by a transverse alpha helix that extends from the most distal core membrane subunit (mt-ND5 in mammals) that lies planar to the membrane with the C-terminus located close to the ubiquinone binding site (Baradaran et al, 2013). However, recent work using chemical crosslinking of the lateral helix to the membrane refutes this hypothesis and that electron transport is coupled to proton translocation by other mechanisms (Zhu & Vik, 2015).

Initial structural characterisation of the membrane arm of bacterial Complex I was first solved at a resolution of 3.9Å (Efremov et al, 2010) and subsequently to 3.0Å (Efremov & Sazanov, 2011). Both structures were found to contain 6 subunits (NuoL, M, N, A, J and K; see Table 1 for a summary of the nomenclature used for the core subunits of Complex I) with a total mass of 222kDa (Efremov et al, 2010; Efremov & Sazanov, 2011). The electron density map obtained was used to model 55 transmembrane α -helices that correlated well with predictions for the formation of a 14 transmembrane motif that is repeated 3 times (Efremov et al, 2010). The latter structure of higher atomic resolution was able to resolve the 55 helices into 6 subunits, including linker domains, and revealed a novel antiporter-like fold consisting of two inverted repeats in each antiporter subunit that formed 4 putative proton channels across the bacterial membrane (Efremov & Sazanov, 2011). The entire Complex I from *Thermus thermophilus* was solved to obtain the structure at 4.5Å resolution (Efremov et al, 2010). The crystal structure of mitochondrial Complex I from the yeast *Y. lipolytica* was also solved to a resolution of 6.3Å (Hunte et al, 2010). From the electron density maps, 17 transmembrane protein subunits were modelled that contained 71 α -helical transmembrane domains, however the resolution was too low to model the molecular detail of the enzyme (Hunte et al, 2010).

The cryo-EM structure of mitochondrial Complex I from bovine heart was solved to 5Å resolution and has provided a model encompassing the 14 core subunits and 13 different accessory subunits (Vinothkumar et al, 2014). Comparison of the bacterial Complex I structure with the core subunits of the bovine Complex I structure revealed striking similarity indicating the highly conserved nature of this molecular machine (Fig. 1.2) (Baradaran et al, 2013; Vinothkumar et al, 2014). As well as the core subunits, the structure also revealed a number of accessory subunits not present in the bacterial enzyme. While the role of these proteins remains unclear, it is thought they do not play a direct role in catalysis but rather may be required for structural stability or protection against oxidative damage (Brandt, 2006; Efremov et al, 2010; Vogel et al, 2007c). Proteomic analysis of the accessory proteins has revealed 18 subunits that have clear orthologues in many species including human (*H. sapiens*), cow (*B. Taurus*), fungi (*N. crassa* and *Y. lipolytica*), algae (*C. reinhardtii*), plant (*A. thaliana* and *O. sativa*), mouse (*M. musculus*), fly (*D. melanogaster*) and worm (*C. elegans*) species (Brandt, 2006). The nomenclature for the accessory subunits of human and bovine Complex I is listed in Table 2.

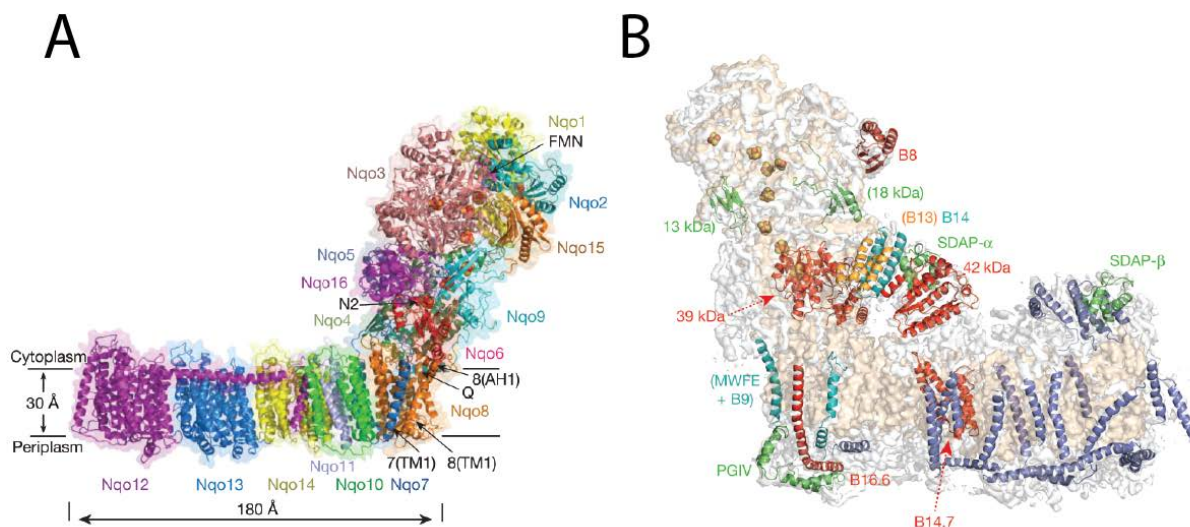


Figure 1.2: The structure of Complex I. Complex I from **(A)** *Thermus thermophilus* (Baradaran et al, 2013) and **(B)** *Bos taurus* (Vinothkumar et al, 2014) exhibit similar 'L' shaped structures. The structure from *T. thermophilus* illustrates the core subunits of Complex I required for electron transport from NADH to ubiquinone and proton translocation across the bacterial membrane. The cryo-EM structure of bovine Complex I also contains these subunits indicated in tan. Additional electron density attributed to the accessory subunits is shown in grey with numerous accessory subunits resolved to sufficient level assigned to particular proteins.

Structural insights into Complex I have revealed that this complex may have evolved from two modules of unrelated function; a family of membrane bound energy converting [NiFe] hydrogenases that utilised molecular hydrogen (H₂) as electron donors and constitute the peripheral arm and the Mrp cation/H⁺ antiporter that provided the enzyme with proton translocation ability (Fig. 1.3) (Hedderich, 2004; Mathiesen & Hägerhäll, 2002; Sazanov, 2015). These evolutionary relationships are supported by a substantial amount of functional evidence that leads to the development of the ‘modular design’ of Complex I (Brandt, 2006). This suggests that the complex has evolved from a number of different modules that have brought together the functions of electron input (by the N or ‘NADH-dehydrogenase’ module responsible for NADH oxidation), electron output (by the Q or ‘hydrogenase’ module responsible for electron guidance and the reduction of ubiquinone) and proton translocation (the P module) across the membrane (Fig 1.4A) (Brandt, 2006; Vogel et al, 2007c). The N- and Q-modules together constitute the peripheral arm of the complex, whereas the P-module forms the membrane arm (Brandt, 2006).

Table 1: Nomenclature of the core subunits of Complex I. Adapted from Sazanov (2015)

Module	<i>H. sapiens</i>	<i>B. taurus</i>	<i>E. coli</i>	<i>T. thermophilus</i>	Cofactors/TMD*
Peripheral Arm					
N-module	NDUFS1	75 kDa	NuoG	Nqo3	N1b (Fe ₂ S ₂) N4 (Fe ₄ S ₄) 4xCys N5 (Fe ₄ S ₄) 3xCys 1xHis
	NDUFV1	51 kDa	NuoF	Nqo1	FMN N3 (Fe ₄ S ₄)
	NDUFV2	24 kDa	NuoE	Nqo2	N1a (Fe ₂ S ₂)
Q-module	NDUFS2	49 kDa	NuoD (NuoCD#)	Nqo4	-
	NDUFS3	30 kDa	NuoC	Nqo5	-
	NDUFS8	TYKY	NuoI	Nqo9	N6a (Fe ₄ S ₄) N6b (Fe ₄ S ₄)
	NDUFS7	PSST	NuoD	Nqo6	N2 (Fe ₄ S ₄)
Membrane Arm					
	ND1	ND1	NuoH	Nqo8	8-9
P-module	ND2	ND2	NuoN	Nqo14	14- Antiporter like
	ND3	ND3	NuoA	Nqo7	3
	ND4	ND4	NuoM	Nqo13	14- Antiporter like
	ND4L	ND4L	NuoK	Nqo11	3
	ND5	ND5	NuoL	Nqo12	16- Antiporter like
	ND6	ND6	NuoJ	Nqo10	5

*Cofactors refer to the iron-sulphur clusters bound by core subunits and where applicable the coordinating residues. TMD represents the number of transmembrane domains possessed by different subunits of the membrane arm. # In some bacteria NuoC and NuoD are fused into a single protein.

Table 2: Nomenclature of the *H. sapiens* and *B. taurus* accessory subunits of Complex I

<i>H. sapiens</i>	<i>B. taurus</i>	<i>H. sapiens</i>	<i>B. taurus</i>	<i>H. sapiens</i>	<i>B. taurus</i>
NDUFV3	10 kDa	NDUFA8	PGIV	NDUFB4	B15
NDUFS4	18 kDa	NDUFA9	39 kDa	NDUFB5	SGDH
NDUFS5	15 kDa	NDUFA10	42 kDa	NDUFB6	B17
NDUFS6	13 kDa	NDUFA11	B14.7	NDUFB7	B18
NDUFA1	MWFE	NDUFA12	B17.2	NDUFB8	ASHI
NDUFA2	B8	NDUFA13	B16.6	NDUFB9	B22
NDUFA3	B9	NDUFAB1	SDAP	NDUFB10	PDSW
NDUFA5	B13	NDUFB1	MNLL	NDUFB11	ESSS
NDUFA6	B14	NDUFB2	AGGG	NDUFC1	KFYI
NDUFA7	B14.5a	NDUFB3	B12	NDUFC2	B14.5b

Additionally, treatment of Complex I with mild detergents has provided evidence for the physical substructure of the complex (Fig 1.4B) (Janssen et al, 2006; Lazarou et al, 2009). Solubilisation results in the resolution of 4 enzyme substructures, I α , which is composed of the peripheral arm and a small section of the membrane arm, and I β , which is the remainder of the membrane arm (Carroll et al, 2003). Changing the experimental conditions (Fearnley, 2001) dissociates the peripheral arm from the membrane arm forming the sub-complex I λ (Carroll et al, 2003; Sazanov et al, 2000). The sub-complex I γ represents any subunits not found in I λ or I β (Sazanov et al, 2000).

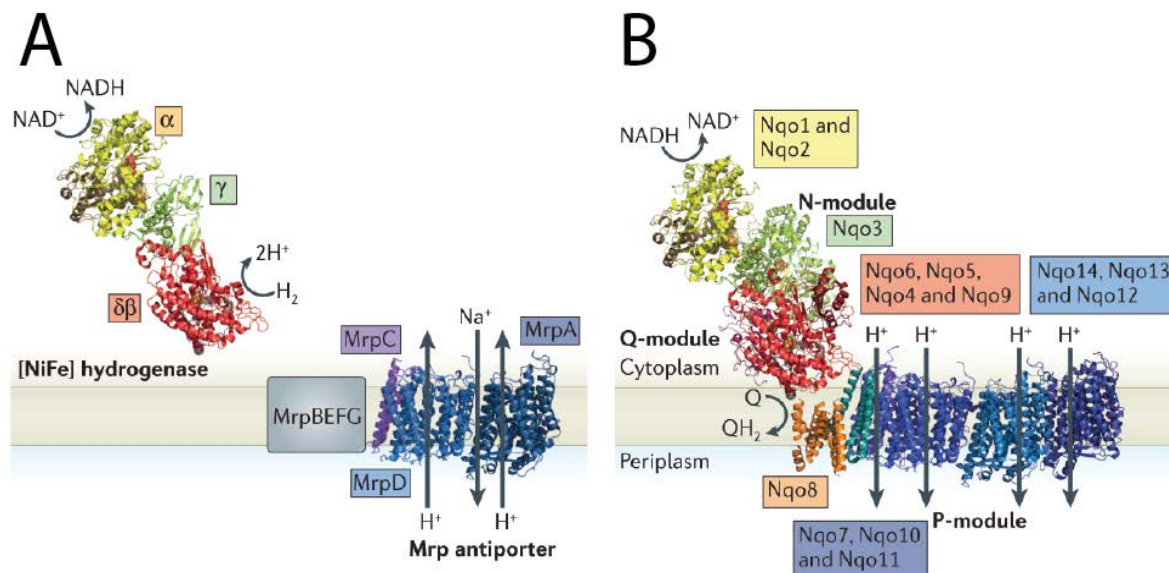


Figure 1.3: The evolution of Complex I. (A) The soluble [NiFe] hydrogenase located in the bacterial cytoplasm is responsible for the reduction of NAD⁺ by molecular hydrogen to generate H⁺ and NADH. The membrane Mrp antiporter is responsible for exchange of Na⁺ and H⁺ across the bacterial membrane. **(B)** Complex I consists of similar modules involved in NADH oxidation and the transfer of electrons to Ubiquinone (Q) and the translocation of protons across the membrane. The domain structure is very similar and Nqo8 (mt-ND1 in mammals) provides a link at the nexus between the modules and introduces the ubiquinone binding site. Taken from Sazanov (2015).

The mature complex assembles in a semi-sequential manner where discrete assembly intermediates, composed of multiple subunits, come together to form the mature complex as opposed to being assembled one subunit at a time (Vogel et al, 2007c). The presence of assembly intermediates has been shown by studies where cells lacking the membrane subunits mt-ND4 and mt-ND5 were still able to produce the peripheral arm sub-complex consisting of at least the subunits NDUFS2, 3 & 8 by immunoprecipitation using anti-NDUFS3 antibodies (Vogel et al, 2007c). Multiple models for the assembly of Complex I have been proposed by various groups, each with subtle distinctions with respect to the order and subunit composition of intermediate incorporation (Fig. 1.5) (Mimaki et al, 2012; Vogel et al, 2007c). Research has also suggested that Complex I also plays an important role in the assembly of respirasomes where subunits of complexes III and IV can interact with the ~815 kDa assembly intermediate before addition of the N-module to Complex I (Moreno-Lastres et al, 2012).

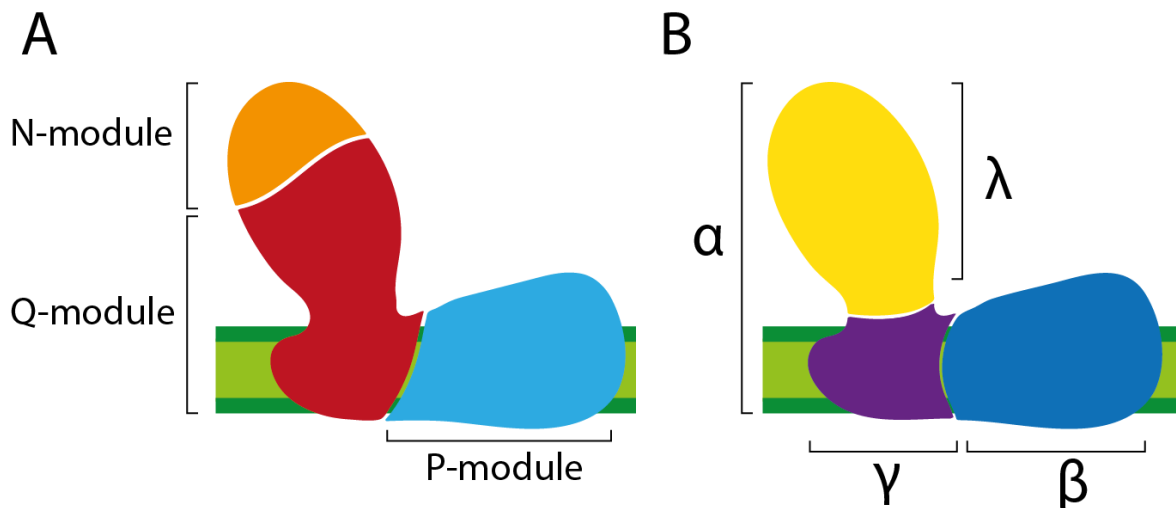


Figure 1.4: Complex I substructure. (A) Complex I is composed of 3 functional modules, The N-module oxidises NADH, the Q-module transports electrons to and oxidises ubiquinone and the P-modules translocates protons across the inner membrane **(B)** A number of sub-complexes have been identified based on various detergent solubilisations. The α sub-complex is composed of the peripheral arm and some of the membrane arm. This complex can further dissociate into the γ and λ sub-complexes. The majority of the membrane arm comprises the β sub-complex.

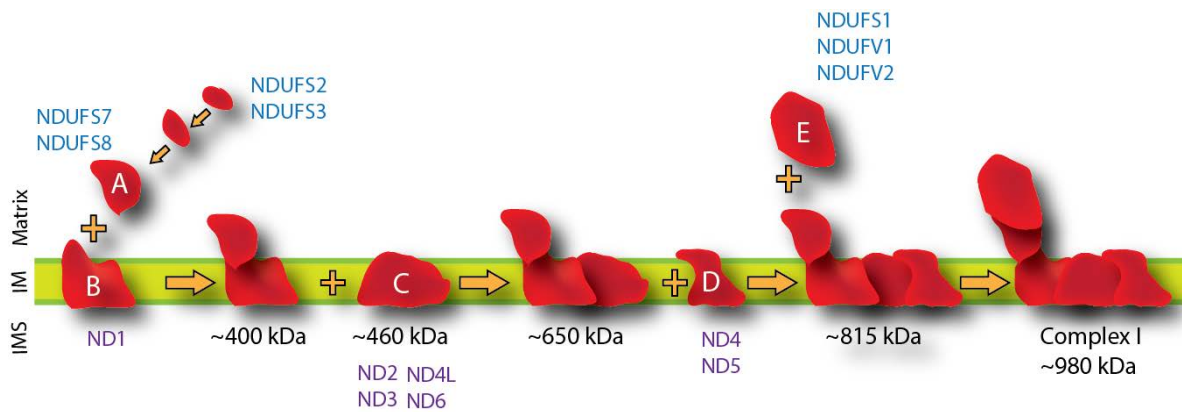


Figure 1.5: Complex I assembly. Biogenesis of Complex I occurs by sequential addition of sub-complexes containing different Complex I subunits that lead to the fully assembled enzyme. Core mtDNA-encoded subunits are labelled in purple and core nuclear encoded subunits indicated in blue. The core subunits NDUFS2 and NDUFS3 form a soluble intermediate that matures by incorporating other subunits including NDUFS7 and NDUFS8 forming a soluble assembly intermediate 'A'. A small seeding membrane intermediate 'B' consisting of at least the mtDNA-encoded subunit mt-ND1 is also formed. The intermediates 'A' and 'B' associate to form the ~400 kDa intermediate. This complex then engages an ~460 kDa intermediate (denoted 'C') that consists of the mtDNA encoded mt-ND2, mt-ND3, mt-ND4L and mt-ND6 subunits to form an ~650 kDa sub-complex. This further engages an intermediate comprising the subunits mt-ND4 and mt-ND5 (sub-complex 'D') to form an ~815 kDa sub-complex. Assembly is completed upon addition of the NADH dehydrogenase module (denoted 'E') that consists of the core subunits NDUFV1, NDUFV2 and NDUFS1, and other accessory subunits to generate the mature Complex I. Figure adapted from Mimaki et al (2012).

1.4 Mitochondrial disease and Complex I deficiency

1.4.1 Identification and molecular diagnosis of mitochondrial disease

Diseases caused by defects in mitochondrial oxidative phosphorylation occur in ~1 in 5,000 live births and as a group, are the most common inborn error of metabolism (Janssen et al, 2006; Skladal et al, 2003; Smeitink et al, 2001). The proper function of the electron transport chain requires in excess of 90 gene products and mutations can lead to a range of clinical phenotypes, which can present at any stage of life and affect a number of tissues and organs (Gerards et al, 2010b; Janssen et al, 2006). The tissues most at risk of mitochondrial dysfunction and defects in oxidative phosphorylation are those that have a large ATP demand and include the brain and nervous tissue, cardiac tissue and skeletal muscle (Janssen et al, 2006).

If a mitochondrial disease is suspected, measurement of the enzyme activities is performed to aid in the diagnosis procedure. This is a robust method and can use samples ranging from muscle biopsies, cultured fibroblasts or more specialised tissue such as the heart, liver or brain (Hoefs et

al, 2012). While cultured fibroblasts are often a good model for OXPHOS deficiency, sometimes these cells may not exhibit the defect in question and other tissues such as the muscle or heart may need to be tested to diagnose the patient (Hoefs et al, 2012; Stroud et al, 2015).

A retrospective study analysing the enzymatic activity of OXPHOS enzymes (excluding Pyruvate Dehydrogenase) identified 40% of cases had an isolated Complex I deficiency, making this the leading cause of mitochondrial disease (Loeffen et al, 2000; Thorburn et al, 2004). While the prevalence of Complex I deficiency can be attributed to the large number of subunits required for the enzyme to be active, only about half the patients with Complex I deficiency have a pathogenic mutation in a known mtDNA or nDNA encoded gene, while the remaining patients lack a molecular diagnosis (Hoefs et al, 2012; Loeffen et al, 2000). Therefore, mitochondrial diseases may arise from mutations in structural subunits encoded by both mtDNA or nDNA or in many cases, can be attributed to mutations leading to the dysfunction of nDNA encoded assembly factors required for the correct assembly (Hoefs et al, 2012; Janssen et al, 2006; Mimaki et al, 2012). Identification of genes with pathogenic mutations has improved since the advent of high throughput and whole genome sequencing, however sequence coverage and handling of sequence data remains a difficult task associated with this technique (Calvo et al, 2010).

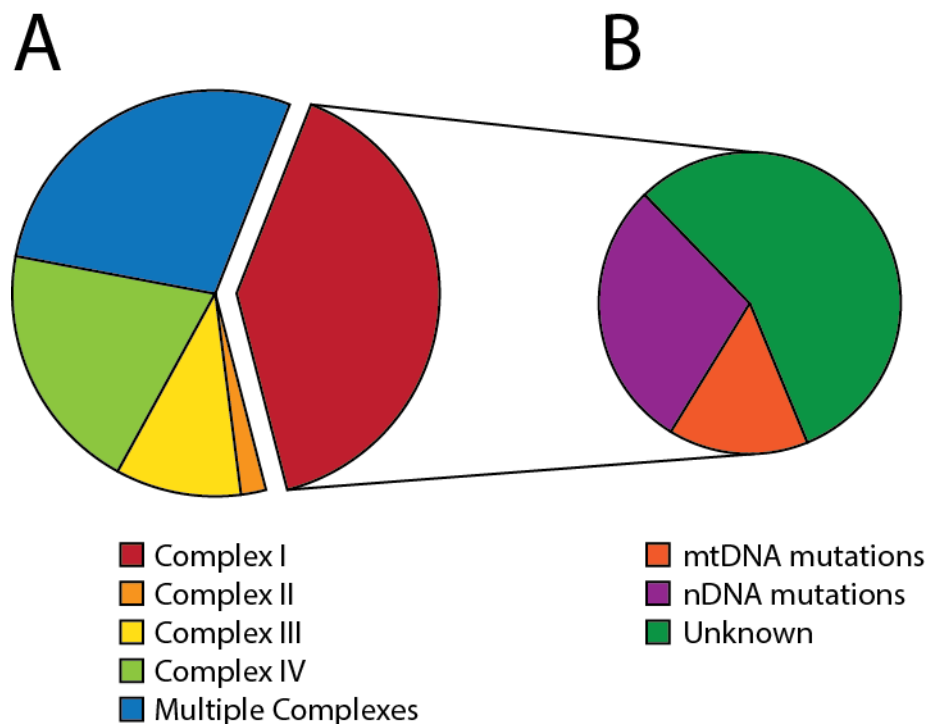


Figure 1.6: Mitochondrial disease distribution. (A) Isolated Complex I deficiency is the leading cause of mitochondrial disease, accounting for approximately 40% of reported cases. **(B)** For those patients diagnosed with Complex I deficiency, 15% have a mutation in mtDNA, 26% have a mutation in nDNA and 59% remain without a molecular diagnosis. Adapted from Thorburn et al (2004) and Hoefs et al (2012).

1.4.2 Inheritance of mitochondrial disease

The diagnosis of a patient with a single nucleotide mutation in mtDNA encoding the *MT-ND4* gene was the first time Complex I deficiency was recognised as a cause of human disease (Wallace et al, 1988). Since then a number of patients have been identified with mutations in other mtDNA or nDNA genes involved with Complex I. Because genes involved in OXPHOS function are located on a variety of chromosomes with varying methods of inheritance, inheritance may follow simple Mendelian rules of autosomal dominant/recessive patterns of X-linked or somatic mutations, or the maternal inheritance of mtDNA. Furthermore, some mutations may arise *de novo*, as observed for example, in a subset of patients harbouring mtDNA deletions (Lebon et al, 2003).

The inheritance of mtDNA is a complex process, and currently is viewed mainly as a stochastic process (White et al, 2008). The mitochondrial genome is present in the order of hundreds to thousands of copies per cell. Furthermore, the mitochondrial genome may be homoplasmic- that is, all copies of the mtDNA are identical in sequence with no variation. Mutations may arise in some mtDNA molecules leading to variation, known as heteroplasmy, where the mtDNA population will be a mixture of both mutant and wildtype genes. If the mutant mtDNA accumulates past a 'threshold' level, symptoms of mitochondrial disease may arise. This poses a serious problem for the inheritance of mtDNA during cell division of somatic cells. While the segregation of nuclear DNA during mitosis is strictly regulated resulting in daughter nuclei containing genetic material identical to the parent cell, the same is not true for mtDNA. During cell division, the cytosolic components including mitochondria, are distributed at random and in the process the daughter cells may inherit a different load of mutant mtDNA (Fig. 1.7). Should one cell receive more of the mutant DNA, clinical symptoms associated with the mtDNA mutation may become apparent due to change in the level of the mutant proteins they encode. Studies of mtDNA inheritance in mice suggest that mtDNA encoding a severe pathogenic mutations, such as an insertion resulting in a frameshift in the *MT-ND6* gene may undergo a process of 'purifying selection' to reduce the mutant load of the zygote, while milder mutations that may still result in mitochondrial disease still persist (Fan et al, 2008).

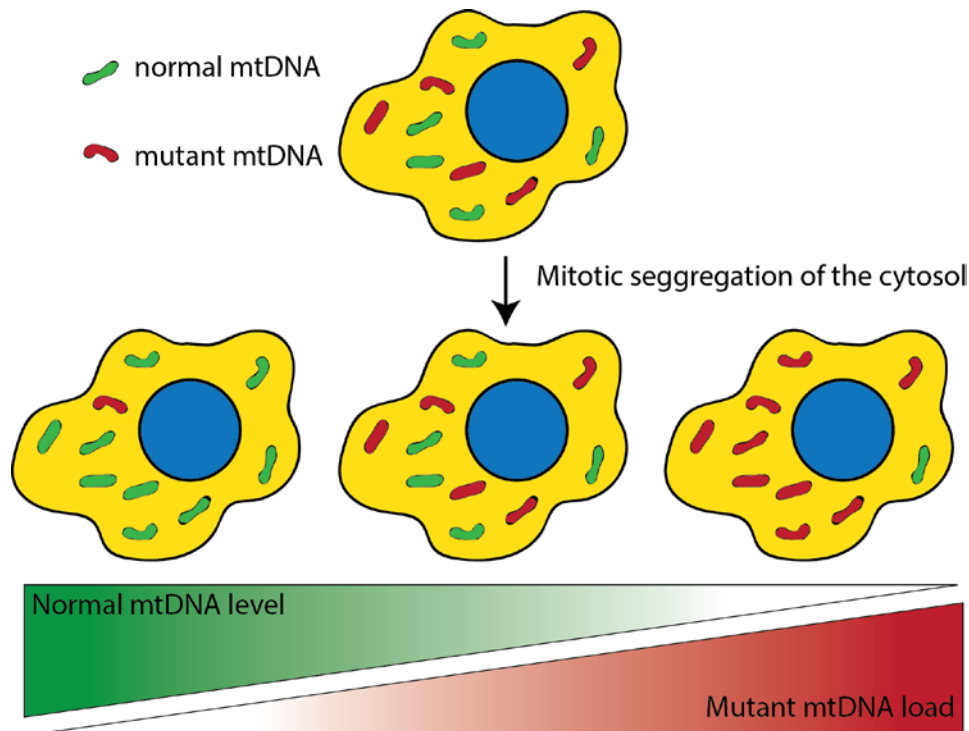


Figure 1.7: Differential mtDNA segregation during cell division may lead to clinical manifestation of mitochondrial disease. During cell division the random segregation of mitochondria may result in cells receiving varying amounts of mutant mtDNA. If the mutant mtDNA load is low, mitochondrial OXPHOS will generally be unaffected. However, if the mutant load increases past the ‘Threshold level’ the cells may lose the capacity to perform OXPHOS and start to exhibit symptoms of mitochondrial disease. Adapted from Taylor and Turnbull (2005)

1.4.3 Clinical presentation of Complex I deficiency

Mutations in both the mitochondrial and nuclear genomes can contribute to mitochondrial disease. Mutations in mitochondrial DNA tend to be associated with late-onset mitochondrial disease and generally diagnosed in adults (Stewart & Chinnery, 2015). Leber hereditary optic neuropathy (LHON) is the most commonly diagnosed disease in patients with mutations in mtDNA and is characterised by bilateral acute or sub-acute vision failure as a result of degeneration of the retinal ganglion and their axons (Man et al, 2003). Mutations in mtDNA-encoded structural genes can also lead to mitochondrial encephalomyopathy with lactic acidosis and stroke-like episodes (MELAS), which is characterised by a range of neurological symptoms including mental retardation, dementia, seizures, migraines and convulsions as well as lactic acidosis (El-Hattab et al, 2015).

In contrast to mutations in mitochondrial DNA, nuclear DNA mutations often present in the neonatal period, infancy or early childhood (Rubio-Gozalbo et al, 2000). Leigh syndrome is one of the most commonly diagnosed paediatric mitochondrial diseases, with mutations in at least 20 genes encoding structural subunits or assembly factors being documented to result in this disease

(Ruhoy & Saneto, 2014). To date, mutations in more than 75 genes involved in various aspects of mitochondrial biology result in Leigh syndrome, including genes involved in Pyruvate Dehydrogenase activity, mitochondrial DNA maintenance and translation as well as other enzyme of the OXPHOS system (Lake et al, 2015). Leigh syndrome is characterised by bilateral symmetric lesions in the basal ganglia, thalamus and brainstem, along with other neural defects including psychomotor retardation, seizures, optic atrophy and dystonia (Finsterer, 2008). The age of onset is also clinically variable, starting *in utero* to early childhood and a median age of death of 2.4 years, ranging from 1 month to 21 years of age (Ruhoy & Saneto, 2014). Other diseases that present early in life associated with Complex I deficiency include fatal infantile lactic acidosis (FILA), leukodystrophy, cardiomyopathy and renal tubulopathy (Janssen et al, 2006).

1.4.4 Neurological defects associated with Complex I deficiency

Complex I deficiency has been identified in the dopaminergic neurons located in the substantia nigra of patients with sporadic Parkinson's Disease (PD) (Schapira et al, 1989). This has been substantiated in a number of studies and recapitulated in a zebrafish model of PD (Flinn et al, 2009; Schapira et al, 1990). Furthermore, inhibition of Complex I by MPTP (1-methyl-4-phenyl-1,2,3,6-tetrahydropyridine) or rotenone in animal models can result in characteristic changes observed in PD including degeneration of dopaminergic neurons, α -synuclein aggregation and increased oxidative damage (Betarbet et al, 2000; Sherer et al, 2007). Reduced levels of Complex I subunits have also been associated with Bipolar Disorder, characterised by recurring episodes of mania, hypomania and depression (Andreazza et al, 2010; Sun et al, 2006). Changes to Complex I levels or activity have also been observed in the brain of patients with Downs Syndrome, Schizophrenia, Alzheimer's Disease and Huntington's Disease (Arenas et al, 1998; Karry et al, 2004; Kim et al, 2001). Taken together, these studies indicate the important role Complex I plays in the progression of neurodegenerative disorders.

1.5 The Complex I assembly machinery- assembly factors required for biogenesis

Mitochondrial Complex I assembles by sequential addition of modules composed of a number of subunits. The assembly of Complex I is orchestrated by a number of assembly factors that function at different stages of the biogenesis pathway.

1.5.1 Early stage assembly factors

1.5.1.1 *NDUFAF3 (C3ORF60) and NDUFAF4 (C6ORF66)*

Defects in the assembly factor C6ORF66 (later renamed 'NADH Dehydrogenase (Ubiquinone) 1 Alpha Subcomplex, Assembly Factor 4'- NDUFAF4) was originally identified in a consanguineous family of Arab-Muslim decent (Saada et al, 2008). Patients presented with high plasma lactate

levels immediately after birth, three patients dying after the first week of life. Patients that survived went on to develop severe encephalopathy. One patient also developed cardiomyopathy. Enzyme activity and blue-native (BN-) PAGE analysis from fibroblast and muscle biopsies revealed lower Complex I activity and complex abundance leading to a diagnosis of an isolated Complex I deficiency. After sequencing of known disease causing genes, homozygosity mapping was used to determine the causative gene. Analysis of the *NDUFAF4* gene revealed a mutation at nucleotide c.194T>C resulting in a p.L65P substitution. All patients presenting with symptoms were homozygous for this mutation. Complementation with wildtype cDNA encoding *NDUFAF4* was able to restore Complex I levels in patient fibroblast, indicating its importance in Complex I biogenesis.

Proteomic analysis of a number of mouse tissue mitochondrial samples were used to generate the 'MitoCarta' catalogue to describe the mitochondrial proteome (Pagliarini et al, 2008). Using phylogenetic profiling of proteins identified in mitochondria, *NDUFAF3* was identified as a candidate assembly factor due to strong evolutionary interactions with Complex I (Pagliarini et al, 2008). In addition, patients presenting with Complex I deficiency were identified to carry mutations in the *NDUFAF3* (*C3ORF60*) gene (Saada et al, 2009). Homozygosity mapping and genetic analysis of 5 patients from 3 families revealed mutations in this gene. Three patients from a single family were homozygous for a c.229G>C mutation resulting in a substitution p.G77R. The fourth patient was homozygous for a mutation c.365G>C resulting in a p.R122P substitution. The final patient was heterozygous for the p.Arg122Pro substitution as well as a c.2T>C mutation that results in a p.M1? mutation, effectively removing the initiating methionine. Complementation of patient-derived fibroblasts with wildtype *NDUFAF3* was able to restore the Complex I defect. It was also shown that *NDUFAF3* and *NDUFAF4* interact together with Complex I subunits *NDUFS2* and *NDUFS3* but not *NDUFA9*, *NDUFA2* and mt-*ND1* (Saada et al, 2009), indicating they may help assemble the early soluble core components. Proteomic analysis also showed that *NDUFAF3* and *NDUFAF4* co-migrate on BN-PAGE further supporting that these proteins function together (Wessels et al, 2009).

1.5.1.2 *NDUFAF5* (*C20ORF7*)

Homozygosity mapping of an Egyptian consanguineous family identified the gene *C20ORF7* to be important in Complex I biogenesis (Sugiana et al, 2008). The patient died 7 days after birth and showed increased lactate levels in both plasma and cerebrospinal fluid. Analysis of the gene revealed a homozygous mutation c.719T>C resulting in a p.L229P substitution in affected individuals. BN-PAGE analysis showed the absence of mature Complex I, while addition of wildtype *NDUFAF5* was able to restore Complex I levels in patient fibroblasts. *NDUFAF5* contains

a predicted S-adenosylmethionine (SAM)-dependent fold and may be important in the post-translational modifications of Complex I subunits (Sugiana et al, 2008). Analysis of NDUFAF5 in the organism *Dictyostelium* also showed it was essential for Complex I biogenesis (Carilla-Latorre et al, 2013). Re-expression of NDUFAF5 harbouring the mutation G86V, which disrupts a highly conserved 'GXGXG' motif in SAM-dependent methyltransferases, was unable to restore the growth phenotype to normal and remained similar to Ndufaf5- cells. This suggested that the methyltransferase function is crucial to NDUFAF5 function (Carilla-Latorre et al, 2013). Patients from a Moroccan consanguineous family also identified with mutations in *NDUFAF5* presented with Leigh syndrome, swallowing and learning difficulties and survived into adulthood (Gerards et al, 2010a). Analysis revealed a homozygous c.477A>C mutation resulting in a p.L159F substitution. A homozygous mutation in *NDUFAF5* (c.749G>T resulting in a p.G250V substitution) was also been identified in patients harbouring Complex I and Complex IV defects (Saada et al, 2012).

1.5.1.3 *NDUFAF6 (C8ORF38)*

Phylogenetic profiling of organisms harbouring Complex I using the MitoCarta catalogue identified *NDUFAF6* as a protein that has evolved with Complex I and is absent in species lacking the enzyme (Pagliarini et al, 2008). Homozygosity mapping for a Lebanese family with Complex I deficiency identified a c.296A>G mutation resulting in a p.N99R mutation in a highly conserved residue. *NDUFAF6* has sequence homology to squalene/phytoene synthetases and may be implicated in the metabolism of branch-chained lipids (Pagliarini et al, 2008). Further analysis of patient fibroblasts revealed a strong Complex I defect and a rapid loss of newly translated mt-ND1 protein (McKenzie et al, 2011). While the mammalian *NDUFAF6* is a peripheral membrane protein localising to the matrix side of the inner membrane (McKenzie et al, 2011), the *Drosophila* homologue *Sicily* was reported to be localised to the cytosol and required for the subcellular transport of ND42 to mitochondria, the homologue of mammalian *NDUFA10* (Zhang et al, 2013).

1.5.1.4 *NDUFAF7 (MidA)*

A functional genomics analysis of *Dictyostelium* first identified *MidA* to be important in mitochondrial function where *MidA*- cells had disrupted size and growth rate (Torija et al, 2006). It was also noted that *MidA* was homologous to the human protein PR01853. Subsequent phylogenetic analysis of mitochondrial proteins in species with and without Complex I identified PR01853 as a likely assembly factor that has co-evolved with Complex I (Pagliarini et al, 2008). Further work then showed that *Dictyostelium* lacking *MidA* harboured a Complex I defect and both human and *Dictyostelium* *MidA* could interact with the subunit *NDUFS2* (Carilla-Latorre et al, 2010). Structural bioinformatics analysis of *MidA* also predicted this protein to have an SAM-

dependent methyltransferase fold and mutagenesis of the putative domain at conserved residues required for enzyme activity were unable to restore the MidA- phenotype in *Dictyostelium* (Carilla-Latorre et al, 2010). Analysis of NDUFS2 by mass spectrometry following MidA (henceforth called NDUF7) depletion in culture showed that it was required for symmetric dimethylation of NDUFS2 on Arg-85 to produce ω -N^G,N^G-dimethylarginine, classifying NDUF7 as a class II methyltransferase (Rhein et al, 2013). Transient knockdown of NDUF7 also showed rapid mt-ND1 turnover in an AFG3L2-dependent manner while attempts to knockout the *NDUF7* gene in mice were unsuccessful and shown to be embryonically lethal by day E10.5 (Rendón et al, 2014).

1.5.1.5 NUBPL (*hInd1*)

Ind1 was first identified in the obligate aerobic yeast *Yarrowia lipolytica* as a specific chaperone required for Complex I biogenesis, as loss of this protein resulted in a strong Complex I defect (Bych et al, 2008). Analysis showed that Ind1 was homologous to other proteins involved in the biogenesis of Fe-S clusters and was able to bind a transferable Fe-S cluster through a 'CXXC' motif that was required for Ind1 function (Bych et al, 2008). Analysis of the human homologue showed that hInd1 functioned in a similar way to the *Y. lipolytica* protein, which required the CXXC motif to bind the Fe-S cluster [Fe₄S₄] *in vitro* in a labile manner (Sheftel et al, 2009). High-throughput pooled sequencing subsequently identified the human homologue hInd1 (later renamed NUBPL) to be involved in mitochondrial disease (Calvo et al, 2010). The patient was identified to be apparently homozygous c.166G>A mutation from the paternal allele that resulted in a p.G56R substitution at a highly conserved residue as well as a c.815-27T>C mutation that likely resulted in exon skipping (Calvo et al, 2010). Further analysis showed that the maternal allele contained a complex chromosomal rearrangement resulting in loss of exons 1-4. Complementation with cDNA encoding wild type NUBPL was able to restore the Complex I deficiency in patient fibroblasts (Calvo et al, 2010).

1.5.2 Mid-stage assembly factors-The MCIA complex

1.5.2.1 NDUF1 (*CIA30*)

Analysis of Complex I assembly in the fungus *Neurospora crassa* revealed two novel chaperones termed Complex I intermediate associated (CIA) protein of 30- and 84 kDa (CIA30 and CIA84 respectively) to be important in Complex I assembly (Kuffner et al, 1998). Analysis of the role of CIA30 and CIA84 demonstrated these proteins were important in the biogenesis of the membrane arm and the loss of these proteins resulted in the accumulation of stalled assembly intermediates (Kuffner et al, 1998). While it was demonstrated these proteins were required for the formation

of Complex I they were not associated with the final holoenzyme indicating that these proteins contained chaperone activity (Kuffner et al, 1998).

A human orthologue of CIA30 was later identified to be important in the biogenesis of Complex I through knockdown studies (Janssen et al, 2002; Vogel et al, 2005). While initial studies observed CIA30 in two assembly intermediates of ~600 kDa and ~700 kDa (Vogel et al, 2005), it was later shown that CIA30 resides in a number of higher molecular weight complexes ranging from 460-830 kDa (Dunning et al, 2007). CIA30 was also shown to be a peripheral membrane protein in the mitochondrial matrix and able to interact with a number of Complex I subunits, but not the fully assembled Complex I (Dunning et al, 2007). Interestingly, co-immunoprecipitation of CIA30 following mtDNA-encoded protein radiolabelling showed that CIA30 interacted with the Complex I subunit mt-ND2 early in the assembly process, but this was lost once subunits entered mature Complex I (Dunning et al, 2007). The first patient identified with mutations in CIA30 harboured a maternal c.1001A>C mutation resulting in a p.T207P mutation, and a paternally derived allele contained a c.1140A>G mutation resulting in a p.K253R substitution (Dunning et al, 2007). The paternal allele also disrupts an intron-exon boundary resulting in an additional splicing of 6 bases resulting in a 2 amino acid deletion Δ Val Δ Lys encoded by the end of exon 3 (Dunning et al, 2007). Mitochondria isolated from patient fibroblasts were unable to form the ~815 kDa intermediate and had a greatly reduced level of assembled Complex I (Dunning et al, 2007).

CIA30 was later renamed NDUFAF1 (Vogel et al, 2005) and a second patient was subsequently identified with two separate mutations; c.631C>T resulting in an p.R211C substitution and c.733G>A resulting in a p.G245R substitution (Fassone et al, 2011). The patient was healthy but died approximately 3 weeks after a viral infection, which initiated a number of symptoms indicative of mitochondrial disease (Fassone et al, 2011). NDUFAF1 was later found to be regulated by the nuclear TR4 receptor as TR4^{-/-} mice developed mitochondrial myopathy, Complex I deficiency and had a specific reduction in NDUFAF1 mRNA (Liu et al, 2011). More recently a third patient was identified with mutations in NDUFAF1 resulting in leukodystrophy (Wu et al, 2014). Both mutations were located in exon 2 and were c.247GA and c.278A>G, leading to p.D83N and p.H93R substitutions respectively (Wu et al, 2014).

1.5.2.2 *Ecsit*

Ecsit (evolutionarily conserved signalling intermediate in toll-signalling) was originally identified as an adaptor protein in Toll-pathways of the innate immune system leading to the expression of pro-inflammatory genes (Kopp et al, 1999). *Ecsit* was also identified as a signalling intermediate in the BMP signalling pathway and loss resulted in embryonic lethality at day E6.5-7.5 (Xiao et al, 2003).

A new role for Ecsit was identified when a population of the cytosolic protein was observed to be targeted to the mitochondrial matrix where it could interact with CIA30 and participate in Complex I biogenesis (Vogel et al, 2007b). Ecsit was observed to co-migrate with CIA30 on BN-PAGE and Ecsit knockdown using RNAi reduced the levels of mature Complex I and the levels of CIA30 (Vogel et al, 2007b). Unifying the role of Ecsit in innate immune signalling and Complex I biogenesis, it was shown that following bacterial infection, a subset of TLR receptors (TLR1, 2 and 4) in macrophages could activate TRAF6 resulting in translocation to mitochondria where it could engage Ecsit (West et al, 2011).

1.5.2.3 ACAD9

ACAD9 (Acyl-CoA dehydrogenase 9) was originally identified as a component of the β -oxidation machinery of fatty acids in mitochondria with high expression in heart, muscle and brain tissue and specificity towards long-chain unsaturated acyl-CoA substrates *in vitro* (Ensenauer et al, 2005; Zhang et al, 2002). ACAD9 was shown to localise to the matrix side of the inner membrane and undergoes a two-step processing by the mitochondrial proteases MPP and MIP to produce the mature ACAD9 protein (Ensenauer et al, 2005). It was noted that while most proteins imported into the mitochondrial matrix undergo processing by the Mitochondrial Processing Peptidase (MPP) to remove the mitochondrial targeting sequence, further processing by the Mitochondrial Intermediate Peptidase (MIP) is generally reserved for proteins that are involved in oxidative phosphorylation (Branda & Isaya, 1995; Chew et al, 1997). ACAD9 was the first of the ACADs to be identified to undergo this process (Ensenauer et al, 2005). It was hypothesised that ACAD9 is responsible for oxidation of Acyl-CoA in the embryonic and fetal central nervous system due to its high expression while an paralogue of ACAD9, Very-long chained Acyl-CoA dehydrogenase (VLCAD) had little to no expression in these tissues (Oey et al, 2006).

The involvement of ACAD9 in disease was first identified when 3 patients presented with liver dysfunction, cardiomyopathy or chronic neurological dysfunction (He et al, 2007). Despite the high homology of ACAD9 with VLCAD, it was obvious that these two proteins could not compensate for one another should one be deficient (He et al, 2007). One patient presented with Reye-like episodes following aspirin ingestion during a minor viral infection (He et al, 2007). No defects in electron transport chain complexes were detected in post mortem muscle biopsies of the patient, as well as no mtDNA mutations, deletions or rearrangements (He et al, 2007). Another patient presented with cardiomyopathy and hepatomegaly. The patient died at 4.5 years of congestive heart failure (He et al, 2007).

Analysis of the *ACAD9* promoter region identified two highly conserved regions homologous to nuclear respiratory factor 1 (NRF-1) and cAMP-responsive element transcription factor binding

sites (CREB), important regulators of gene expression for many respiratory chain enzyme subunits (He et al, 2007). Analysis of the promoter region also failed to identify any putative 'direct repeat site 1' (DR1) binding site for the peroxisomal proliferation-activated receptors (PPARs), which are common in the 5' promoter region of the VLCAD gene and other ACADs, suggesting ACAD9 is differentially regulated when compared to other ACADs involved in the oxidation of fatty acids (He et al, 2007).

In a later study endogenous ACAD9 was identified to interact with C-terminal TAP-tagged CIA30 and Ecsit through affinity purification (Nouws et al, 2010). In a similar way, ACAD9-TAP could interact with both CIA30 and Ecsit, suggesting a tight interaction between these proteins (Nouws et al, 2010). Also suggesting a close role with Complex I biogenesis, ACAD9 containing complexes co-migrated with NDUFAF1 and Ecsit and all three proteins were tightly associated with the matrix face of the inner membrane (Nouws et al, 2010). Knockdown studies of ACAD9 showed a reduction of mature Complex I, as well reduced levels of CIA30 and Ecsit (Nouws et al, 2010). Analysis of a cohort of patients with isolated Complex I deficiency identified two unrelated patients with mutations in ACAD9; one patient was homozygous for a c.1553G>A mutation resulting in a p.R518H substitution, while the second patient was heterozygous for c.187G>T resulting in a premature stop codon (p.E63*) and c.1237G>A resulting in an p.E413K mutation (Nouws et al, 2010). Transduction of patient cells with wild type ACAD9 could rescue the defect, indicating that this gene was the cause of the Complex I deficiency. Interestingly, ACAD9 deficient cells had normal dehydrogenation of palmitoyl-CoA and oxidation of oleic acid, whereas VLCAD knockdown severely reduced both activities (Nouws et al, 2010). This strongly suggested a specific role of ACAD9 in Complex I biogenesis, whereas VLCAD is involved in β -oxidation. Phylogenetic analysis showed that ACAD9 evolved from a gene duplication of VLCAD at the root of the vertebrates and has acquired a new function in the biogenesis of Complex I (Nouws et al, 2010).

Exome sequencing was also used to identify *ACAD9* mutations as a cause of Complex I deficiency (Haack et al, 2010). The patients presented with a range of symptoms indicative of a mitochondrial disease and Complex I deficiency, including cardiomyopathy, lactic acidosis, exercise intolerance and encephalopathy (Haack et al, 2010). A number of point mutations were identified including c.130T>A (p.F44I), c.797G>A (p.R266N), c.976G>A (p.A362P), c.1249C>T (p.R417C) and c.1594C>T (p.R532W) as likely pathogenic mutations in the *ACAD9* gene (Haack et al, 2010). Expression of ACAD9 in patient cells was also able to restore enzyme activity back to nearly control levels (Haack et al, 2010). Interestingly, riboflavin supplementation in ACAD9 patient fibroblasts was able to significantly increase Complex I activity suggesting metabolic intervention may help patients with ACAD9 mutations and Complex I deficiency (Haack et al,

2010). ACAD9 is an FAD-containing flavoprotein and so supplementation with riboflavin, a metabolic precursor of FAD could explain the increase in Complex I activity observed in ACAD9 deficient fibroblasts (Haack et al, 2010). Another study identified a Dutch double consanguineous family with patients suffering from easy fatigability, exercise intolerance and lactic acidosis and to have an isolated Complex I deficiency that was attributed to mutations in ACAD9 (Gerards et al, 2010b). The patients harboured a homozygous c.1594C>T mutation resulting in a p.R532W substitution in a highly conserved residue. An unrelated patient with similar symptoms was also screened for mutations in *ACAD9* and was identified to be compound heterozygous for c.380G>A and c.1405C>T resulting in the substitutions p.R127Q and p.R469W respectively (Gerards et al, 2010b). All patients identified were responsive to riboflavin treatment (Gerards et al, 2010b; Scholte et al, 1995). A novel pathogenic mutation, c.1240C>T resulting in the point mutation p.R414C was later identified in a patient with Complex I deficiency (Garone et al, 2013). Again fibroblasts from this patient had restored Complex I activity when supplemented with riboflavin, suggesting that ACAD9 deficiency could be widely treated with this metabolite.

After mounting evidence that ACAD9 deficiency could be widely treated with riboflavin supplementation, a patient was identified with a c.659C>T mutation that resulted in the substitution p.A220V, mutating a residue that is highly conserved in both ACAD9 and VLCAD (Nouws et al, 2014b). The patient presented with high lactate levels soon after birth and was later diagnosed with hypertrophic cardiomyopathy and hypotonia at age 7 weeks. Analysis showed an isolated Complex I deficiency, but unlike other ACAD9 patients, fibroblasts supplemented with riboflavin did not respond and enzyme activity levels remained unchanged.

More recent evidence suggests that ACAD9 indeed possesses enzyme activity catalysing the formation of *trans*-2-enoyl-CoA from acyl-CoA *in vivo* (Nouws et al, 2014a). Knockdown of ACAD9 in VLCAD deficient fibroblasts revealed that it was required for the production of C14:1-carnitine from oleate and C12-carnitine from palmitate, providing a biochemical explanation as to why these acyl-carnitines are produced and used to identify cases of VLCAD deficiency (Nouws et al, 2014a). Because ACAD9 was observed to have catalytic activity *in vivo*, a catalytically inactive mutant of ACAD9 (E426Q-resulting in the removal of an essential nucleophile in the catalytic triad) was generated and was also able to restore Complex I levels indicating ACAD9's catalytic activity related to β -oxidation of fatty acids was not required for Complex I biogenesis (Nouws et al, 2014a).

In order to clarify the extent of β -oxidation attributed to ACAD9, HEK293 cells deficient of ACAD9 were tested for palmitate oxidation and palmitoyl-CoA dehydrogenase activity, which were both reduced in the absence of ACAD9 (Schiff et al, 2015). To determine the effect of patient mutations

on the ability of ACAD9 to catalyse oxidation of palmitoyl-CoA *in vitro*, a number of recombinant ACAD9 proteins harbouring patient mutations were generated (Schiff et al, 2015). While some ACAD9 mutations have a severe reduction in enzyme activity and trypsin stability, some mutations behaved similar to wild type ACAD9 suggesting little correlation with the role of ACAD9 enzyme activity and a defect in Complex I assembly (Schiff et al, 2015).

1.5.2.4 *TMEM126B*

Using complexome profiling, which integrates BN-PAGE and mass spectrometry analysis, TMEM126B was identified as a protein that co-migrated with CIA30, Ecsit and ACAD9 (Heide et al, 2012). TMEM126B is an integral membrane protein located in the mitochondrial inner membrane and knockdown in 143B osteosarcoma cells resulted in decreased levels of mature Complex I and reduced oxygen consumption (Andrews et al, 2013; Heide et al, 2012). Interestingly, certain other MCIA-containing assembly intermediates remained largely unchanged in the absence of TMEM126B (Heide et al, 2012). The role of TMEM126B in Complex I function/assembly is unclear and as yet, patient mutations in the gene encoding this protein have not been reported.

1.5.2.5 *TIMMDC1 (C3ORF1)*

The human gene *C3ORF1* was originally identified as a protein of unknown function (Escarceller et al, 2000). Sequence analysis of *C3ORF1* identified a homologue in *Mus musculus* and was also homologous to the essential *Drosophila* RP140-upstream gene (Escarceller et al, 2000). Northern blot analysis showed this gene was ubiquitously expressed, with enhanced expression of *C3ORF1* in heart and skeletal muscle (Escarceller et al, 2000). Following this, *C3ORF1* was identified to be an assembly factor required for the membrane arm of Complex I (Andrews et al, 2013). Later renamed TIMMDC1, it was shown that this assembly factor associates at an early stage of Complex I assembly and was able to interact with a number of subunits in a ~315 kDa intermediate (Andrews et al, 2013). It was later shown that TIMMDC1 performs its function in Complex I assembly in association with the MCIA complex, a mid-stage assembly complex required for Complex I assembly (Guarani et al, 2014). TIMMDC1 belongs to the TIM17/22/23 family of protein translocases and so may have an important role in the integration of transmembrane proteins into the mitochondrial inner membrane (Guarani et al, 2014).

1.5.3 *Late stage assembly factors*

1.5.3.1 *NDUFAF2 (B17.2L)*

The yeast *Saccharomyces cerevisiae* has been a useful genetic tool to understand the biogenesis of components of the electron transport chain. However, studies into Complex I assembly have not

been able to take advantage of this organism as it lacks a Complex I as seen in the mitochondria of higher eukaryotes. In a whole-genome subtractive study to compare genes in aerobic yeast (*Y. lipolytica* and *D. hansenii*) but absent in fermentative yeast, the protein B17.2L was identified as a possible candidate for a Complex I assembly factor (Ogilvie et al, 2005). This protein was of particular interest as it appeared to have arisen from a gene duplication event of the B17.2 gene (NDUFA12 in humans), a structural subunit of Complex I present in α -proteobacteria and eukaryotic mitochondria but absent in the *nuo* operon in other bacteria including *E. coli* (Ogilvie et al, 2005). A patient was identified with Complex I deficiency and analysis of the *NDUFAF2* gene that encodes B17.2L revealed a homozygous c.182C>T mutation producing a premature stop codon at p.R45 (Ogilvie et al, 2005). Analysis of the patient fibroblasts showed a large reduction in the levels of mature Complex I that were rescued upon retroviral expression of B17.2L (Ogilvie et al, 2005). Immunodetection of B17.2L in fibroblasts from various Complex I deficient patients showed that this protein was present in the ~815 kDa intermediate (present in NDUFS4 patient fibroblasts) but not in control suggesting it may play a role late in Complex I assembly (Ogilvie et al, 2005). This was further illustrated in a cohort of Complex I deficient patients with defects at different stages of assembly that showed a specific interaction of B17.2L with the same stalled intermediate in patients with NDUFS4 or NDUFV1 mutations that lack the 'N module' of Complex I (Vogel et al, 2007d). Similar observations were made when *in vitro* translated B17.2L was imported into mitochondria isolated from patients with NDUFS4 and NDUFS6, whereas no stable complex was observed in mitochondrial isolated from control fibroblasts (Lazarou et al, 2007). Subsequently, a patient was identified to harbour a homozygous triple gene deletion encompassing *NDUFAF2* (the human gene encoding B17.2L), *ERCC8* (encoding a protein involved in transcription coupled nucleotide excision repair pathway for DNA damage) and *ELOVL*, encoding a putative elongase involved in fatty acid biosynthesis (Janssen et al, 2009). While fatty acid biosynthesis was normal, the patient had a severe Complex I defect with no detectable B17.2L and a defective DNA repair pathway when exposed to UV light suggesting the severe phenotype was due to the loss of both B17.2L and ERCC8 (Janssen et al, 2009).

1.5.4 Putative assembly factors

1.5.4.1 Apoptosis inducing Factor (AIF)

Apoptosis Inducing Factor was originally identified as a mitochondrial intermembrane space protein capable of inducing caspase independent chromatin condensation and DNA fragmentation when added to isolated nuclei (Candé et al, 2002). Upon apoptotic induction the membrane anchored protein can translocate from the mitochondria to the cytosol and finally the nucleus to carry out the pro-apoptotic function (Candé et al, 2002). This protein contains a membrane anchor and an oxidoreductase domain facing the intermembrane space. Further

studies into AIF function suggested that it was required for Complex I biogenesis as loss resulted in decreased levels of assembled Complex I along with its individual subunits (Vahsen et al, 2004). Studies using specific liver and muscle deletions of AIF demonstrated a loss of Complex I and an OXPHOS deficiency that resembles human insulin resistance, possibly indicating a molecular cause of the disease (Pospisilik et al, 2007). Recent work suggests that AIF is required for the import and stabilisation of CHCHD4, an intermembrane space protein disulphide oxidoreductase/isomerase with a homologue found in yeast termed MIA40 (Hangen et al, 2015). Once stable, CHCHD4 can then catalyse the oxidative folding of a number of intermembrane space proteins that contain twin CX_nC motifs in OXPHOS subunits (for example, NDUFA8 and NDUFS5) and assembly factors (Hangen et al, 2015; Meyer et al, 2015). Thus, loss of AIF is likely to cause defects in the biogenesis of a number of Complex I subunits leading to decreased Complex I assembly.

1.5.4.2 FOXRED1

FAD-dependent oxidoreductase 1 (FOXRED1) is a member of the D-amino acid oxidase family of proteins and has a wide distribution among organisms of the different kingdoms of life including bacteria, archaea and metazoa (Lemire, 2015a). Using high-throughput pooled sequencing of a cohort of Complex I deficient patients, FOXRED1 (Flavin-dependant oxidoreductase 1) was identified as a candidate gene involved in Complex I assembly (Calvo et al, 2010). The patient was compound heterozygous for a c.694C>T mutation resulting in a premature stop codon at p.Q232 while the other allele contained a c.1289A>G mutation resulting in the substitution p.N430S (Calvo et al, 2010). Analysis of fibroblasts from the patient revealed decreased Complex I activity that was rescued upon viral complementation with wild-type FOXRED1 (Calvo et al, 2010). A second patient was later identified to harbour a homozygous c.1054C>T mutation resulting in an p.R352W substitution (Fassone et al, 2010). The point mutation was predicted to interfere with FAD binding, a predicted co-factor of FOXRED1 (Fassone et al, 2010). Complex I activity in the skeletal muscle was 7% of the control while a milder defect of 70% activity was observed in patient-derived fibroblasts (Fassone et al, 2010). Phylogenetic analysis of FOXRED1 homologues suggest that this protein has a wide distribution even in organisms that lack Complex I and may play a metabolic function in these organisms, with a role in Complex I assembly a more recently evolved function of this protein (Lemire, 2015a). While a number of lower organisms lack FOXRED1 but still harbour Complex I, metazoans appear to require the presence of FOXRED1 to assemble this enzyme (Lemire, 2015a). Operon analysis of bacteria containing FOXRED1 homologues places this gene downstream of N-methylhydantoinase genes involved in creatine and creatinine degradation (Lemire, 2015a). Furthermore, a structural model of FOXRED1 suggested an FAD-binding site analogous to the highly similar protein monomeric sarcosine

oxidase and a putative oxygen binding site indicating that FOXRED1 may have oxidoreductase activity *in vivo* (Lemire, 2015b).

1.5.4.3 *LactB* and *LYRM5*

Both *LactB* and *LYRM5* were identified as proteins that have co-evolved with, and are absent in organisms that lack Complex I (Pagliarini et al, 2008). *LactB* is an active-site serine enzyme that is evolutionarily related to the bacterial penicillin-binding protein (Polianskyte et al, 2009). In bacteria, this enzyme is responsible for peptidoglycan metabolism and cell wall biosynthesis, which is not present in mammalian mitochondria, suggesting a new role for this protein (Polianskyte et al, 2009). Biochemical analysis of *LactB* demonstrated that it localises to the mitochondrial intermembrane space and forms filaments that may aid in micro-compartmental organisation of the intermembrane space (Polianskyte et al, 2009). A causal link between *LactB* and obesity was demonstrated in transgenic mice overexpressing *LactB* indicating a link to metabolism, but how this relates to Complex I remains unclear (Chen et al, 2008).

The LYR superfamily consists of at least 13 proteins with a highly conserved N-terminal leucine (L), tyrosine (Y) and arginine (R) residues and an invariant phenylalanine (Angerer, 2013). This family of proteins is involved in Fe-S biogenesis and a number of these proteins are subunits or assembly factors of a number of respiratory complexes (Angerer, 2013). While the role of *LYRM5* remains elusive, two accessory subunits of Complex I (NDUFA6 and NDUFB9) are also members of this family and may function together with *LYRM5* in Complex I assembly (Angerer, 2013).

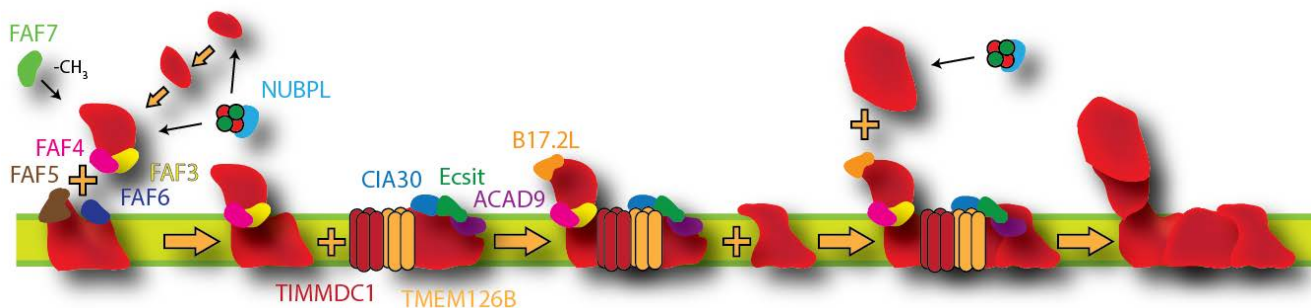


Figure 1.8: Complex I assembly requires a number of assembly factors. While the assembly of Complex I occurs by the assembly of a number of modules, a number of assembly factors have been implicated at various stages of the pathway. NUBPL delivers Fe-S clusters to Complex I subunits, while NDUFAF7 is required to methylate NDUFS2. The assembly factors NDUFAF3-6 are also implicated in early stage assembly. The proteins CIA30, Ecsit, ACAD9, TMEM126B and TIMMDC1 function in mid-stage assembly, while B17.2L functions at a late stage. Adapted from Mimaki et al (2012) and McKenzie and Ryan (2010).

1.6 Aims of this study

Complex I assembly is an intricate process requiring the incorporation of subunits from two distinct genomes into an enzyme of nearly 1 MDa in size. This process is orchestrated by a number of factors that have been shown to be important for Complex I assembly, however molecular detail on how these proteins function is lacking. Also, the assembly of this complex containing 44 different subunits is hypothesised to have more assembly factors than those described in the literature. Therefore, the aims of this thesis are as follows:

1. Characterisation of the known assembly machinery of Complex I.

Complex I biogenesis requires the cooperation of at least 13 known assembly factors. While it is known these proteins are important, what role they play at the molecular level is largely unknown. Here, genome editing, proteomic analysis and traditional biochemical techniques will be used to dissect the molecular pathway these proteins are involved in to understand how these proteins contribute to Complex I biogenesis. This will help in the understanding of the assembly pathway, how different proteins contribute to Complex I biogenesis and the development of future treatment for patients with Complex I deficiency.

2. Identification of novel assembly machinery involved in the biogenesis of Complex I.

The model organism *S. cerevisiae* lacks Complex I, and so this genetic toolbox is not available to interrogate and investigate Complex I assembly. Indeed, Complex IV in yeast contains 11 subunits but requires at least 14 proteins for correct biogenesis, with a similar ratio of structural to assembly proteins observed in mammalian mitochondria (Soto et al, 2012). By extension, it is plausible that many Complex I assembly factors remain to be identified. Further to this, more than 50% of Complex I deficient patients lack pathogenic mutations in structural subunits or known assembly factors, suggesting that many proteins involved in this process are yet to be identified. To investigate this, precipitation of close-proximity proteins to known Complex I assembly proteins followed by proteomic analysis will be utilised. This will allow for the identification of proteins that may not be known to be involved in the Complex I assembly pathway and increase the repertoire of genes that can be screened for patients with Complex I deficiency and lack a molecular diagnosis of the disease.

Chapter 2
Materials and Methods

2.1 Chemical Reagents

General laboratory reagents for this work were purchased from Sigma, Thermo Scientific, Amresco and Merck.

2.2 Cloning and Molecular Biology

2.2.1 Plasmid Purification

The required plasmids were prepared from an overnight culture containing an appropriate antibiotic as a selective agent. The culture was incubated at 37°C overnight and purified using the Qiagen® Plasmid Plus Mini/Midi Kit or the Promega Wizard® Plus SV Miniprep kit according to manufacturer's instructions. The concentration of DNA was determined by measuring the absorbance at 260nm using the Nanodrop ND-1000 UV-Vis Spectrophotometer (Nanodrop Technologies).

2.2.2 Polymerase Chain Reaction (PCR)

2.2.2.1 PCR from a plasmid as template

Amplification of the appropriate open reading frame was performed using PCR with Vent™ DNA Polymerase (New England Biolabs) according to manufacturer's instructions. Primer design incorporated appropriate restriction enzyme recognition sites to facilitate insert incorporation during ligation. The PCR reaction was carried out in a PCRExpress® (BioRad) machine according to Sambrook and Russell (2001).

2.2.2.2 PCR from genomic DNA

Preparation of genomic DNA was performed according to Sambrook and Russell (2001). Briefly, 100µg of cells were resuspended in 133µL of genomic DNA extraction buffer (67 mM Tris-Cl pH 8.8, 6.7 mM MgCl₂, 2 µM SDS, 50 µg/mL Proteinase K) and incubated for 1 hour at 37°C followed by 10 minutes at 80°C.

To amplify the region of interest, primers were designed using 'PRIMER-BLAST' software (<http://www.ncbi.nlm.nih.gov/tools/primer-blast/>) using the human genomic DNA database. Primers were selected based on the fewest off-target PCR products or those that would fail to generate a product similar in size. To amplify the region of interest, Herculase II polymerase (Aligent) was used according to manufacturer's instructions, using 1µL of the prepared genomic DNA as template.

2.2.2.3 PCR from a human cDNA library

A cDNA library was constructed from whole RNA isolated from HEK293T cells using TRIzol (Chomczynski & Sacchi, 2006) followed by reverse transcription using random hexamer priming using the SuperScript® III First strand synthesis system (Invitrogen) according to the manufacturer's instructions. Primers were designed to amplify the gene of interest that also incorporated the restriction endonuclease sites to allow insertion into a vector backbone. Amplification was carried out using Herculase II polymerase (Aligent) according to manufacturer's instructions.

2.2.2.4 Mutagenesis using inverse PCR

In order to generate plasmids incorporating a desired mutation, Inverse PCR was employed (Sambrook & Russell, 2001). Mutagenic primers were designed to incorporate nucleotides that would result in the desired mutation being translated. For amino acid substitutions, nucleotides were changed according to the standard codon usage in mammalian cells to minimise the number of nucleotide changes required. For deletions, primers were designed to flank the 5' and 3' region to amplify the entire vector without the region to be deleted. Amplification was performed using Phusion Polymerase (New England Biolabs) according to manufacturer's instructions. Following amplification, template was digested using DpnI and the 5' ends of the amplicon were phosphorylated using T4 polynucleotide kinase (New England Biolabs) in the presence of 1 mM ATP. Circularisation of the plasmid was achieved using T4 DNA ligase followed by transformation into *E. coli*.

2.2.3 Restriction enzyme digestion and DNA ligation

The PCR amplicon and/or purified plasmid were subject to restriction enzyme digestion using restriction enzymes purchased from Promega or New England Biolabs. The digestions were performed at 37°C before separation on a 1% (w/v) agarose gel. The bands were excised and purified using the Promega Wizard® SV PCR clean-up kit. The plasmid and insert were incubated with 1U T4 DNA ligase (New England Biolabs) in the presence of 1mM ATP at room temperature for at least 2 hours before bacterial transformation.

2.2.4 Bacterial Transformation

The ligation products were transformed as described in Sambrook and Russell (2001) in chemically competent XL-1 Blue *E. coli* cells prepared by the 'One-step' method (Chung et al, 1989).

2.2.5 Dideoxynucleotide Sequencing

Sequencing was carried out by the Australian Genome Research Facility (AGRF) at the Walter and Eliza Hall Institute of Medical Research (WEHI). Samples were prepared by the addition of 10 pmol of appropriate primers directed against the vector to be sequenced as well as 600-1200 ng of purified plasmid DNA made up to 12 μ L. The primers were designed to be approximately 40-50 bp upstream and downstream of the multiple cloning site.

2.3 Genome Editing

2.3.1 TALEN design and construction

Transcription activator-like effector nucleases were designed using ZiFiT Targeter version 4.2 and generated using the FLASH (Fast ligation-based automatable solid-phase high-throughput) assembly method (Reyon et al, 2012; Sander et al, 2010; Sander et al, 2007).

2.3.2 CRISPR-Cas9 design and construction

Crispr-Cas9 targets were identified and designed using the online tool 'CHOP CHOP' <https://chopchop.rc.fas.harvard.edu/> and generated using oligoduplex ligation into a Crispr-Cas9 vector backbone (Montague et al, 2014; Ran et al, 2013).

2.4 Tissue Culture

2.4.1 Cell Culture

Tissue culture cell lines were cultured in incomplete Dulbecco's modified eagles media (DMEM) supplemented with fetal calf serum (FCS-10% (v/v)) and 10 mL/L Penicillin/Streptomycin (denoted as complete DMEM). Cell lines depleted of mtDNA or those that contained a respiratory defect also required the addition of uridine (50 μ g/mL) to the culture medium. For SILAC, cells were cultured in SILAC DMEM (Thermo-Fisher Scientific; 4.5 g/L glucose, 4 mM L-glutamine, 110 mg/L sodium pyruvate) containing 10% (v/v) dialysed FCS, supplemented with penicillin/streptomycin, 50 μ g/ml uridine, 600 mg/L L-proline and either 'light' amino acids (146 mg/L L-lysine.HCl and 42 mg/L L-arginine.HCl), or 'heavy' amino acids (180 mg/L $^{13}\text{C}_6^{15}\text{N}_2$ -L-lysine.2HCl and 44 mg/L $^{13}\text{C}_6^{15}\text{N}_4$ -L-arginine.HCl; Cambridge Isotope Laboratories). All cells were cultured in a humidified environment at 37°C under 5% CO₂, 95% air.

2.4.2 Transient transfection of cultured cells

Approximately 18-24 hours prior to transfection, cultured cells were trypsinised (1:250 Trypsin and EDTA pH 7.0, GIBCO) and seeded at ~80% confluency. Transfection was performed using

Lipofectamine™ 2000 (Invitrogen) according to manufacturer's instructions. Cells were incubated for the desired time in DMEM containing 10% (v/v) FCS in the absence of penicillin/streptomycin.

2.4.3 Cell sorting, screening and validation of disruptions

Following transient transfection of either TALENs or pCRISPR-Cas9 constructs, cells were trypsinised and resuspended in PBS containing 10% (v/v) FBS and 1mM EDTA, filtered through a 70 µm cell strainer (Falcon) and sorted using a BD Biosciences FACS Aria III gated on GFP and/or mCherry fluorescence to isolate single cell populations. After cells were expanded, cells were trypsinised and divided into DMEM containing either glucose or galactose as the carbon source. Any clones that failed to grow in galactose DMEM were expanded and tested by Western blotting for the loss of the target protein by SDS-PAGE (provided an antibody was available), loss/disruption of Complex I by BN-PAGE or indel sequencing of the target region. Disruptions causing a subtle OXPHOS defect may not have resulted in a strong growth phenotype, and so were screened by BN-PAGE or SDS-PAGE as described. Specificity was confirmed by complementation by re-introduction of the target protein.

2.4.4 Generation of pseudotyped pantropic retrovirus for stable protein expression

The generation of stable cell lines expressing a protein of interest was performed according to Morgenstern and Land (1990) with modifications. All work was carried out in a certified PC2 facility and all viral related material was treated with bleach and UV-irradiated to inactivate live virus. Briefly, HEK293T cells were co-transfected with a viral vector (pBABE with open reading frame of the protein of interest) and helper vectors (gag-pol and VSV-G) using Lipofectamine LTX (Invitrogen) overnight according to manufacturer's instructions. Following transfection, media was removed and replaced with 1 mL of complete DMEM for a further 24 hours. The viral supernatants were then harvested and centrifuged at 2,000g for 5 minutes to remove cellular debris. The viral supernatant was then filtered through a Millex-HV PVDF 0.45 µm filter (Millipore) onto the recipient cells. Polybrene was added to a final concentration of 8µg/mL to allow viral attachment and transduction of cells to occur. Transduced cells were selected for by adding galactose DMEM if the transduced cells harboured a respiratory defect, or by the addition of 1 µg/mL puromycin until control cells were no longer viable. Positive cells were expanded, and protein expression was verified by SDS-PAGE and western blot analysis.

2.4.5 Oxygen consumption and enzyme activity measurements

Oxygen consumption and ECAR measurements were performed using Seahorse Biosciences XF24-3 analyser with the kind assistance of Dr Ann Frazier according to Formosa et al (2015).

Enzyme activity measurements were performed with the assistance of Ms Tegan Stait according to Frazier and Thorburn (2012).

2.4.6 *[³⁵S]-Met pulse-chase labelling of mtDNA encoded subunits*

To determine synthesis and turnover of mtDNA encoded subunits, pulse-chase analysis was performed according to Formosa et al (2016).

2.4.7 *Mitochondrial Isolation*

Mitochondrial isolations were carried out according to Johnston et al (2002) with modifications. Tissue culture cells were grown to ~95% confluency, and were removed from the plate with mechanical scraping followed by washing with PBS. The cells were pelleted (800g, 4°C, 5 minutes) and resuspended in 5mL Solution A (20mM Hepes-KOH pH 7.6, 220mM Mannitol, 70mM Sucrose, 1mM EDTA, 0.5mM PMSF, 2mg/mL BSA) followed by incubation on ice for 15 minutes to facilitate swelling. This was then homogenised using a drill-fitted pestle with 12-20 strokes. The homogenate was centrifuged (800g, 4°C, 5 minutes) and the supernatant containing mitochondria was centrifuged further (10,000g, 4°C, 10 minutes) to enrich for mitochondrial membranes. The pellet containing crude mitochondria were then resuspended in Solution B (As per Solution A without BSA) and centrifuged (10,000g, 4°C, 20 minutes). The final pellet was then resuspended in Sucrose Storage Buffer (10mM HEPES-KOH pH 7.4, 0.5M Sucrose) before quantitation of mitochondrial protein amount using the BCA protein quantitation kit (Thermo Scientific) according to manufacturer's instructions.

2.4.8 *Trichloroacetic acid precipitation*

The samples were subjected to trichloroacetic Acid (TCA) precipitation according to Rosenberg (1996). This was performed by resuspending the pellet in 12% (v/v) TCA and incubating on ice for 20 minutes or at -20°C overnight. The sample was then centrifuged at 16,000g for 30 minutes at 4°C and washed with acetone. The samples were centrifuged again (16,000g, 2 minutes, 4°C) and allowed to dry. Samples were analysed using SDS-PAGE (Tris-Tricine buffer system) as required.

2.5 Analysis of interacting proteins

2.5.1 *Co-immunoprecipitation of exogenously expressed FLAG-tagged protein*

Co-immunoprecipitation of FLAG-tagged protein was performed according to Formosa et al (2015). Briefly, cells were transiently transfected with a plasmid encoding the protein of interest with a C-terminal FLAG epitope. Following expression, mitochondria were isolated and

solubilised as above described in section 2.4.7. Once clarified, lysate was then bound to anti-FLAG M2-affinity gel (Sigma) for at least 2 hours at 4°C with gentle rotation. Washing was performed as described, and bound protein was eluted using 100 µg/mL FLAG peptide (Sigma).

2.5.2 Streptavidin-mediated pulldown of BirA* biotinylated proteins

Cells were incubated for 24 hours in DMEM containing 50µM Biotin (Sigma) prior to harvesting. Mitochondria were isolated and 600 µg of mitochondrial protein was lysed in 2 mL RIPA buffer (50 mM Tris pH 7.5, 150 mM NaCl, 1% (v/v) NP40, 1 mM EDTA, 1 mM EGTA, 0.1% (w/v) SDS) supplemented with 1x Protease cocktail inhibitor (Roche) 0.5% (w/v) deoxycholate, 250 U Benzoylase, with rotation at 4°C for 1 hour. Lysate was clarified by centrifugation (16,000g, 4°C, 30 mins) and applied to prewashed 20 µL bead volume of Streptavidin magnetic beads (Pierce). Streptavidin-biotin complexes were formed with gentle rotation at 4°C for 3 hours, followed by collection using a magnetic stand. Beads were washed twice in RIPA buffer, followed by three washes in TAP lysis buffer (50 mM HEPES-KOH pH 8, 100 mM KCl, 10% (v/v) glycerol, 2 mM EDTA, 0.1% (v/v) NP40) followed by three washes in 50 mM ammonium bicarbonate (ABC). Following the final wash, on-bead tryptic digest was performed using 1µg mass-spectrometry grade trypsin overnight at 37°C with agitation. Magnetic beads were collected and the supernatant containing peptides was transferred to a fresh tube. The beads were rinsed twice with mass spectrometry grade water. Samples were then lyophilised using vacuum centrifugation and resuspended in 10 µL of 5% formic acid and 3 µL was used for analysis.

2.6 Proteomics and data analysis

Sample preparation, mass spectrometry and data analysis was performed with the kind assistance of Dr David Stroud according to Formosa et al (2015) and Stroud et al (2015).

2.7 Polyacrylamide Gel Electrophoresis

2.7.1 Tris-Tricine SDS-PAGE

Tris-Tricine PAGE was performed according to Schagger and von Jagow (1987) with modifications. The separating gel consisted of a continuous 10%-16% acrylamide gradient (49.5% Acrylamide, 3% Bisacrylamide) in Tris-Tricine gel buffer (1 M Tris pH 8.45, 0.1% (w/v) SDS) and the stacking gel was prepared using 4% acrylamide. Polymerisation was initiated by the addition of 0.044% (v/v) APS and 0.033% (v/v) TEMED.

Samples were prepared as required and mixed with SDS loading buffer (50 mM Tris-HCl pH 6.8, 100 mM DTT, 2% (w/v) SDS, 10% (v/v) glycerol, 0.05% (w/v) Bromophenol blue) and boiled for 5 minutes. Samples were loaded onto the gel with molecular weight markers (MBP-β-

galactosidase (175kDa), MBP-Paramyosin (80kDa), MBP-CBD (58kDa), Aldolase (46kDa) Triosephosphate Isomerase (30kDa), CBD-BmFKBP13 (25kDa), Lysozyme (17kDa) and Aprotinin (7kDa)) and run at ambient temperature for 16 hours at 100 V and 25 mA per gel in Anode buffer (0.2M Tris pH 8.9) and cathode buffer (100mM Tris pH 8.25, 100mM Tricine, 0.1% (w/v) SDS) or until the dye front reached the end of the gel.

2.7.2 Blue Native PAGE

Blue Native PAGE was performed according to Schagger and von Jagow (1991) and McKenzie et al (2007). The separating gel consisted of a continuous 4%-13% acrylamide gradient (49.5% Acrylamide, 3% Bisacrylamide) in BN gel buffer (50 mM Bis-Tris pH7.0, 66 mM ϵ -amino n-caproic acid) and the stacking gel was prepared as a 4% gel. The gel was polymerised by the addition of 0.044% (v/v) APS and 0.033% (v/v) TEMED.

For BN-PAGE samples, the pellet was gently resuspended in 50 μ L of solubilisation solution (20 mM Bis-Tris pH 7.0, 50 mM NaCl, 10% (v/v) glycerol, 1% (w/v) Digitonin (Sigma) or 1% (v/v) Triton X-100) and was incubated on ice for 30 minutes to facilitate solubilisation. This was then centrifuged (16,000g, 4°C, 15 minutes) to remove any insoluble or aggregated material. To this, 10 \times BN loading dye (0.5% Coomassie blue G, 50 mM ϵ -amino n-caproic acid, 10 mM Bis-Tris pH 7.0) was added and loaded onto the BN PAGE gel. The molecular weight markers consisted of Thyroglobulin (669kDa), Ferritin (440kDa) and Bovine Serum Albumin (134kDa and 67kDa).

The gel was run in BN anode buffer (50 mM Bis-Tris pH 7.0) and BN cathode buffer (50 mM Tricine, 15 mM Bis-Tris, 0.02% (w/v) Coomassie blue G). The gel was run at 100 V and 10 mA per gel for 16 hours. After 3 hours, the cathode buffer was replaced with 'clear' cathode buffer (as above, without Coomassie blue G) and allowed to run for a further 13 hours.

2.8 Protein detection

2.8.1 Antibodies

Antibodies used during this work were produced in-house or purchased from commercial sources. Antibodies produced by the MTR lab included CIA30, NDUFAF2, NDUFAF4, Ecsit, ACAD9, NDUFA9, NDUFS5, and NDUF6. Commercially available antibodies were purchased for TIMMDC1 (Sigma), TMEM126B (Sigma), NDUFS2 (Abcam), NDUFS3 (Abcam), NDUFA13 (Sapphire Biosciences), NDUFV2 (Abcam), COI (Abcam), COIV (Abcam), Core I (Life Technologies), SDHA (Abcam) and FLAG (Sigma). The mtHsp70 antibody was a kind gift from Prof. Nick Hoogenraad (La Trobe University) and the mt-ND1 polyclonal antibody was a kind gift from Dr Anne Lombes (Institut De Myologie, Paris, France).

2.8.2 Western Blot analysis

2.8.2.1 Western Transfer

Proteins from gels were transferred onto a PVDF (Immobilon, Millipore) membrane using the semi-dry transfer method (Harlow & Lane, 1999). Following electrophoresis, the gel was removed and soaked briefly in transfer buffer (50 mM Tris, 40 mM glycine, 0.37% (w/v) SDS, 20% (v/v) methanol). A PVDF membrane was cut to an appropriate size, activated in methanol and blotting paper were soaked in transfer buffer. Proteins were transferred using 200mA (limiting) and 20 V for 2 hours. Following transfer, proteins were fixed and stained using 50% (v/v) methanol, 7% (v/v) acetic acid and 0.05% (w/v) Coomassie blue R, and then destained using a solution containing 50% (v/v) methanol and 7% (v/v) acetic acid. Finally, all Coomassie was removed using total destain (90% (v/v) methanol, 10% (v/v) acetic acid) before proceeding.

2.8.2.2 Immunoblot analysis

Once transfer was complete, the PVDF membrane was blocked for one hour with 5% (w/v) skim milk in PBS containing 0.05% (v/v) Tween20 (Sigma, denoted as PBS-tween). Once blocked, the skim milk was removed and the membrane was washed three times with PBS-tween over 30 minutes. The primary antibody was then added (made up in 5% (w/v) skim milk in PBS-Tween) and incubated overnight at 4°C with gentle rotation. Following incubation, the primary antibody was removed and the membrane was again washed with PBS-tween (three changes over 20 minutes). To this, a secondary antibody (goat anti-rabbit or goat anti-mouse IgG conjugated to horse radish peroxidase, Sigma) was made to 1:5000 dilution using 5% (w/v) skim milk in PBS-tween and incubated at ambient temperature for one hour. After washing, the membrane was analysed using electrochemiluminescence (ECL) reagents (Amersham) and a Molecular Imager® ChemiDoc™ XRs imaging system (BioRad).

2.8.3 Autoradiography of [³⁵S]-labelled proteins

Following transfer of [³⁵S]-labelled proteins, the membrane was exposed to a Phosphor imager screen (Amersham) for 24-48 hours and imaged using a Typhoon Trio DIGE Phosphor Imager (Amersham).

2.9 Fluorescence Microscopy

2.9.1 Immunofluorescence assay

Cells were fixed with 4% (w/v) paraformaldehyde in PBS (pH 7.4), permeabilised with 0.2% (w/v) Triton X-100 in PBS and incubated with primary antibodies for 60 minutes at room temperature. Primary antibodies were labelled with either Alexa Fluor 488 or Alexa Fluor 568 conjugated anti-mouse or anti-rabbit secondary antibodies (Molecular Probes). Hoechst (10 µg/mL) was used for nuclear staining.

2.9.2 Confocal Microscopy

Confocal microscopy was performed with the kind assistance of Mr Abeer Singh. Confocal microscopy was performed using a Leica TCS SP8 microscope equipped with HyD detectors. Z-sectioning was performed using 1 µm slices and combined. All images were processed using Image J (Schneider et al, 2012).

Chapter 3

Characterisation of FOXRED1 in Complex I assembly

3.1 Introduction

Proteomic analysis of mouse tissue followed by phylogenetic profiling, identified Flavin-dependant Oxidoreductase 1 (FOXRED1) as a putative assembly factor required for Complex I biogenesis (Pagliarini et al, 2008). Subsequently, lentiviral mediated knockdown of FOXRED1 was shown to result in a modest decrease in Complex I activity to approximately 80% of the control (Pagliarini et al, 2008). Further studies uncovered two patients with mutations in the *FOXRED1* gene and both presenting with Complex I deficiency (Calvo et al, 2010; Fassone et al, 2010).

Recently it was reported that FOXRED1 lacks a cleavable mitochondrial targeting signal and associates peripherally with the matrix side of the inner membrane (Formosa et al, 2015). Investigation of mitochondria isolated from patient fibroblasts confirmed decreased levels of mature Complex I suggesting that the pathogenic mutations may represent a partial loss of function, perhaps explaining why the patients have survived into adulthood. Furthermore, FOXRED1 deficient patient fibroblasts harboured a non-functional ~475kDa sub-complex that contained most mtDNA encoded subunits (Formosa et al, 2015).

While the use of patient fibroblasts has been useful in understanding the role of proteins in the biogenesis of Complex I, they have a number of drawbacks. Firstly, an isogenic control for comparison to patient fibroblasts is not possible, as these cells are derived from human sources with different genetic backgrounds. Secondly, patient cells are slow to grow and mitochondrial yield is poor making analysis difficult. Thirdly, fibroblasts are not amenable to manipulation such as transient transfections and require stable viral-mediated expression of target proteins. To address these issues, tissue culture cell lines such as HEK293T cells offer a range of advantages; ease of culture and improved yield of mitochondria compared to fibroblasts and ease of transfection. Furthermore, parental non-manipulated cells provide the most appropriate “isogenic” control. Together with new genome editing techniques (Gaj et al, 2013), the investigation of Complex I biogenesis is no longer restricted to the use of patient fibroblasts and allows deeper examination as to how these proteins function. In order to address whether FOXRED1 is critical for Complex I biogenesis, ‘transcription activator-like effector nuclease’ (TALEN) mediated gene disruption was employed to produce cells that lack FOXRED1 expression, denoted as Δ FOXRED1.

The use of TALENs offer a highly specific approach to gene disruption in mammalian cells. Originally identified in the plant pathogen *Xanthomonas*, these DNA-binding proteins are composed of a repeating domain, termed a transcription activator-like (TAL) domain that specifically recognise and bind to a single nucleotide (Sugio et al, 2007). A series of TAL domains can then recognise and bind to a specific region of the genome to elicit a biological effect. In plants,

the natural protein results in an upregulation of genes that allow the invading bacterium to colonise the host (Sugio et al, 2007). Since their discovery, these DNA-binding arrays have been functionalised with the non-specific nuclease *FokI* to allow the introduction of DNA double strand breaks (DSB). To introduce a DSB in the region of interest, a TALEN pair is designed to bind upstream and downstream of the target region. Upon binding of the TAL domains to the DNA, the *FokI* from each TALEN can homo-dimerise and becomes active resulting in a DSB that can be repaired by non-homologous end joining (NHEJ). This DNA repair mechanism is generally inefficient resulting in the introduction or deletion of nucleotides, which result in a frameshift and loss of protein expression.

Because the majority of mitochondrial targeted proteins are directed to the matrix by an N-terminal mitochondrial targeting signal, disruption of the gene encoding this region can result in a lack of protein being able to localise correctly (Stroud et al, 2013) and/or block protein synthesis altogether. The work presented here solidifies the role of FOXRED1 in Complex I assembly by analysing the consequences of protein loss as well as investigating the behaviour of FOXRED1 *in vivo*.

3.2 A TALEN pair targeting the *FOXRED1* gene can result in disruption

In order to generate a HEK293T cell line that lacks FOXRED1, a TALEN pair was designed to target the initiating methionine of the gene (Fig. 3.1A). TALENs were constructed by the FLASH assembly method described by Reyon et al (2012). Following transfection and single cell sorting, clonal populations were subjected to screening by impaired growth in galactose-containing DMEM (gal-DMEM). When galactose is used in place of glucose, cells with a defect in a oxidative phosphorylation are not able to proliferate and so this was used as an initial screen to identify cells that may be deficient in Complex I (Robinson et al, 1992). Clones that were observed to have a growth phenotype on gal-DMEM were then grown and digitonin-solubilised cell extracts were subjected to BN-PAGE and western blotting to determine the presence or absence of respiratory super-complexes, of which Complex I is a component. Analysis revealed that three clones (A6, C9 and H2) lacked respiratory super-complexes when immunodecorated for the Complex I subunit NDUFA9, suggesting these clonal populations do not contain an active OXPHOS system (Fig. 3.1B, upper panel). Immunoblotting for the outer membrane protein VDAC1 confirmed equal loading of samples (Fig. 3.1B, lower panel).

To determine the nature of the genome modification, two clones were selected for further genomic analysis (A6 henceforth known as Δ FOXRED1 and C9 henceforth known as Δ FOXRED1^{C2}).

Following genomic DNA extraction, the genomic region encompassing the TALEN binding site was amplified and sub-cloned to isolate individual alleles prior to Sanger sequencing. The Δ FOXRED1 cell line returned two different alleles, one harbouring a 16 base-pair deletion and the other with a 17 base-pair deletion. The Δ FOXRED1^{C2} cell line was found to contain 6 and 15 base-pair deletions, in all cases removing the initiating methionine (Fig. 3.1C). These results indicate that successful gene disruption of the FOXRED1 gene was performed through TALEN mediated gene-disruption technology.

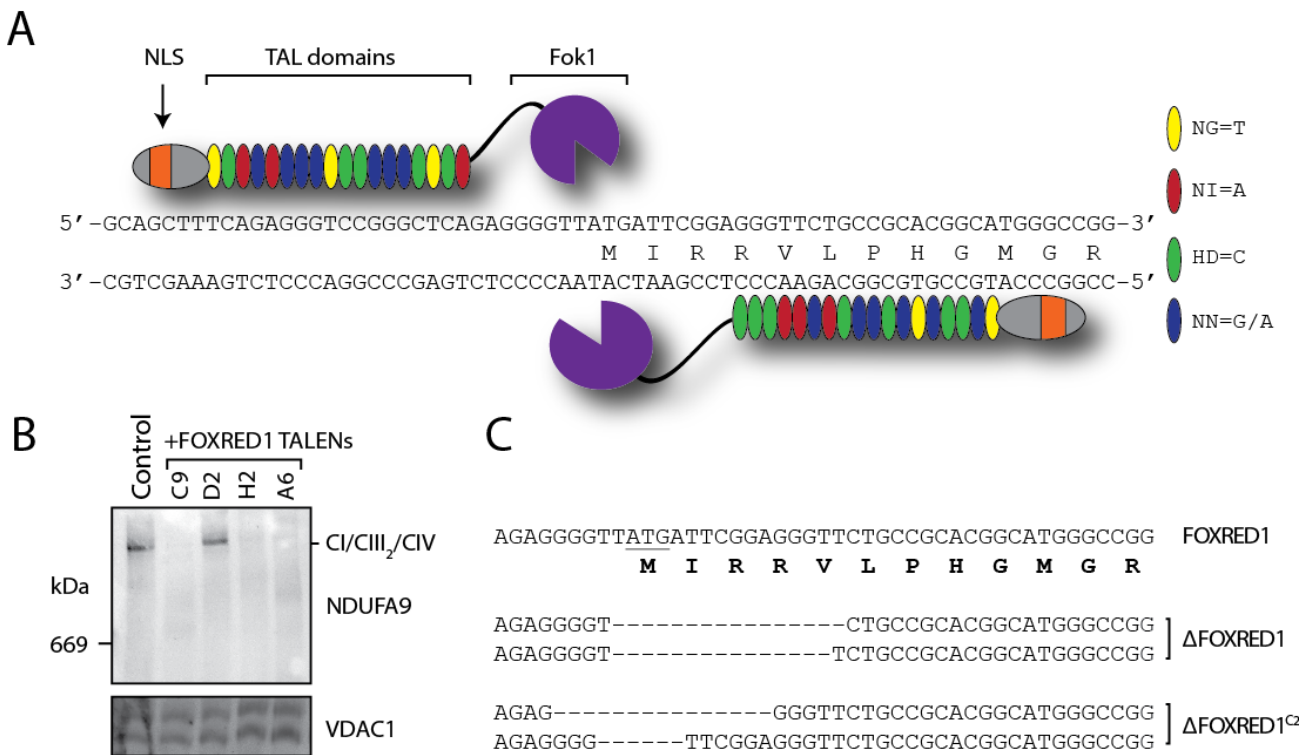


Figure 3.1: TALEN design, screening and validation of a Δ FOXRED1 cell line. (A) Schematic representation of the TALEN binding site. The TALEN is composed of an N-terminal domain containing the nuclear localisation sequence (NLS), the repeated arrays of TAL domains and a non-specific FokI endonuclease. TALENs bind upstream and downstream of the region of interest. The TAL domain colour indicates specificity for a particular nucleotide in the genomic DNA. (B) BN-PAGE analysis of putative Δ FOXRED1 clones following solubilisation in 1% (w/v) digitonin. Immunoblotting for the Complex I subunit NDUFA9 was used to determine the presence or absence of respiratory super-complexes. Immunoblotting for VDAC1 served as a loading control. (C) Nucleotide sequence spanning the TALEN-targeted region in the *FOXRED1* gene present in the first coding exon. Sequence analyses of corresponding alleles in Δ FOXRED1 and Δ FOXRED1^{C2} cells indicate a deletion of 6-16 nucleotides encompassing the initiation codon.

3.3 Δ FOXRED1 cells harbour a specific Complex I defect

To investigate the effect of the loss FOXRED1 on components of the OXPHOS system, BN-PAGE, in-gel activity (IGA) assay and immunoblotting were employed. Following mitochondrial isolation and BN-PAGE analysis Complex I activity was assayed (Fig. 3.2A-CI IGA). In-gel activity of Complex I was observed in control cells when solubilised in either digitonin or Triton X (TX)-100 that dissociates super-complexes into the respective holo-enzymes (Fig. 3.2A, lanes 1 and 3), but was absent in Δ FOXRED1 mitochondria (Fig. 3.2A, lanes 2 and 4). Analysis of other respiratory complexes (CII, CIII and CIV) revealed that the loss of FOXRED1 does not impact the levels of CII and CIII, however, an increase in assembled CIV was observed (Fig. 3.2A, lane 16). Furthermore, the loss of FOXRED1 resulted in an inability of respiratory complexes CIII and CIV to assemble into super-complexes due to the loss of Complex I (Fig. 3.2A, compare lanes 9 and 13 to lanes 10 and 14 respectively). Analysis of mitochondria isolated from control, Δ FOXRED1 and Δ FOXRED1^{C2} cells revealed a strong Complex I defect with reduced NDUFA9 and NDUF55 in respiratory super-complexes (Fig. 3.2B; compare lane 1 with lanes 2 and 3, and lane 7 with 8 and 9) and also a strong reduction in the levels of holo-Complex I (Fig. 3.2B; compare lane 4 with lanes 5 and 6, and lane 10 with 11 and 12). Interestingly, digitonin-solubilised Δ FOXRED1 and Δ FOXRED1^{C2} mitochondria accumulate a number of NDUF55-containing sub-complexes (Fig. 3.2B, lanes 8 and 9), similar to what is observed in mitochondria isolated from FOXRED1 patient fibroblasts (Formosa et al, 2015). Analysis of other Complex I subunits (NDUFS2, NDUFS3 and NDUF6) also showed a strong Complex I defect indicating a specific role of FOXRED1 in the biogenesis of Complex I (Fig. 3.2C). To determine the extent of Complex I decrease relative to the control cells, densitometry measurements of the Complex I subunit NDUF55 immuno-signal from BN-PAGE were made. Quantitation of NDUF55 signal from Δ FOXRED1 mitochondria revealed that ~7% of super-complex and ~10% of holo-Complex I remained (Fig. 3.2D).

To analyse the steady state levels of proteins in the mitochondria of Δ FOXRED1 cells, SDS-PAGE and immunoblotting were used. Immunoblotting for the N-module subunit NDUFV2 and the Q-module subunits NDUFS2 and NDUFS3 showed a strong decrease in the levels relative to control mitochondria, while NDUFA9 showed a modest decrease relative to the control (Fig. 3.2E-upper panels). The intermembrane space subunit NDUF55 and the membrane arm subunit NDUF6 appeared to be largely unchanged relative to the control mitochondria (Fig. 3.2E-upper panels). Also, analysis of a selection of other Complex I assembly factors (NDUFAF1, NDUFAF2, NDUFAF4, Ecsit and ACAD9) were unchanged, suggesting that the loss of FOXRED1 does not alter the other assembly machinery and is sufficient for Complex I deficiency (Fig. 3.2E-middle panels).

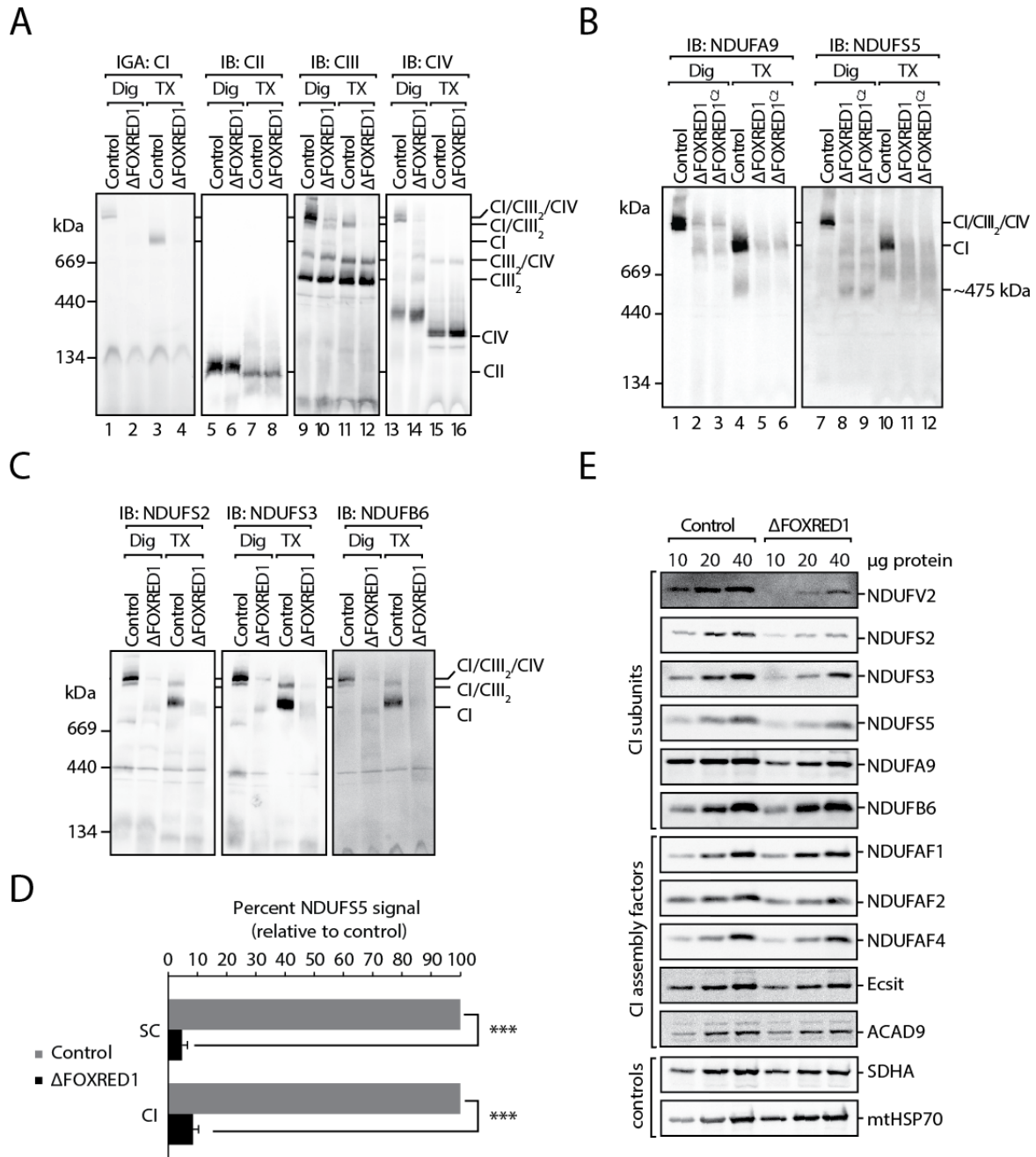


Figure 3.2: Δ FOXRED1 cells have a severe Complex I deficiency. (A) Mitochondria from control and Δ FOXRED1 cells were subjected to BN-PAGE followed by an in-gel activity assay (IGA) for Complex I or western blot analysis using antibodies for Complexes II (SDHA), III (Core I) and IV (COXIV). (B) Mitochondria isolated from control, Δ FOXRED1 and Δ FOXRED1^{C2} clones were solubilised in Digitonin (Dig) or Triton X-100 (TX) before BN-PAGE followed by immunodecoration with the antibodies against Complex I subunits NDUF9 and NDUF55. (C) Mitochondria isolated from control and Δ FOXRED1 cells were subjected to BN-PAGE as in (B) followed by immunodecoration with the antibodies against Complex I subunits NDUF52, NDUF53 and NDUFB6. (D) Densitometry analysis of NDUF55 assembled into super-complex (SC) or holo-Complex I (CI) relative to the control (n=3, mean \pm SEM; paired two-tailed student t-test *** p<0.005). (E) Mitochondria from control and Δ FOXRED1 cells (10-40 μ g protein) were subjected to SDS-PAGE and western blot analysis using antibodies against Complex I subunits, assembly factors and control proteins, as indicated.

3.4 The ~815 kDa intermediate is still produced in the Δ FOXRED1 cell line

The biogenesis of Complex I requires the coordinated assembly of subunits from two distinct genomes. In order to determine the effect of the loss of FOXRED1 on translation of mtDNA encoded subunits, pulse-chase analysis using [35 S]-Methionine/Cysteine was performed according to Formosa et al (2016). Following chloramphenicol treatment for 15 hours, control and Δ FOXRED1 cells were treated with the reversible cytosolic ribosome inhibitor anisomycin for 2 hours in the presence of [35 S]-Methionine/Cysteine to specifically label mtDNA encoded proteins. Following pulse labelling, a chase was performed for 0, 3 and 24 hours to determine how the loss of FOXRED1 may affect translation, assembly and stability of these proteins.

Analysis of isolated mitochondria by BN-PAGE revealed that while mtDNA encoded subunits could assemble into mature Complex I in control cells, Δ FOXRED1 cells were unable to do so (Fig. 3.3A). Interestingly, mtDNA-encoded subunit from both control and Δ FOXRED1 cells could assemble into an ~815 kDa intermediate (CI*) that in control cells matures to the holo-complex, but falls apart in the absence of FOXRED1 (Fig. 3.3A). Analysis of the mtDNA-encoded proteins by SDS-PAGE suggested that the translation and stability of the proteins was similar to control during the chase period (Fig. 3.3B). These data suggest that FOXRED1 may not perform a direct role in the translation or stability of mtDNA encoded subunits, but is crucial in the latter assembly stages for the maturation of the ~815 kDa intermediate into fully-assembled Complex I.

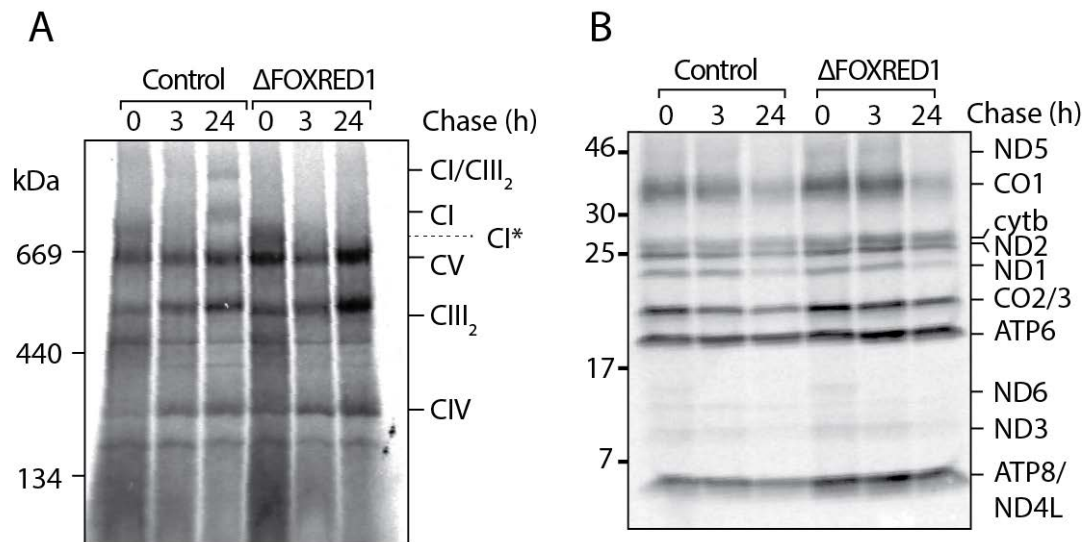


Figure 3.3: Δ FOXRED1 cells do not have an mtDNA translation defect. Control and Δ FOXRED1 cells were subjected to [35 S]-Methionine/Cysteine radiolabelling of mtDNA-encoded proteins and pulse-chase analysis. **(A)** BN-PAGE analysis followed by radiography of samples indicating the assembly of mature CI, CIII₂, CIV and CV and the ~815 kDa Complex I intermediate (CI*). **(B)** SDS-PAGE analysis followed by radiography indicating the translation of the mtDNA encoded subunits.

3.5 Global proteomic analysis of Δ FOXRED1 cells suggests an isolated Complex I deficiency

To determine the overall effect of the loss of FOXRED1 on the mito-proteome, quantitative proteomic studies using SILAC (stable isotope labelling of amino acids in cell culture) was undertaken. Because the individual cell lines are differentially labelled with either heavy or light amino acids, the samples can be mixed and analysed simultaneously, allowing for a direct comparison between two sample populations (Hoedt et al, 2014).

Analysis of the proteomic data revealed a strong Complex I defect, in agreement with western blot analysis of the Δ FOXRED1 cell line. Interestingly, the N-module subunits NDUFV1, NDUFV2, NDUFV3, NDUFS1, NDUFS4, NDUFS6 and NDUFA12 were strongly decreased 1.5 to 4 fold to that of control mitochondria, suggesting that the loss of FOXRED1 results in a strong defect in this module (Fig. 3.4A, red circles). Other subunits that associate with the Q- or P-module of Complex I were also decreased (NDUFA2, NDUFA7, NDUFA9 and NDUFA11, as well as NDUFB7, NDUFB8 and NDUFB9). Of the mitochondrial-encoded subunits, mt-ND5 had a 1.5 fold decrease, indicating that the mtDNA encoded subunits were less affected. A number of non-OXPHOS related proteins were also decreased in the absence of FOXRED1, however the decrease, while significant was to a lesser extent than Complex I subunits with less than a two-fold decrease in all cases (Fig. 3.4B, orange circles).

Interestingly, subunits of Complex IV (mt-CO2, mt-CO3, COX5B, COX6C, COX7A2, COX7A2L, COX15 and NDUFA4) were increased relative to the control (Fig. 3.4A. green circles). Other proteins that were upregulated included those in amino acid (PYCR1 and GPT2) and phosphoenol pyruvate (PCK2) metabolism, RNA binding or metabolism (MACROD1, C14ORF166 and CHCHD2). Other proteins not thought to be directly involved in OXPHOS processes (Fig. 3.4B, blue circles) that were significantly increased included redox and ROS related proteins, proteins involved in protein or metabolite transport, as well as proteins involved in signalling, apoptosis or cristae organisation. How these proteins are related to the loss of FOXRED1 remains to be determined.

In conclusion, proteomic analysis of mitochondria from Δ FOXRED1 cells suggest that the loss of FOXRED1 results in an isolated Complex I deficiency.

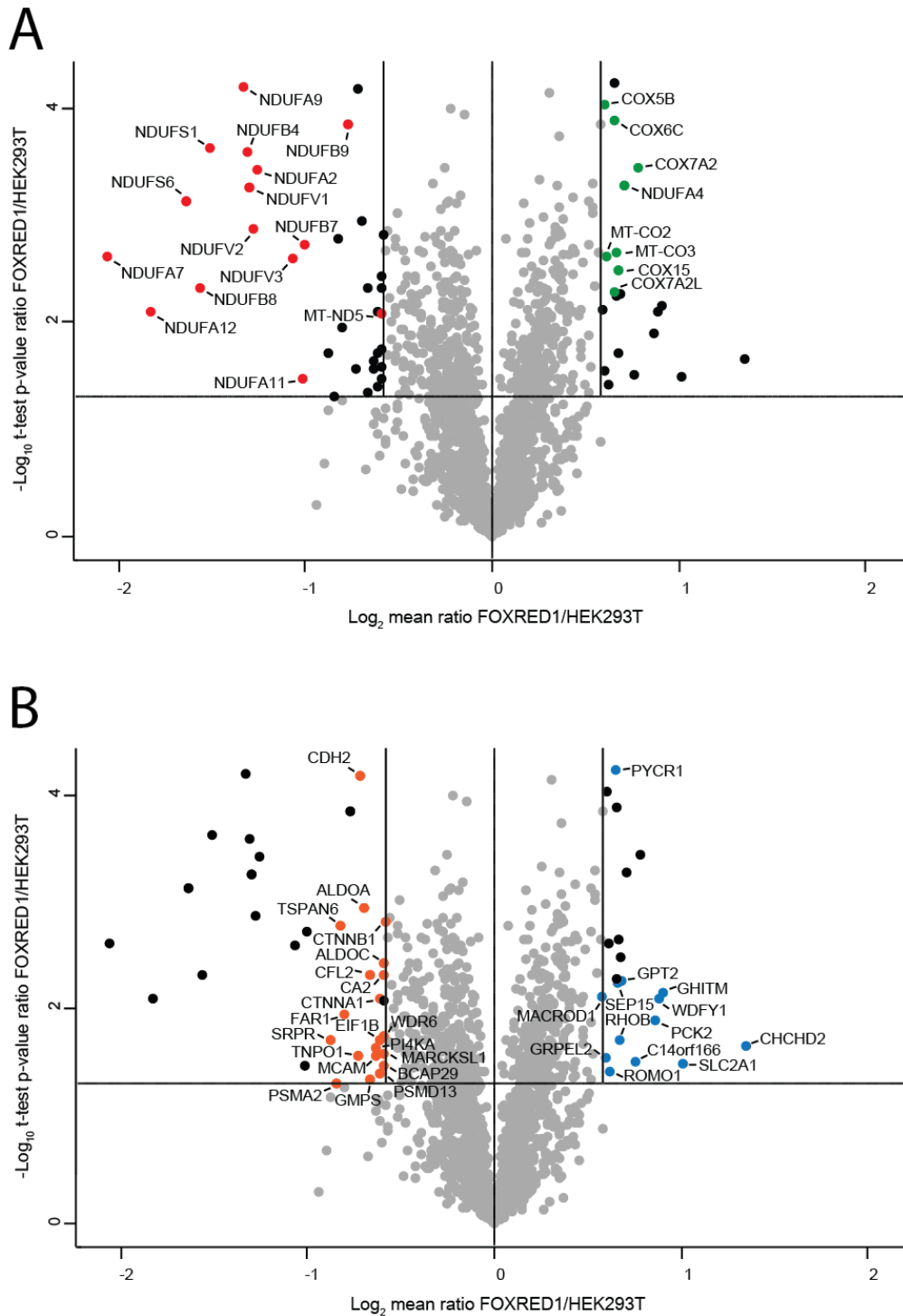


Figure 3.4: Global proteomic analysis reveals a specific loss of Complex I subunits.

Mitochondria from control and Δ FOXRED1 were subject to SILAC proteomic analysis to determine global changes in the proteome. Volcano plots showing global proteomic changes in Δ FOXRED1 vs control cells. Each circle represents one protein. The \log_2 fold change of SILAC pairs is indicated on the x-axis, with solid vertical lines indicating a 1.5-fold increase/decrease. The \log_{10} of the p value is shown on the y-axis, with the solid horizontal line indicating a p-value of 0.05. **(A)** Indicated circles highlighting the increase (green) or decrease (red) of OXPHOS related proteins **(B)** Indicated circles highlighting the increase (blue) or decrease (orange) of non-OXPHOS proteins.

3.6 Δ FOXRED1 cells have a reduced respiratory capacity

In order to investigate the effect of the loss of FOXRED1 on respiration, analysis of oxygen consumption rates (OCR) and extracellular acidification rate (ECAR) were performed using a Seahorse analyser, performed with the kind assistance of Dr Ann Frazier (Murdoch Children's Research Institute). Analysis of the OCR in Δ FOXRED1 cells revealed a reduced basal respiration rate, a reduced oligomycin-sensitive respiration rate due to membrane proton leak and a reduced maximal respiration rate relative to control cells (Fig. 3.5A). In the presence of the drugs rotenone and antimycin A, which inhibit Complexes I and III respectively, oxygen consumption was comparable, indicating no significant difference in non-mitochondrial oxygen consumption (Fig. 3.5A). In addition, the oxygen consumption rates of both Δ FOXRED1 and Δ FOXRED1^{C2} cell lines were indistinguishable (Fig. 3.5B). The basal ECAR/OCR ratio was greater in Δ FOXRED1 cells, indicating an increased reliance on glycolysis for energy production in this cell line (Fig. 3.5C).

To determine the enzyme activity of respiratory chain complexes, spectrophotometric enzyme activity analysis was performed by Ms Tegan Stait (Murdoch Children's Research Institute). Enzyme activity analysis revealed a strong reduction in Complex I activity (13% and 11% of the control levels for Δ FOXRED1 and Δ FOXRED1^{C2} respectively), while Complexes II and III were unchanged. Interestingly, there appeared to be a large increase in isolated CIV activity in both Δ FOXRED1 and Δ FOXRED1^{C2} cell lines (Fig. 3.5D). In addition, both Δ FOXRED1 clones were unable to grow on media containing galactose as opposed to glucose with ~80% cell death by Trypan blue staining observed after 72h, again suggesting the absence of FOXRED1 results in a deficiency in oxidative phosphorylation in the cells (Fig. 3.5E). From these data it can be concluded that while FOXRED1 is not essential for assembly *per se*, it is nevertheless critical for ensuring efficient Complex I assembly to levels that sustain oxidative phosphorylation.

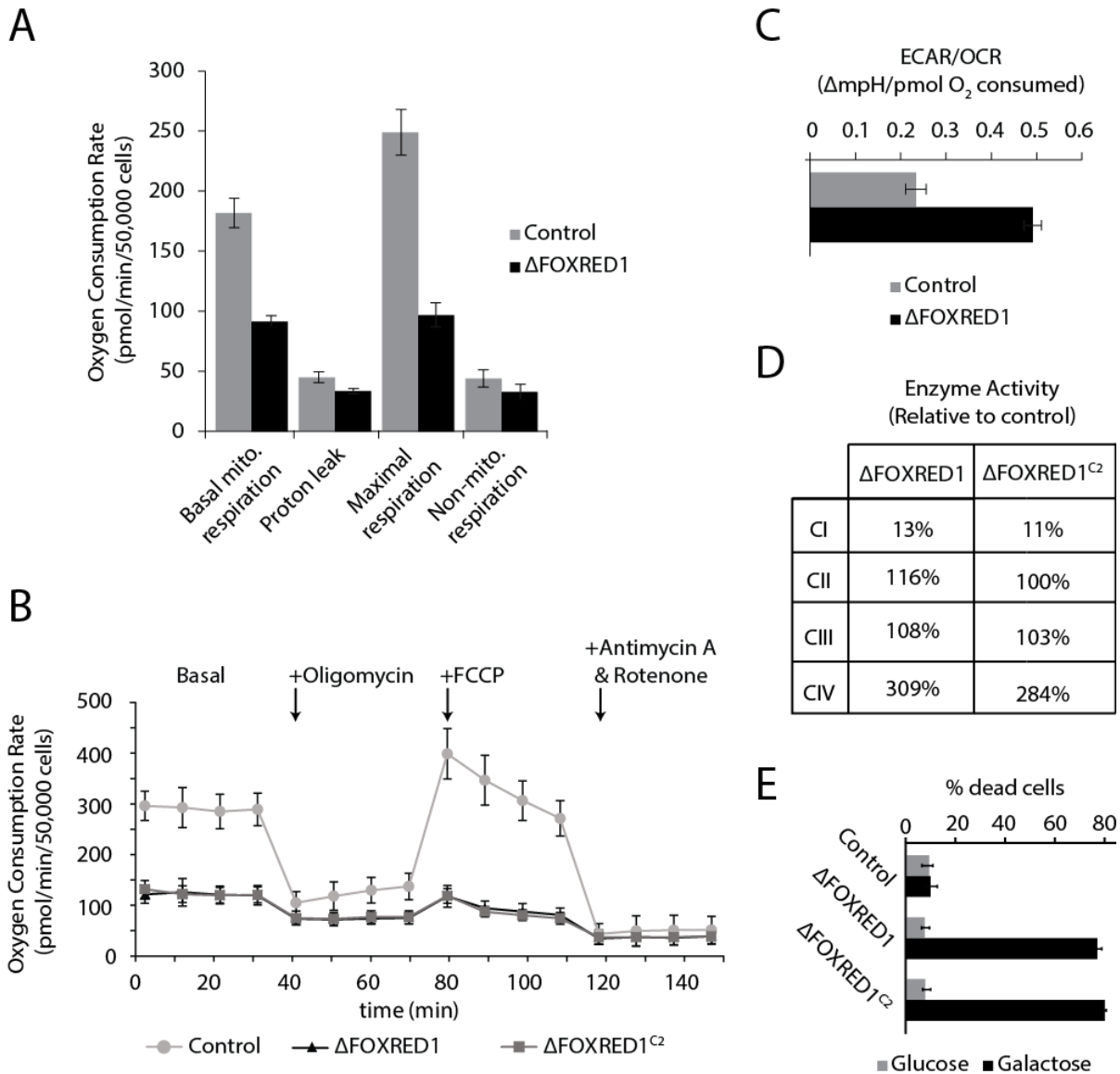


Figure 3.5: ΔFOXRED1 cells have a strong respiratory defect. (A) The oxygen consumption rate of control and ΔFOXRED1 cells was measured over a 170 min period. The addition of oligomycin was used to measure proton leak, while the maximal respiration was measured by addition of the membrane potential uncoupler FCCP. Non-mitochondrial respiration was measured by addition of rotenone and antimycin A, which inhibit CI and CIII, respectively. n=3, SEM. **(B)** Representative traces of oxygen consumption rates for control, ΔFOXRED1 and ΔFOXRED1^{c2} cells as described in (A). Error bars represent the SEM of 6-7 replicates/sample **(C)** Measurement of the basal ECAR: basal OCR ratio for control and ΔFOXRED1 cells. (n=3, SEM). **(D)** Enzyme activity measurements of ΔFOXRED1 and ΔFOXRED1^{c2} relative to control, normalised to Citrate Synthase. Data presented as the average percentage of 6-7 replicates per sample. **(E)** Control and ΔFOXRED1 clones were plated on glucose or galactose containing media, incubated for 72h and analysed for cell viability by trypan blue staining (>300 cells/assay; n=3, SD).

3.7 Complementation analysis of Δ FOXRED1 cells

Rescue studies were undertaken in order to confirm that the loss of Complex I in Δ FOXRED1 cells was due to a lack of FOXRED1 protein. Transient expression of FOXRED1 fused to either a FLAG epitope tag or GFP (both at the C-terminal end) was able to rescue the defect in Complex I assembly (Fig. 3.6A, BN-PAGE). In addition, no defects in Complex I assembly were seen following FOXRED1 overexpression in control HEK293T cells. Ectopic expression of FOXRED1^{FLAG} and FOXRED1^{GFP} was confirmed by SDS-PAGE and immunoblotting for the FLAG epitope and GFP protein respectively, while Tom20 served as a loading control (Fig. 3.6A, SDS-PAGE)

Two separate missense mutations have been reported in FOXRED1 that lead to Complex I deficiency – p.R352W (Fassone et al, 2010) and p.N430S (Calvo et al, 2010). Each mutation disrupts a highly conserved residue (Fig. 3.6B). Interestingly, overexpression of either FOXRED1^{R352W} or FOXRED1^{N430S} was able to rescue Complex I assembly in Δ FOXRED1 cells (Fig. 3.6C, upper panel). Analysis by SDS-PAGE and western blotting using anti-FLAG antibodies confirmed similar expression of FOXRED1 forms (Fig. 3.6C, lower panel). Transfected cells were also able to efficiently grow on galactose-containing media, indicating that mitochondrial respiration was restored (data not shown). These results suggest that the mutations are hypomorphic in nature.

In order to search for key residues involved in FOXRED1 function, site directed mutagenesis was performed. Mutagenesis was carried out on a subset of highly conserved tyrosine residues to investigate their role in FOXRED1 function and possible FAD binding. Tyrosine, cysteine and histidine residues are capable of being covalently flavinated, while tyrosine and phenylalanine are also capable of non-covalent stabilisation of FAD through interactions with the phenyl moiety and the isoalloxazine ring system (Ma & Ito, 2002; Mewies et al, 1998; Zhou et al, 1998). Residues Y327, Y349 and Y359 were chosen based on high conservation within FOXRED1 of different species. Also, the predicted structural similarity of FOXRED1 with sarcosine oxidase (MSOX) (Fassone et al, 2010) led us to select residues Y410 and Y411, as these two tyrosine residues align closely with the residue C316, the site of covalent attachment of FAD in MSOX (Trickey et al, 1999). While mutations in residues Y327, Y349, Y410 and Y411 to either phenylalanine or alanine were able to restore Complex I levels to that of wild-type cells, the mutation Y359A was not (Fig. 3.6D, lane 9). As the Y359F mutation was still functional (Fig. 3.6D, lane 8), it suggests that the phenyl moiety at position 359 is critical for the function of FOXRED1 in the biogenesis of Complex I. Equal levels of expression were confirmed by SDS-PAGE and western blot analysis (Fig. 3.6D, bottom panel).

To determine the nature of the FOXRED1^{Y359A} mutant, it was expressed in wild-type cells to investigate if it functions in a dominant-negative manner, hindering Complex I assembly or inactivating the wildtype FOXRED1 protein. Ectopic expression of FOXRED1^{Y359A} did not have an effect on Complex I assembly in control cells, while also not being able to restore levels of Complex I in Δ FOXRED1 cells as expected (Fig. 3.6E, upper panel). Equal expression of FOXRED1 was confirmed by SDS-PAGE using anti-FLAG antibodies, while Tom20 was used as a loading control (Fig. 3.6E, lower panels).

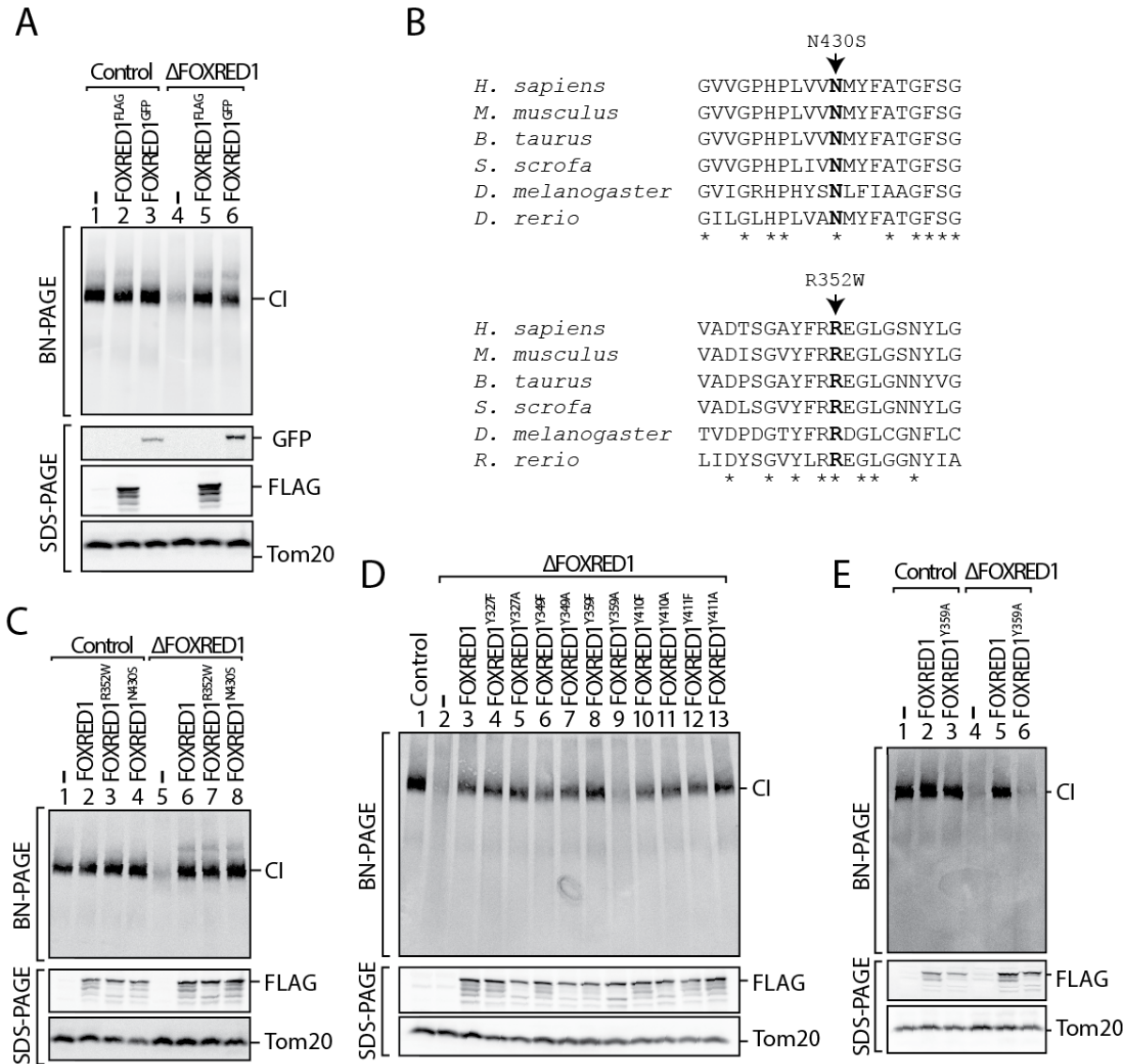


Figure 3.6: Complementation of Δ FOXRED1 can restore Complex I assembly (A) Control or Δ FOXRED1 cells expressing FOXRED1^{FLAG} or FOXRED1^{GFP} were subjected to BN-PAGE and immunoblotting with NDUFA9 antibodies to detect Complex I. SDS-PAGE analysis and western blotting using FLAG and GFP antibodies was used to confirm expression of the fusion proteins. Tom20 was used as a loading control. (B) Partial sequence alignment of FOXRED1 from various species. The position of the patient mutations p.R352W and p.N430S is indicated. (C) Mitochondria isolated from control or Δ FOXRED1 cells transiently expressing FLAG-tagged FOXRED1 or patient mutations, p.R352W and p.N430S were subjected to BN-PAGE and immunoblot analysis for Complex I (NDUFA9; top panel). Expression was confirmed using SDS-PAGE and immunoblot analysis with FLAG antibodies, while Tom20 was used as a loading control. (D & E) Mitochondria isolated from control or Δ FOXRED1 cells transiently expressing FLAG-tagged FOXRED1 variants were subjected to BN- and SDS-PAGE and immunoblot analysis as described in (C).

3.8 FOXRED1 may not associate with the ~815 kDa subcomplex

It was observed that in cells lacking FOXRED1, a late stage ~815 kDa Complex I intermediate was visible after 2 hours of pulse labelling (Fig. 3.3A). Because this intermediate further matures into complete Complex I (Lazarou et al, 2007), it was hypothesised that FOXRED1 may function to stabilise this intermediate allowing proper assembly to occur. Indeed, the Complex I assembly factor B17.2L is known to associate with this complex and functions in a late state of Complex I biogenesis (Lazarou et al, 2007; Ogilvie et al, 2005) While B17.2L does not form stable complexes in control fibroblasts, analysis of patient fibroblasts that lack the subunit NDUFS4 identified the accumulation of the ~815 kDa intermediate harbouring B17.2L (Lazarou et al, 2007; Ogilvie et al, 2005). This suggests that B17.2L may function late in the assembly pathway, and the same may therefore apply to FOXRED1.

To investigate this, control or Δ NDUFS4 HEK293T cells (prepared by Dr David Stroud, unpublished) were transiently transfected with FOXRED1 or FOXRED1^{Y359A} to determine if the exogenous protein could form any complexes detectable by BN-PAGE. Analysis of isolated mitochondria solubilised in TX-100 followed by BN-PAGE and immunoblotting for the Complex I subunit NDUFS5 revealed that Δ NDUFS4 harboured an ~815 kDa intermediate (denoted CI*; Fig. 3.7A, upper panel). Mitochondria subjected to SDS-PAGE and immunoblotting for FLAG confirmed expression of the exogenous protein and Tom20 was used as a loading control (Fig. 3.7A, lower panels). To determine if FOXRED1 was associated with this intermediate, mitochondria were solubilised in the mild detergent 1% (w/v) digitonin and analysed by BN-PAGE to maintain any transient interactions present and immunoblotted for the FLAG epitope. Under these mild conditions, no complexes containing FOXRED1-FLAG or FOXRED1^{Y359A}-FLAG in either control or Δ NDUFS4 mitochondria were observed (Fig. 3.7B). Rather, FOXRED1-FLAG was observed to migrate in an unassembled form. To eliminate the possibility that the FLAG epitope was being obscured during one dimensional BN-PAGE, two dimensional BN/SDS-PAGE was performed. Immunoblotting for the FLAG epitope failed to identify any complexes containing the FOXRED1-FLAG protein (Fig. 3.7C). Immunodetection of the NDUFS5 subunit was used as a control to identify the CI*/CIII₂/CIV complex (Fig. 3.7C). These data suggest that FOXRED1 may not associate with the ~815 kDa intermediate that can be resolved by BN-PAGE analysis.

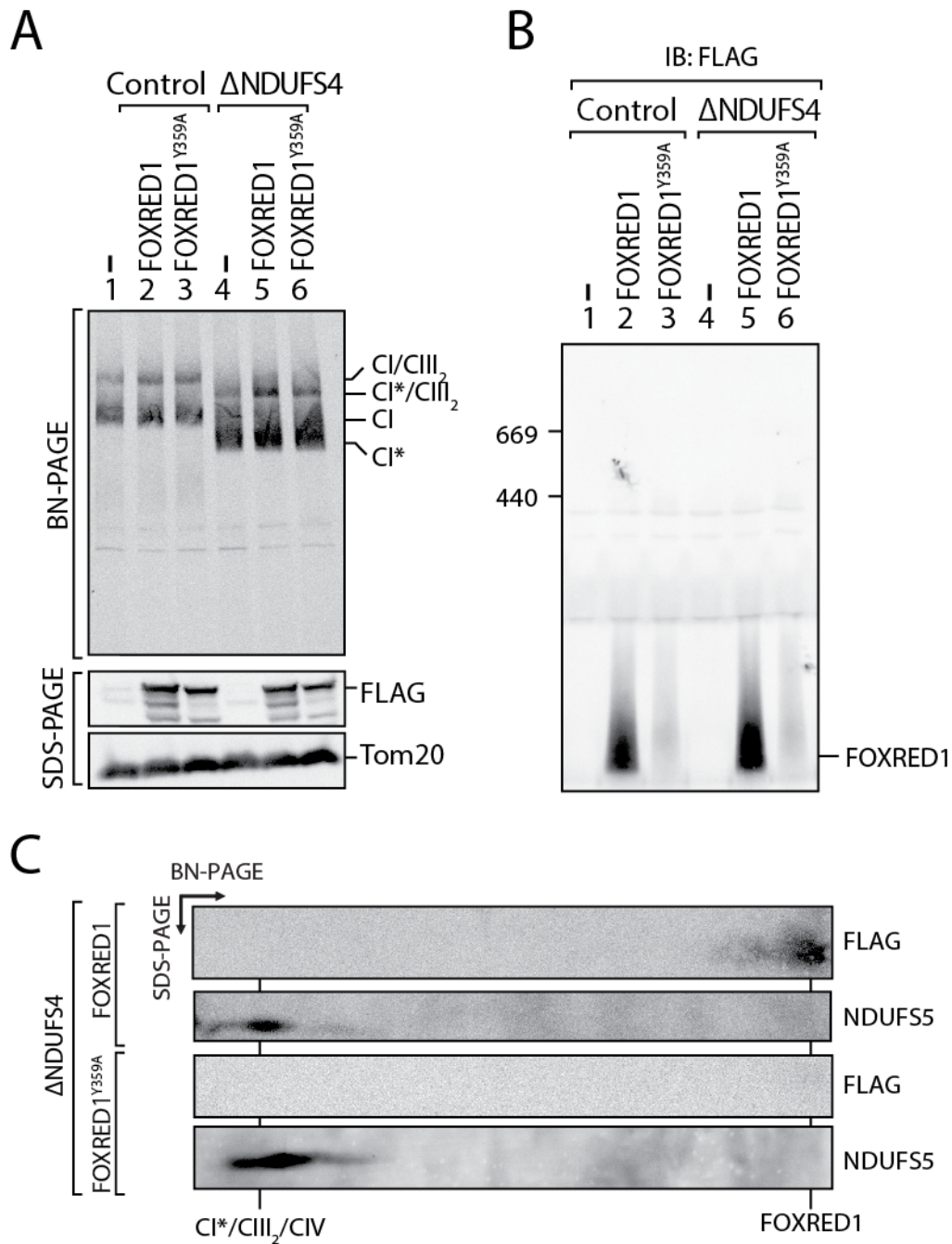


Figure 3.7: FOXRED1 may not form stable complexes observable by BN-PAGE. (A) Control or Δ NDUFS4 cells expressing FOXRED1 or FOXRED1^{Y359A} were subjected to 1% (v/v) TX-100 solubilisation, BN-PAGE and immunoblotting with NDUFS5 antibodies to detect Complex I (CI) or the ~815 kDa intermediate (CI*). SDS-PAGE analysis and western blotting using FLAG antibodies was used to confirm expression of the fusion proteins. Tom20 was used as a loading control. **(B)** Control or Δ NDUFS4 cells expressing FOXRED1 or FOXRED1^{Y359A} were subjected to 1% (v/v) Digitonin solubilisation, BN-PAGE and immunoblotting with FLAG antibodies. **(C)** Following BN-PAGE as shown in (B), Δ NDUFS4 cells expressing FOXRED1 or FOXRED1^{Y359A} were subjected to second dimension SDS-PAGE and immunoblotted using FLAG or NDUFS5 antibodies. The CI*/CIII₂/CIV complex is indicated.

3.9 FOXRED1 can associate with a subset of Complex I subunits

Given the lack of specific antibodies for FOXRED1, it was not possible to determine whether the endogenous protein forms stable complexes. Furthermore, following ectopic expression of epitope-tagged FOXRED1 in control, Δ FOXRED1 or Δ NDUFS4 cells, specific FOXRED1 containing complexes were not detected by BN-PAGE. FOXRED1 may therefore transiently or loosely associate with Complex I intermediates that are refractory to BN-PAGE.

To investigate FOXRED1 interactions, co-immunoprecipitation analysis of FOXRED1-FLAG expressed in Δ FOXRED1 cells was performed. In this case, stable-isotope labelling of cells (SILAC) (Oeljeklaus et al, 2014; Ong et al, 2002) and subsequent quantitative mass spectrometry of eluted proteins was employed. To correct for potential bias due reduced levels of Complex I subunits in Δ FOXRED1 mitochondria (Fig. 3.2E), FOXRED1 lacking the C-terminal FLAG epitope was also expressed in Δ FOXRED1 cells (see Fig. 3.8A for more details). In addition to this, co-immunoprecipitation analysis of the inactive FOXRED1^{Y359A}-FLAG mutant was also performed in the same manner to determine proteins specifically bound to the functional FOXRED1 (Fig. 3.8A). As can be seen (Fig. 3.8B and Fig. 3.8C), FOXRED1, but not the mutant FOXRED1^{Y359A}, co-immunoprecipitated with a number of Complex I subunits including NDUFB10, NDUFS5, NDUFA10, NDUFA8, NDUFS3 and NDUFA5. The potential association of FOXRED1 with components of the import machinery (e.g. Tom20, Tom22, MPP) and chaperones (e.g. mtHsp70, Hsp60/10) may be related to the biogenesis of FOXRED1 due to its ectopic expression. Importantly, specific association with subunits of the other respiratory chain complexes was not observed, indicating that the interactions are specific and are likely to occur at stages in assembly prior to assembly of Complex I intermediates into super-complexes (Moreno-Lastres et al, 2012).

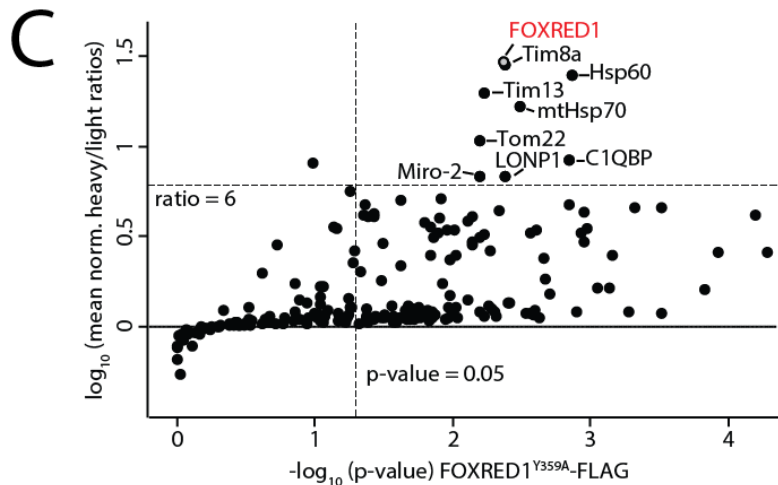
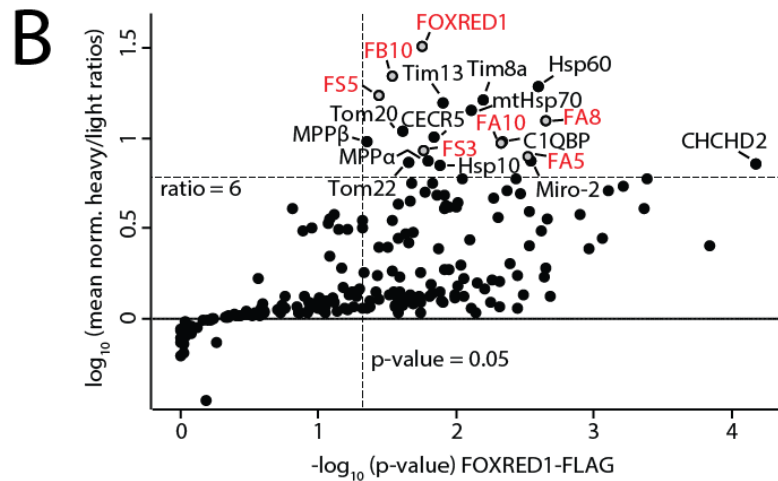
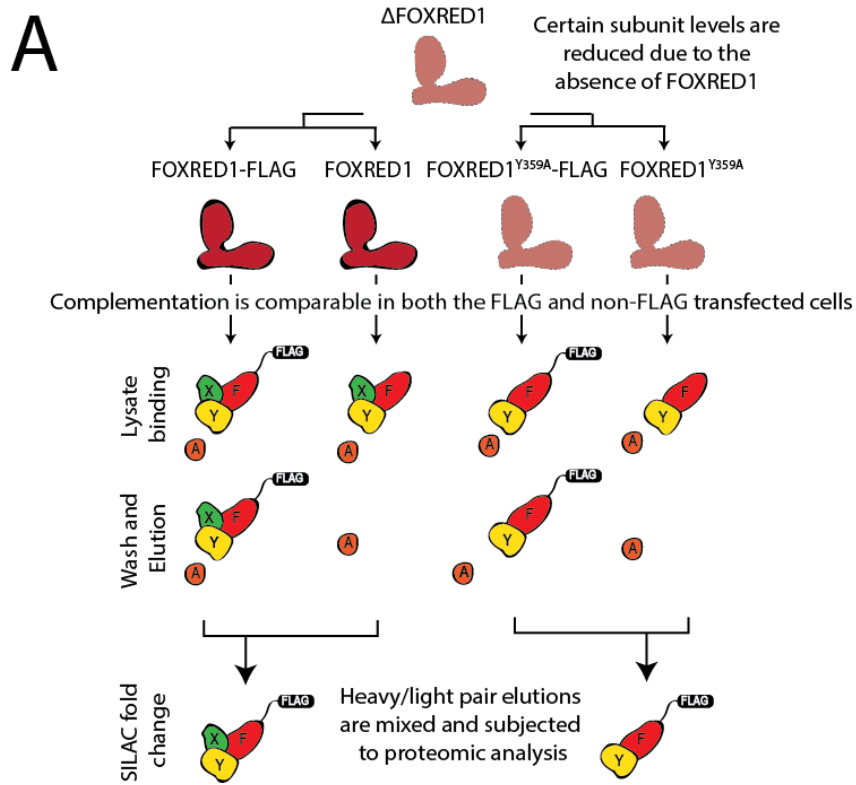


Figure 3.8: Figure legend on the following page

Figure 3.8: FOXRED1-FLAG co-immunoprecipitates with a subset of Complex I subunits.

(A) Schematic representation of FOXRED1 co-immunoprecipitation approach. Δ FOXRED1 cells were transfected with a construct encoding wild-type or inactive mutant p.Y359A FOXRED1, with and without a FLAG tag. Expression of FOXRED1 is able to restore levels of Complex I subunits in both the tagged and untagged samples. FOXRED1 (denoted 'F') is able to bind to interacting partners (X represents an interacting protein while Y represents a protein required for import or biogenesis) while contaminating proteins (A) bind non-specifically to the resin in all cases. Upon washing and elution, FOXRED1 containing complexes are enriched in FLAG-tagged elutions while contaminating proteins elute in all samples. Following SILAC analysis, contaminating proteins are removed, while true FOXRED1-binding proteins are enriched. **(B)** Mitochondria from heavy or light amino-acid labelled Δ FOXRED1 cells expressing FOXRED1 or FOXRED1^{FLAG} were subjected to immunoprecipitation with anti-FLAG beads. Elutions were mixed and analysed by LC-MS. The means of normalised heavy/light ratios (\log_{10}), identified in at least two replicates (including a label switch; N=4) were plotted against their p-values ($-\log_{10}$). Thresholds were set at p-values < 0.05 and mean heavy/light enrichment ratios > 6 . For simplicity, only *bona fide* mitochondrial proteins present in the MitoCarta dataset are shown, Complex I subunits are abbreviated indicated in red and commonly used protein names are substituted for gene names (Hsp10, *HSPE1*; Hsp60, *HSPD1*; mt-Hsp70, *HSPA9*; Miro-2, *RHOT2*; MPP α , *PMPCA*; MPP β , *PMPCB*; Tim8a, *TIMM8A*; Tim13, *TIMM13*; Tom20, *TOMM20*; Tom22, *TOMM22*). **(C)** Mitochondria from heavy or light amino-acid labelled HEK293T cells expressing FOXRED1^{Y359A} or FLAG-tagged FOXRED1^{Y359A} were subjected to anti-FLAG immunoprecipitation and analysis performed as in B.

3.10 Discussion

3.10.1 Loss of FOXRED1 leads to impaired Complex I assembly and the presence of a crippled subassembly

While it has been established that FOXRED1 is involved in Complex I biogenesis (Pagliarini et al, 2008) and mutations in its gene cause mitochondrial disease related to Complex I deficiency (Calvo et al, 2010; Fassone et al, 2010), little information is available regarding its functional role. In this chapter, it was found that loss of FOXRED1 leads to defects in the latter stages of Complex I assembly, resulting in the accumulation of a crippled ~475 kDa sub-complex that contains the Complex I subunit NDUFS5. Furthermore, quantitative proteomic analysis also suggested that most of the reduced subunits were those of the NADH-dehydrogenase module, resulting in the crippled sub-complex observed. The observed ~475 kDa sub-complex represents a non-productive breakdown of a stalled assembly intermediate. Pulse chase assembly analysis indicated that at early time points, Δ FOXRED1 mitochondria (as well as FOXRED1-deficient patient fibroblasts) could form a late stage ~815 kDa Complex I intermediate, but this was unproductive, as mature Complex I could not be observed. The reason for such instability of the ~815 kDa intermediate is not clear, but similar observations have been seen in cells lacking the NDUFA9 subunit (Δ NDUFA9) that sits at the interface between the matrix and membrane arms of Complex I (Stroud et al, 2013). Indeed, the non-productive complex observed in Δ NDUFA9 mitochondria also contained the late assembly subunit NDUFS5, suggesting the non-productive complex to also be a breakdown product of the ~815 kDa complex. The late stage ~815 kDa complex also interacts with various assembly factors including CIA30, Ecsit, ACAD9 and other proteins that form the MCIA complex (Guarani et al, 2014), as well as B17.2L, which stabilises the assembly in the absence of N-module subunits (Ogilvie et al, 2005). Given the involvement of multiple assembly factors converging at this point, and the observation that loss of FOXRED1 leads to instability and breakdown of the ~815 kDa species, this suggests that the late stages of Complex I assembly represent a critical nexus in the enzyme's biogenesis.

3.10.2 FOXRED1 is found in association with Complex I subunits

The exact molecular role played by FOXRED1 still remains unclear, but this is also the case for many Complex I assembly factors that have been identified in the past decade (Mimaki et al, 2012). FOXRED1 has putative oxidoreductase activity and has homology to FAD binding proteins that are involved in redox reactions related to amino acid catabolism (dimethylglycine dehydrogenase, sarcosine dehydrogenase, L-pipecolic acid oxidase, peroxisomal sarcosine oxidase) and metabolic regulation (pyruvate dehydrogenase regulatory subunit)(Calvo et al, 2010; Fassone et al, 2010). However, there is still no direct evidence for FAD binding or oxidoreductase activity.

Mutations of residues involved in potential FAD binding did not result in inhibition in FOXRED1 activity, except for the substitution of Y359 for Alanine. It remains to be determined whether this mutation leads to potential defects in FAD binding, or if it causes other defects, such as impairing protein folding. Nevertheless, this construct served as a useful control to determine the proteins that can form a complex with FOXRED1.

The recent determination of a 5Å cryo-EM structure of bovine Complex I revealed not only conservation of the core subunits from *T. thermophilus* but also the presence of density attributed to the accessory subunits (Vinothkumar et al, 2014). This structure revealed that the conserved subunits identified as co-immunoprecipitating with FOXRED1 (NDUFS3, NDUFA10 and NDUFA5) are located in close proximity to each other and to the mitochondrial inner membrane, consistent with the sub-mitochondrial localisation of FOXRED1. Furthermore, HA-tagged NDUFS5 has been found in association with FOXRED1 (Guarani et al, 2014), while FOXRED1 was also identified in stalled Complex I subcomplexes lacking NDUFA11 (Andrews et al, 2013). Together, these data suggest that FOXRED1 may function in a complex comprising at least the core subunit NDUFS3 and the accessory subunits NDUFA5, NDUFA10, NDUFB10 and NDUFS5. Interestingly, proteomic analysis failed to detect any subunits of other respiratory complexes, suggesting FOXRED1 performs its function prior to incorporation of Complex I intermediates with other respiratory complexes. Assembly of Complex I with other complexes has been suggested to occur following assembly of the ~815 kDa subcomplex, and before assembly into holo-Complex I (Lazarou et al, 2007; Moreno-Lastres et al, 2012). Because subunits belonging to other respiratory complexes were unable to be identified, it can be concluded that FOXRED1 most likely exerts its function prior to this stage, thus being a mid-to-late stage assembly factor for the biogenesis of Complex I.

3.10.3 FOXRED1 patient mutations remain partially functional

Two separate missense mutations in FOXRED1, resulting in the substitutions p.R352W (Fassone et al, 2010) and p.N430S (Calvo et al, 2010), lead to loss of Complex I activity and mitochondrial disease. Most patients with nuclear gene defects and Complex I dysfunction display severe symptoms and do not survive to adulthood. Interestingly, both patients harbouring FOXRED1 mutations survived to adulthood (Nouws et al, 2012). This indicates that the mutations result in only partial loss of function of FOXRED1 and/or loss of FOXRED1 can be compensated by other factors. The study reported here indicate that the former is most likely true since total loss of FOXRED1 leads to severe reduction in Complex I levels while overexpression of either of the mutant forms in these cells restores Complex I. Thus, the pathogenic mutations in FOXRED1 are most likely hypomorphic in nature. Similar observations have also been for the Complex I assembly factor NUBPL where overexpression of a p.G56R missense mutation could overcome a

Complex I defect in patient cell lines (Tucker et al, 2012). It is therefore possible that future therapeutic treatments could involve mechanisms to increase the synthesis of these mutant proteins so that the reduced assembly activity is dampened. Current therapies for Complex I deficiency and mitochondrial disease include supplementation with various cofactors and other potential therapeutic agents such as dichloroacetate (DCA), CoQ₁₀, creatine or riboflavin (DiMauro & Rustin, 2009; Kerr, 2010). While symptoms may improve for some patients, it has been shown that responsiveness may depend on the particular gene mutation present, leading to a non-responsive phenotype (Haack et al, 2010; Nouws et al, 2014b). The data presented in this chapter suggests that future therapies could include the identification of pharmacological agents that enhance expression of the mutant protein, thereby overcoming effects of pathological mutations and restoring levels of Complex I.

Chapter 4

Functional Analysis of the Mitochondrial Complex I Assembly (MCIA) Complex

4.1 Introduction

The biogenesis of the membrane arm of Complex I requires integration of subunits encoded by both the mitochondrial and nuclear genomes. Many of the known Complex I assembly factors interact with, or influence, the translation or stability of various mtDNA encoded subunits (Dunning et al, 2007; McKenzie et al, 2011; Rendón et al, 2014; Vinothkumar et al, 2014). The first evidence that extrinsic factors are required for the biogenesis of the membrane arm of Complex I came from the aerobic fungus *N. crassa*, where two chaperones known as CIA30 and CIA84, were found to interact with an assembly intermediate of the membrane arm (Kuffner et al, 1998). The loss of either protein resulted in loss of the mature complex, and the accumulation of membrane arm assembly intermediates (Kuffner et al, 1998). A homologue of CIA30 was identified in humans, and was also shown to be required for the proper assembly of Complex I (Dunning et al, 2007; Vogel et al, 2005). It was later identified that the protein Ecsit also interacted with CIA30 in Complex I assembly (Vogel et al, 2007b). ACAD9 was subsequently identified to function in this process (Nouws et al, 2010), followed by TMEM126B (Heide et al, 2012) and most recently TIMMDC1 (Andrews et al, 2013; Guarani et al, 2014). Together, these proteins are known as the mitochondrial Complex I assembly (MCIA) complex. The MCIA complex is thought to function in the biogenesis of the membrane arm, however the role of each protein in the complex remains elusive. Furthermore, while patients have been identified with mutations in CIA30 (Dunning et al, 2007; Fassone et al, 2011) and ACAD9 (Haack et al, 2010; Nouws et al, 2010), no patients have yet been identified with mutations in genes encoding Ecsit, TMEM126B or TIMMDC1.

In order to investigate the contribution of each component of the MCIA complex, cell lines harbouring a separate gene disruption were generated. The data presented in this chapter details the biochemical characterisation of the MCIA complex. To do this, TALEN-mediated gene disruption as well as 'clustered, regulatory interspaced short palindromic repeat' (CRISPR)-Cas9 genome editing was employed. The CRISPR-Cas9 system was first described as an adaptive immune response in bacteria against invading phage or plasmids (Marraffini, 2015). After incorporation of the foreign DNA into the host genome, silencing of the invading DNA is accomplished by a CRISPR RNA (crRNA) that is partly derived from the invading DNA sequence, which can hybridise with another RNA known as a trans-activating crRNA (tracrRNA) (Deltcheva et al, 2011). This partial dsRNA structure can guide the Cas9 nuclease to elicit dsDNA cleavage of the invading DNA (Fig 4.1A) (Jinek et al, 2012). The advent of RNA-guided genome editing was made possible by a chimeric RNA, combining both the crRNA and the tracrRNA into a single transcript known as the guide-RNA (gRNA) (Jinek et al, 2012). In a similar way, the gRNA can be programmed to target a specific site in the genome to direct and elicit DNA breakage and gene disruption in mammalian cells (Fig.4.1B) (Jinek et al, 2012).

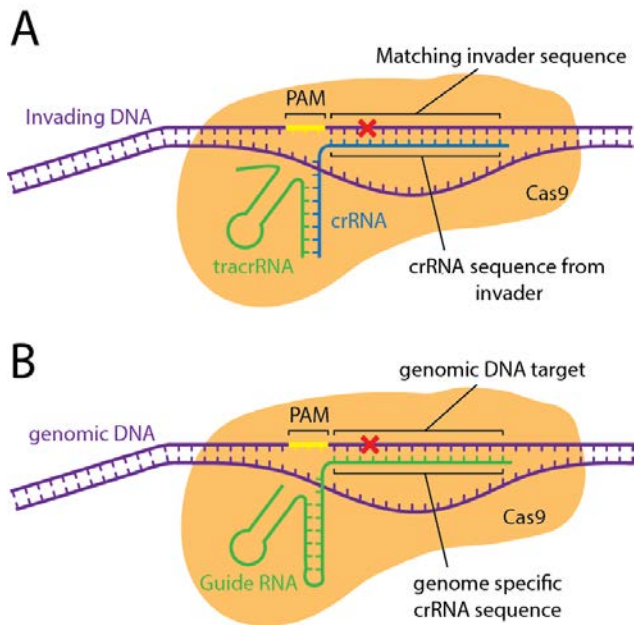


Figure 4.1: Mechanism of CRISPR-Cas9 DNA binding. (A) CRISPR-Cas9 utilises an invading DNA sequence from phage or plasmids to inactivate these genetic elements. Following infection, part of the invading genome is incorporated into the host genome and used to produce specific CRISPR RNAs (crRNAs) that are complementary to the invading DNA. The crRNA binds to the trans-activating crRNA (tracrRNA) and together these guide the CRISPR-Cas9 complex to cleave the foreign genetic material. (B) The CRISPR-Cas9 system has been adapted to use a single guide RNA (gRNA) that is able to modify genomic DNA. Complementary RNA sequence is used as a guide to direct the nuclease Cas9 to the desired region in eukaryotic cells. Adapted from Jinek et al. (2012).

4.2 Design and validation of MCIA complex gene disruptions

In order to investigate the contribution of each component of the MCIA complex, HEK293T cells with individual disruptions were generated. In order to disrupt genes encoding CIA30, Ecsit, ACAD9 and TIMMDC1, the mitochondrial localisation sequence located at the N-terminus of these proteins was targeted (Fig 4.2A). This required the design of TALEN pairs for CIA30 and TIMMDC1 as well as CRISPR-Cas9 constructs for Ecsit and ACAD9 to target exon 1 in the vicinity of the initiation codon (Fig 4.2B). Because TMEM126B lacks a predicted N-terminal mitochondrial targeting sequence (Fig 4.2A), the first common exon among the predicted five isoforms was targeted for disruption (Fig 4.2B). While annotation of the TMEM126B gene indicates the presence of five isoforms produced by alternative splicing of the pre-mRNA transcript, mass spectrometry analysis by Andrews et al. (2013) suggests that only isoforms 1 and 5 are present in mitochondria with no proteomic evidence for isoforms 2, 3 or 4. To ensure that all possible transcripts were disrupted, the first common exon was targeted for CRISPR-Cas9 editing.

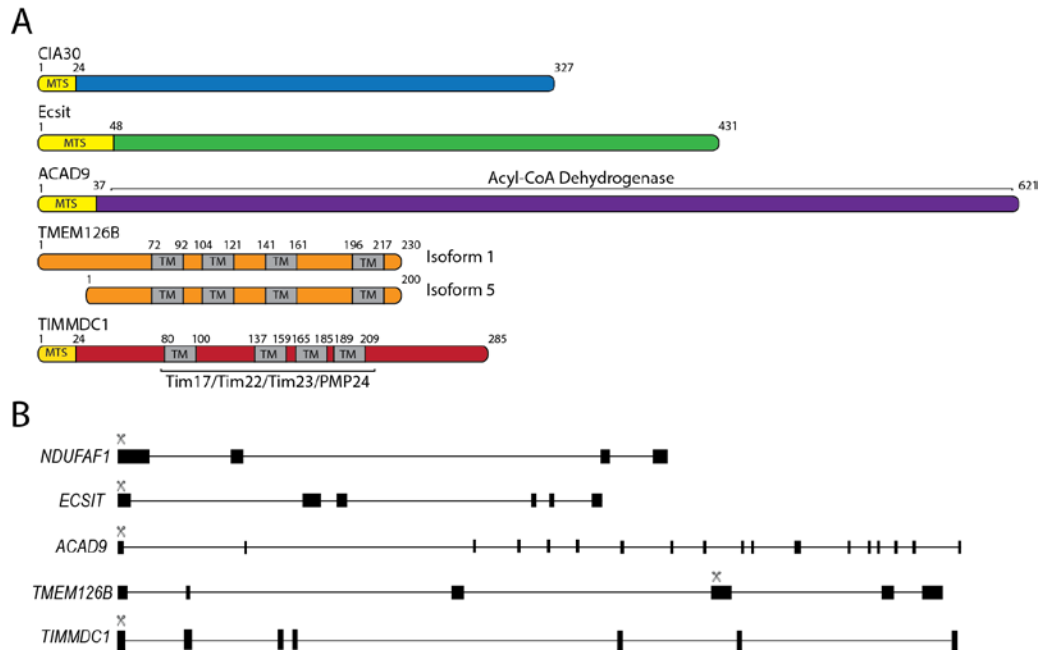


Figure 4.2: MCIA complex protein domain and gene structure. (A) Proteins of the MCIA complex with an N-terminal mitochondrial targeting signal (MTS) are indicated in yellow. Proteins with transmembrane (TM) domain regions are indicated in grey. The protein ACAD9 belongs to the Acyl-CoA dehydrogenase family of proteins, while TIMMDC1 belongs to the Tim17/Tim22/Tim23/PMP24 family of protein translocases. **(B)** Gene structure of each component of the MCIA complex. Squares represent exons, while connecting lines represent introns. The region targeted for disruption is indicated by scissors above the target exon. CIA30 is encoded by the *NDUFAF1* gene.

Following the transfection of TALEN pairs or CRISPR-Cas9 plasmids, clonal populations were generated using fluorescence activated cell sorting (FACS). The single cell colonies were then tested for growth defects on media containing galactose and cells that failed to grow were expanded in glucose-containing media. To ensure biological reproducibility, two independent clones were selected for each cell line for further analysis. The genomic region encompassing the target site was amplified by PCR using genomic DNA and sub-cloned followed by Sanger sequencing. The results of the generated indel sequences are summarised in Table 4.1. Analysis revealed that Δ CIA30-1 contained a single nucleotide deletion resulting in a frame-shift, while Δ CIA30-2 contained a deletion that encompassed the initiation codon, thereby producing no protein. The Δ Ecsit-1 cell line contained a deletion removing the initiation methionine, while Δ Ecsit-2 contained a small indel resulting in a premature stop codon after an additional 5 codons. Both Δ ACAD9 lines contained deletions that eliminated the initiation codon. Analysis of Δ TMEM126B-1 showed a deletion that removed an intron-exon boundary (intron underlined), while Δ TMEM126B-2 and both Δ TIMMDC1-1 and Δ TIMMDC1-2 contained small indels resulting in frame shifts and premature termination of protein synthesis. Since these cell lines contained disruptions to the required genes, they were used for further analysis.

Table 4.1: Genomic sequencing of gene disruptions in MCIA complex cell lines. The target region is shown with deletions and insertions indicated in blue. Translation of the wildtype (WT) or modified gene is indicated in red. Introns are underlined.

Cell lines	Method	Target region	Clone	Allele	Indel
ΔCIA30	TALEN	Exon 1 - MTS		WT	TTCTTGGTGGCCCTTGCTAGCCCAGGAAGAACTTACATTTTGATTTTTTTGTACCATGGCTTTGGTTCACAAATTGCTGCGTGGTACTTATTTTCTCAGAAAATTCTCTAA M A L V H K L L R G T Y F L R K F S K
			1	A	TTCTTGGTGGCCCTTGCTAGCCCAGGAAGAACTTACATTTTGATTTTTTTGTACCATGGCTT-GGTTACAAATTGCTGCGTGGTACTTATTTTCTCAGAAAATTCTCTAA M A W F T N C C V V L I F S E N S L
			2	A	TTCTTGGTGGCCCTTGCTAGCCCAGGAAGAACTTAC-----AAATTGCTGCGTGGTACTTATTTTCTCAGAAAATTCTCTAA
ΔECSIT	CRISPR	Exon 1 - MTS		WT	AAGGTGCCAGGCTAATGCTGAATCTTCTTTTGGGCCAGGTGATTGTCTGACAAGCAGAGGCATGAGCTGGGTCCAGGCCACCCTACTGGCCCCAGGCCCTCTGTAGGGCCTGG M S W V Q A T L L A R G L C R A W
			1	A	AAGGTGCC-----CTCTGTAGGGCCTGG
			2	A	AGGTGCCAGGCTAATGCTGAATCTTCTTTTGGGCCAGGTGATTGTCTGACAAGCAGAGGCATGAGCTGGGTCCAGGCCACCCGA---GGCCCCAGGCCCTCTGTAGGGCCTGG M S W V Q A T R G P R P L *
ΔACAD9	CRISPR	Exon 1 - MTS		WT	CGTCATCAGACGTGTGTGTGTCCCTGCGGGCGCTAAGAAGGGGAGACTGAGGCTGAGGCTGGGGAACATCGGGCAGCATGAGCGGCTGCGGGCTCTTCTGCGCACCACGGCTG M S G C G L F L R T T A
			1	A	CGTCATCAGACGTGTGTGTGTCCCTGCGGGCGCTAAGAAGGGGAGACTGAGGCTGAGGCTGGGGAACATCGGGCAGC-----GGGCTCTTCTGCGCACCACGGCTG
				B	CGTCATCAGACGTGTGTGTGTCCCTGCGGGC-----TGCGGGCTCTTCTGCGCACCACGGCTG
				C	CGTCATCAGACGTGTGTGTGTCCCTGCGGGCGCTAAGAAGGGGAGACTGAGGCTGAGGCTGGGGAACATCGGGCAGC-----GGCTGCGGGCTCTTCTGCGCACCACGGCTG
			2	A	CGTCATCAGACGTGTGTGTGTGTCCCTGCGGGCGCTAAGAAGGGGAGACTGAGGCTGAGGCTGGGGAACATCGGGCAGC-----GGCTGCGGGCTCTTCTGCGCACCACGGCTG
B	CGTCATCAGACGTGTGTGTGTGTCCCTGCGGGCGCTAAGAAGGGGAGACTGAGGCTGAGGCTGGGGAACATCGGGC-----TCTTCTGCGCACCACGGCTG				
ΔTMEM126B	CRISPR	Exon 4 - First Common Exon		WT	TATTAGGACACAAAATATATATCAAATGGCGACATTTGAAACACAGCTGGTTTCTCTGGAATATTCTCAAACCTCCTGTTTCAGACGCTGCTTCAAGGTTAAACATGATGCTT T Q N I Y Q M A T F G T T A G F S G I F S N F L F R R C F K V K H D A
			1	A	-----CAGCTGGTTTCTCTGGAATATTCTCAAACCTCCTGTTTCAGACGCTGCTTCAAGGTTAAACATGATGCTT
			2	A	TATTAGGACACAAAATATATATCAAATGGCGACATTTGAAAC---CAGCTGGTTTCTCTGGAATATTCTCAAACCTCCTGTTTCAGACGCTGCTTCAAGGTTAAACATGATGCTT T Q N I Y Q M A T F E T S W F L W N I L K L P V Q T L L Q G *
B	TATTAGGACACAAAATATATATCAAATGGCGACATTTGAAAC---AGCTGGTTTCTCTGGAATATTCTCAAACCTCCTGTTTCAGACGCTGCTTCAAGGTTAAACATGATGCTT T Q N I Y Q M A T F G K L V S L E Y S Q T S C S D A A S R L N M M L *				
ΔTIMMDC1	TALEN	Exon 1 - MTS		WT	GGCCATGGAGGTGCCGCCACCGGCACCGCGGAGCTTTCTCTGTAGAGCATTGTGCCTATTTCCCGAGTCTTTGCTGCCGAAGCTGTGACTGCCGATTTCGGAAGTCCCTTGAGG M E V P P P A P R S F L C R A L C L F P R V F A A E A V T A D S E V L E
			1	A	GGCCATGGAGGTGCCGCCACCGGCACCGCGGAGCTTTCTCTGTAGAGCATTGTGCCTATT-----GAGG M E V P P P A P R S F L C R A L C L L R
				B	GGCCATGGAGGTGCCGCCACCGGCACCGCGGAGCTTTCTCTGTAGAGCATTGTGCCTATTTCCCT-----CCGAAGCTGTGACTGCCGATTTCGGAAGTCCCTTGAGG M E V P P P A P R S F L C R A L C L F P L R S C D C R F G S P *
			2	A	GGCCATGGAGGTGCCG-----AAGCTGTGACTGCCGATTTCGGAAGTCCCTTGAGG M E V P K L *
				B	GGCCATGGAGGTGCCGCCACCGGCACCGCGGAGCTTTCTCTGTAGAGCATTGTGCCTATTTCCCGA-----TTCCGGAAGTCCCTTGAGG M E V P P P A P R S F L C R A L C L F P R F G S P *

4.3 Steady state levels of MCIA complex proteins differ in the absence of various proteins

To confirm loss of the MCIA components at the protein level and the effect of other components of this complex, mitochondria were isolated from control and disruption cell lines and analysed by SDS-PAGE and immunodecoration (Fig 4.3). Analysis of the Δ TIMMDC1-1 and Δ TIMMDC1-2 cell lines showed a clear loss of the TIMMDC1 protein (Fig. 4.3A), while the levels of the other MCIA complex proteins remained unchanged. The same results were observed in the Δ TMEM126B-1 and Δ TMEM126B-2 cell lines, where there was a clear loss of the TMEM126B protein in both cell lines while the other proteins appeared unchanged (Fig. 4.3B). Immunodecoration of mitochondrial lysates from the Δ CIA30-1 and Δ CIA30-2 cell lines indicated a clear loss of the CIA30 protein in these mitochondria as expected (Fig. 4.3C). Interestingly, the loss of CIA30 also resulted in a decrease in the steady state levels of Ecsit and TMEM126B relative to the control mitochondria, while the levels of ACAD9 and TIMMDC1 remained unchanged (Fig 4.3C). The Δ Ecsit-1 and Δ Ecsit-2 cell lines were analysed in a similar way, with no Ecsit detected in both cell lines and a reduction in the levels of CIA30 and TMEM126B (Fig. 4.3D). In the absence of Ecsit, the levels of ACAD9 and TIMMDC1 appeared unchanged (Fig. 4.3D). In the cells lacking ACAD9 (Δ ACAD9-1 and Δ ACAD9-2), the levels of CIA30, Ecsit and TMEM126B were all reduced, while the levels of TIMMDC1 remained unchanged (Fig. 4.3E). While there was variation in the levels/stability of the MCIA complex proteins among different cell lines, the levels of the early stage assembly factor NDUFAF4 (Saada et al, 2008) and the late stage assembly factor B17.2L (Ogilvie et al, 2005) were unaffected. The Complex II subunit SDHA was used as a loading control and its levels were also unchanged as expected. These data indicate that while TIMMDC1 levels remain stable in the absence of other known MCIA complex components, there is strong interplay between the remaining MCIA complex proteins where the loss of one component can impact on the levels and stability of other proteins in the complex (Fig 4.3F).

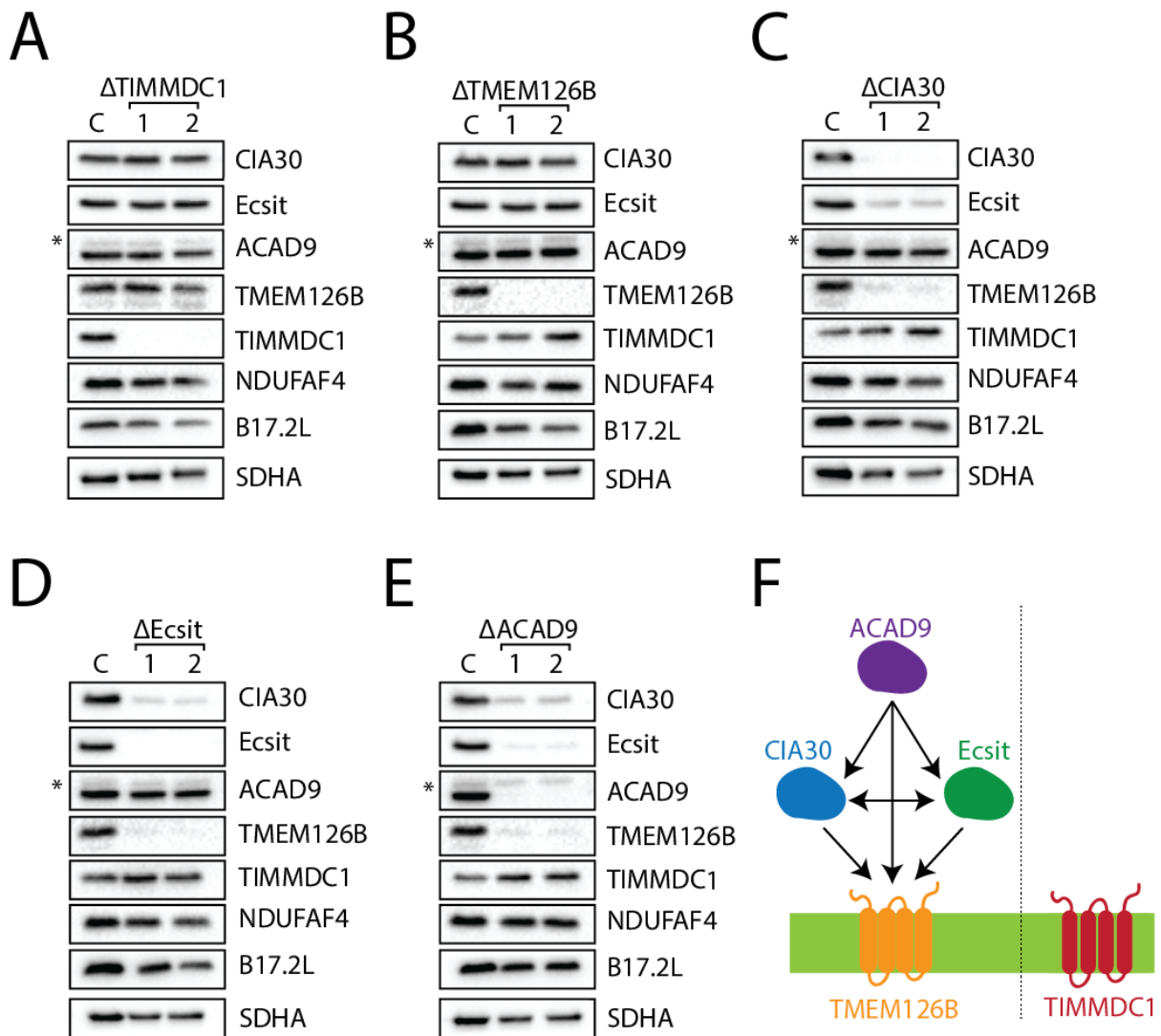


Figure 4.3: Steady state analysis of MCIA complex components in deletion cell lines. Mitochondria were isolated from HEK293T control and **(A)** Δ TIMMDC1-1 and Δ TIMMDC1-2 **(B)** Δ TMEM126B-1 and Δ TMEM126B-2, **(C)** Δ CIA30-1 and Δ CIA30-2, **(D)** Δ Ecsit-1 and Δ Ecsit-2 and **(E)** Δ ACAD9-1 and Δ ACAD9-2 cells, analysed by SDS-PAGE and immunoblotted against indicated proteins. **(F)** Model depicting how the loss of a component of the MCIA complex affects other proteins. Arrows indicate how deletion of one protein affects the loss of another MCIA complex component.

4.4 Loss of any MCIA complex component results in a strong Complex I defect

In order to assess the effect of loss of the MCIA complex proteins on the level of Complex I, mitochondria were isolated from control and gene-disrupted cell lines, solubilised in Triton X-100 and subjected to BN-PAGE and immunoblotting (Fig. 4.4). Analysis of NDUFA9 revealed the presence of Complex I in control mitochondria, while all MCIA complex disruptions lacked any detectable Complex I (Fig 4.4A-E). This is consistent with previous findings from patient cell and knockdown studies indicating that all components of the MCIA complex are critical for Complex I assembly, and loss of any single component is sufficient to result in a severe Complex I defect (Dunning et al, 2007; Heide et al, 2012; Vogel et al, 2007b).

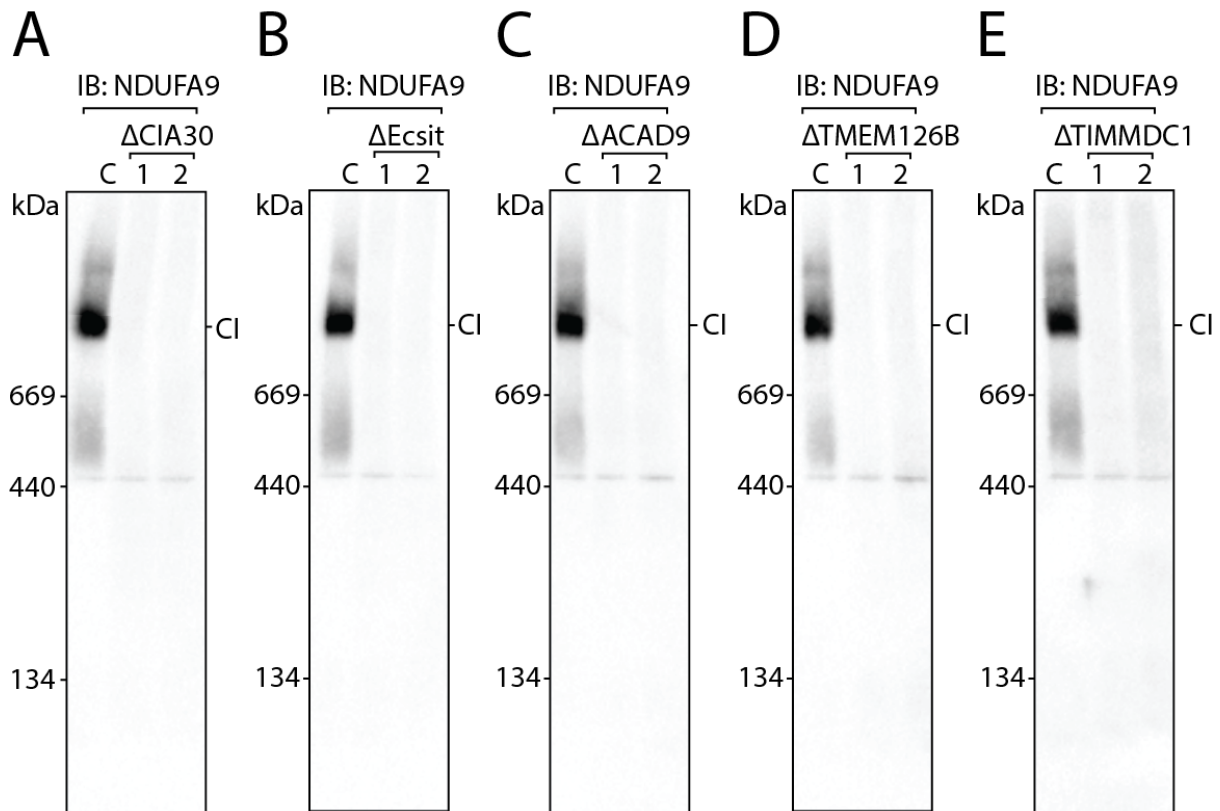


Figure 4.4: All MCIA complex components are critical for Complex I biogenesis. Mitochondria were isolated from control and (A) Δ CIA30-1 and Δ CIA30-2, (B) Δ Ecsit-1 and Δ Ecsit-2, (C) Δ ACAD9-1 and Δ ACAD9-2, (D) Δ TMEM126B-1 and Δ TMEM126B-2 and (E) Δ TIMMDC1-1 and Δ TIMMDC1-2 cells and analysed by BN-PAGE following solubilisation in 1% (v/v) TX100. Analysis of Complex I was performed by immunodecoration with NDUFA9 antibodies.

4.5 Complex I subunits are reduced in MCIA complex disruptions

To assess the effect of the loss of MCIA complex components on the steady state levels of Complex I subunits, mitochondria were isolated and subjected to SDS-PAGE and immunoblotting for various Complex I proteins (Fig. 4.5). Due to the L-shaped structure of Complex I, subunits corresponding to various regions were selected for analysis (Fig 4.5A). Immunodecoration of mitochondrial lysates from the Δ TIMMDC1 cell lines revealed a strong defect in the levels of mt-ND1, NDUFA13 and NDUF5, with no protein being detected (Fig. 4.5B). While mt-ND1 and NDUFA13 are thought to assemble early in the Complex I biogenesis pathway, NDUF5 is thought to assemble at a later stage suggesting that loss may lead to defects at various stages of assembly (Ugalde et al, 2004; Vogel et al, 2007a). The levels of subunits NDUF2, NDUF3 and NDUFA9 were also strongly reduced relative to the control mitochondria, while the levels of NDUF6 appeared similar to the control (Fig. 4.5B). The Complex II subunit SDHA was used as a loading control (Fig 4.5B). Analysis of Δ TMEM126B, Δ CIA30, Δ Ecsit and Δ ACAD9 all showed a similar steady state protein profile (Fig. 4.5C-F) with a strong loss of the NDUF5 subunit and reduced amounts of the subunits NDUF2, NDUF3 and NDUFA9. Analysis of mt-ND1 and NDUFA13 in the absence of CIA30, Ecsit, ACAD9 and TMEM126B also showed decreased levels relative to the control cells, however the decrease was not as strong as that observed in the absence of TIMMDC1 (Fig. 4.5C-F). These results, along with the steady state level profiles of MCIA complex subunits indicate that TIMMDC1 may have a separate function to the remainder of the MCIA complex in Complex I biogenesis.

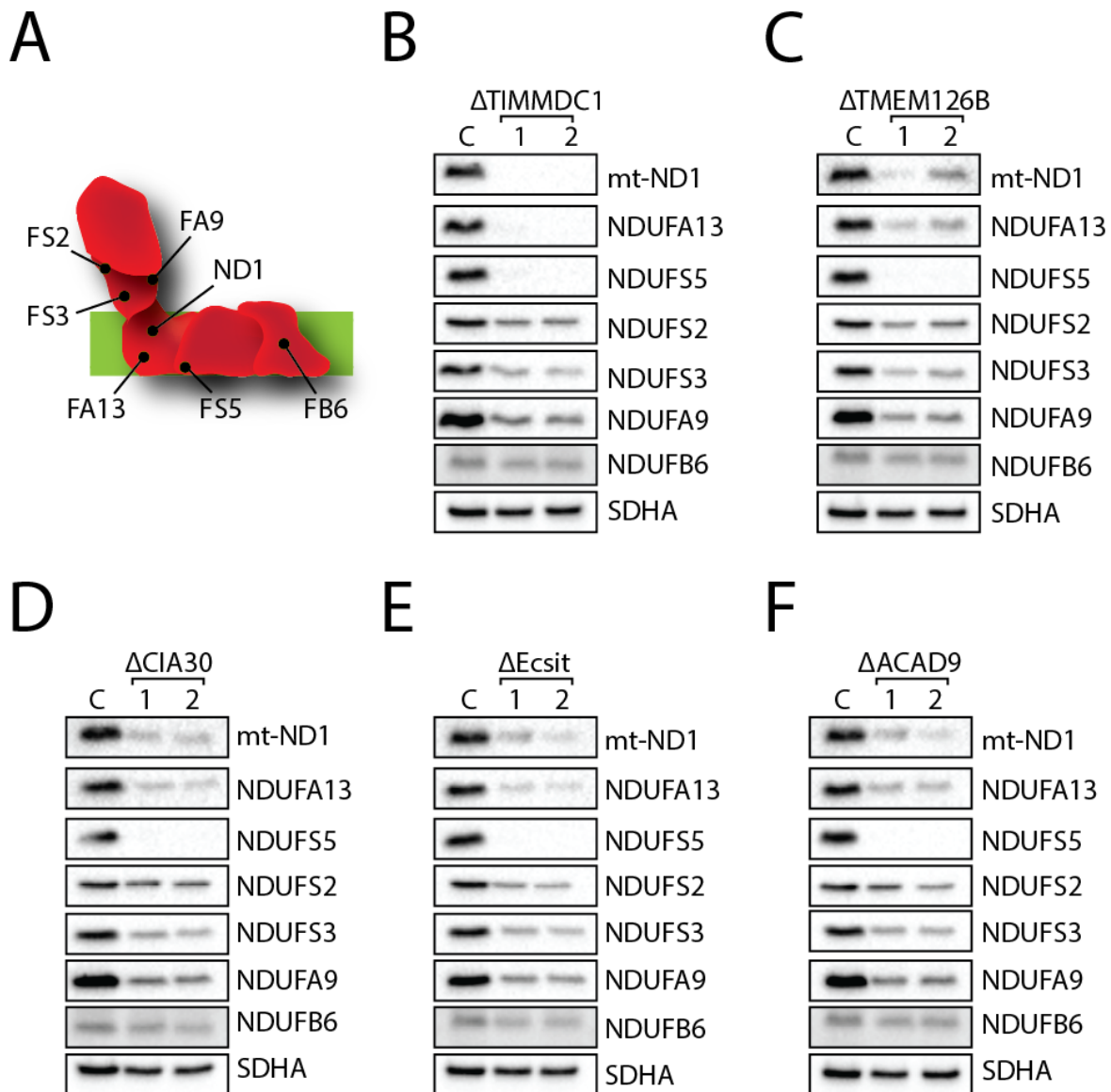


Figure 4.5: Analysis of Complex I subunits in MCIA disrupted cell lines. (A) Schematic representation of the position of Complex I subunits analysed. Mitochondria were isolated from control, **(B)** Δ TIMMDC1-1 and Δ TIMMDC1-2, **(C)** Δ TMEM126B-1 and Δ TMEM126B-2, **(D)** Δ CIA30-1 and Δ CIA30-2, **(E)** Δ Ecsit-1 and Δ Ecsit-2 and **(F)** Δ ACAD9-1 and Δ ACAD9-2 cells, analysed by SDS-PAGE and immunoblotted against indicated proteins.

4.6 Complementation of MCIA complex disruption cell lines with the missing protein is sufficient for Complex I biogenesis

Analysis of the MCIA complex cell lines revealed a similar overall Complex I defect, while defects in the assembly factors themselves differ depending on the missing MCIA complex component. In order to discard potential off-target effects from genome editing, complementation analysis was performed. Plasmids encoding FLAG-tagged MCIA complex components were transiently transfected into their respective cell lines and grown for a further 48 hours to express the protein and promote Complex I assembly. Whole cell extracts were solubilised in digitonin-containing buffer and analysed by BN-PAGE and immunoblotting (Fig. 4.6A). Immunodecoration with antibodies directed to the Complex I subunit NDUFA9 showed that respiratory super-complexes containing Complex I were observed when compared to the untransfected control in each case (Fig 4.6A, CI/CIII₂/CIV). The absence of complete restoration of super-complex levels can be attributed to the transfection efficiency not being 100%, and some cells remain deficient of the missing protein. Expression of the ectopic protein was confirmed by SDS-PAGE and immunodecoration analysis of cell lysates using anti-FLAG antibodies. In each case, the presence of a FLAG signal in the transfected samples corresponded to the size of each of the MCIA complex components (Fig. 4.6B, arrowheads). Equal loading was verified using the Complex II protein SDHA.

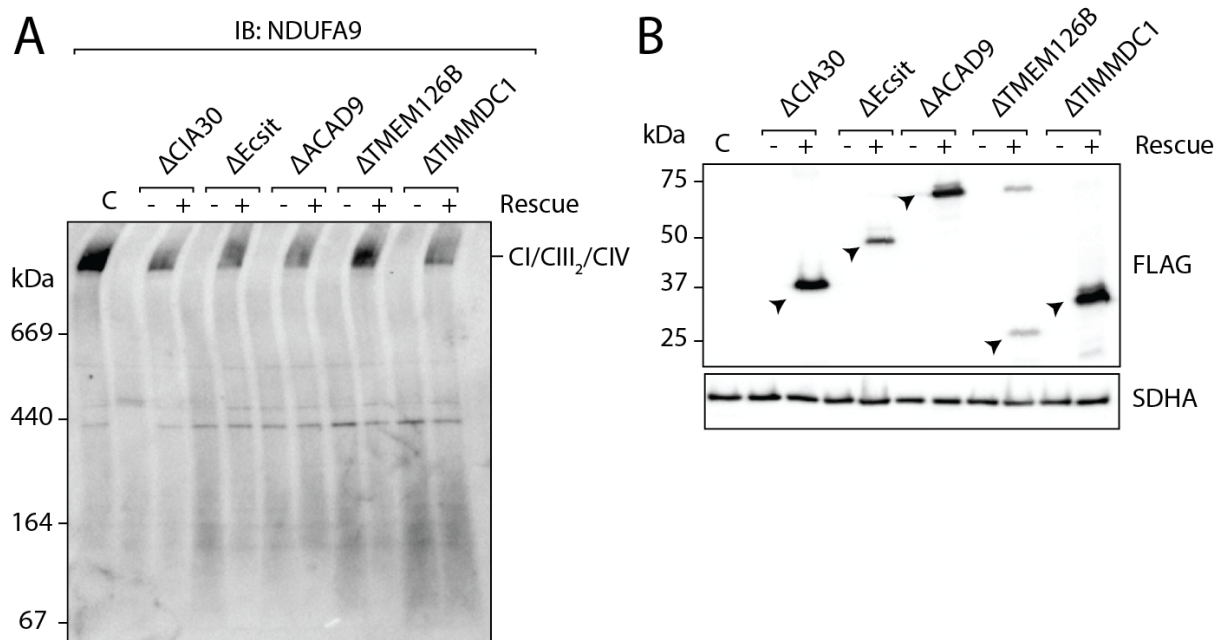


Figure 4.6: Complementation analysis of MCIA complex disruption cell lines. The MCIA complex cell lines were either untreated (-) or rescued (+) with a plasmid encoding the missing protein. **(A)** Cells were analysed by BN-PAGE following solubilisation with 1% (w/v) digitonin and immunodecorated for NDUFA9. **(B)** Cells were analysed by SDS-PAGE and immunodecorated with FLAG antibodies. The Complex II protein SDHA was used as a loading control.

4.7 ACAD9 fails to assemble into higher order complexes in the absence of CIA30 and Ecsit

In analysing the steady state levels of the MCIA complex components, it was observed that while the disruption of ACAD9 resulted in the reduction of CIA30, Ecsit and TMEM126B, the converse was not true as the levels of ACAD9 were stable in the absence of the other proteins (Fig. 4.3). To investigate the behaviour of ACAD9 further, mitochondria from the MCIA complex disruptions were isolated, subjected to digitonin solubilisation and BN-PAGE followed by immunodecoration for ACAD9 (Fig. 4.7). As expected, there were no ACAD9-containing complexes present in either the Δ ACAD9-1 or Δ ACAD9-2 cell lines (Fig 4.7A). In the absence of CIA30 or Ecsit, ACAD9 was unable to assemble into higher order complexes (Fig. 4.7B and C). This data suggests that ACAD9 assembles into higher order complexes with CIA30 and Ecsit.

Analysis of ACAD9 in the Δ TMEM126B-1 and Δ TMEM126B-2 cell lines indicated that in contrast to the loss of CIA30 and Ecsit, the loss of TMEM126B did not change the ability of ACAD9 to form higher molecular weight complexes (Fig. 4.7D). While ACAD9 could still be found in higher order complexes, the profile differed between control and Δ TMEM126B cell lines, suggesting the loss of TMEM126B did not inhibit ACAD9 forming higher order complexes. Interestingly, additional higher molecular weight complexes were observed in the Δ TMEM126B cell lines in comparison to the control (Fig 4.7D). Similarly, in the Δ TIMMDC1 cell lines, ACAD9 also assembled into higher order complexes, however, these were distinct from those seen in the control and Δ TMEM126B cells (Fig. 4.7E). This suggests that the loss of TMEM126B or TIMMDC1 results in different outcomes for the assembly of ACAD9 into higher order complexes. In summary, in the absence of CIA30 or Ecsit, ACAD9 fails to assemble at all, while in the absence of TMEM126B or TIMMDC1, ACAD9 complexes are formed but differ from control mitochondria.

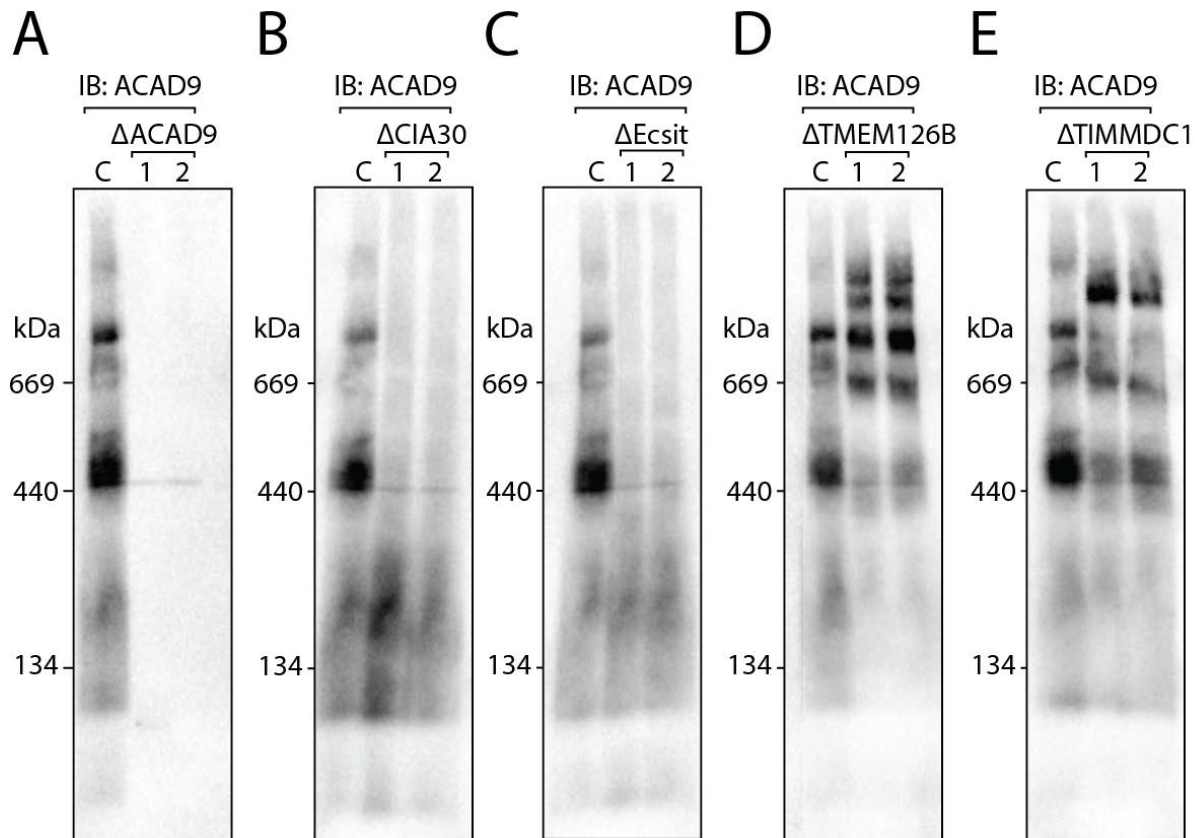


Figure 4.7: ACAD9-containing complexes differ in the absence of various MCIA complex components. Mitochondria were isolated from control and (A) Δ ACAD9, (B) Δ CIA30, (C) Δ Ecsit, (D) Δ MEM126B and (E) Δ TIMMDC1 cell lines, solubilised in 1% (w/v) digitonin and analysed by BN-PAGE and immunodecoration using ACAD9 antibodies.

4.8 Pathogenic mutations in CIA30 deficient patients are either hypomorphic in nature or result in a total loss-of-function

To date, three patients with Complex I deficiency have been diagnosed with pathogenic mutations in the *NDUFAF1* gene that encodes the CIA30 protein (Dunning et al, 2007; Fassone et al, 2011; Wu et al, 2014). In all cases, patients were compound heterozygotes for various point mutations in the *NDUFAF1* gene. Using the Δ CIA30 cell line as a tool to investigate the nature of these mutations, each patient mutation was generated in the pCIA30-FLAG construct by site directed mutagenesis. In each case, the mutation resulted in an amino acid substitution of a highly conserved residue (Fig. 4.8A). Following transient transfection of Δ CIA30 cells with the plasmids encoding wild-type CIA30 or CIA30 harbouring pathogenic mutations, the cells were harvested and solubilised in Triton X-100 and analysed by BN-PAGE and immunoblotting for the presence assembled Complex I (Fig. 4.8B). Analysis showed that control cells had Complex I, while untransfected Δ CIA30 cells did not. Re-introduction of wild-type CIA30 was able to restore the Complex I defect as expected. In addition, expression CIA30 harbouring the mutations D83N, H93R, R211C or K253R were able to restore the levels of Complex I (Fig. 4.8B), suggesting these mutations are hypomorphic in nature with restoration of CIA30 function through overexpression. Notably however, CIA30 with mutations T207P or G245R were both unable to restore the Complex I defect, and likely represent loss-of-function mutations (Fig 4.8B). To confirm expression of the mutant proteins, cell lysates were subjected to SDS-PAGE analysis and immunodecoration (Fig 4.8C). As can be seen, all CIA30 variants were expressed in cells to a similar level (Fig 4.8C). Furthermore, the re-introduction of wild-type CIA30 or CIA30 mutants that could restore the levels of Complex I (i.e. D83N, H93R, R211C and K253R) also restored the levels of Ecsit and the Complex I subunit NDUFS5, which are both reduced in the Δ CIA30 cells. CIA30 harbouring the mutations T207P or G245R were unable to restore the levels of these proteins further supporting that these mutations lead to inactive CIA30. The levels of ACAD9 were unaltered, as was the Complex II subunit SDHA.

In order to assess if the mutant CIA30 proteins or the CIA30-interacting protein ACAD9 could assemble into their higher order complexes as observed in control cells, transfected cells were solubilised in digitonin and subjected to BN-PAGE and immunoblotting (Fig. 4.9). CIA30 mutants T207P and G245R were unable to assemble suggesting intermolecular interactions with partner proteins were lost (Fig. 4.9A). This was further illustrated by immunodecoration with ACAD9 antibodies demonstrating that while wildtype and hypomorphic CIA30 variants were able to restore ACAD9-containing complexes, the inactive T207P and G245R mutants were unable to do so (Fig. 4.9B). These data suggest the T207P and G245R mutants are unable to engage the Complex I assembly machinery and lead to the production of Complex I.

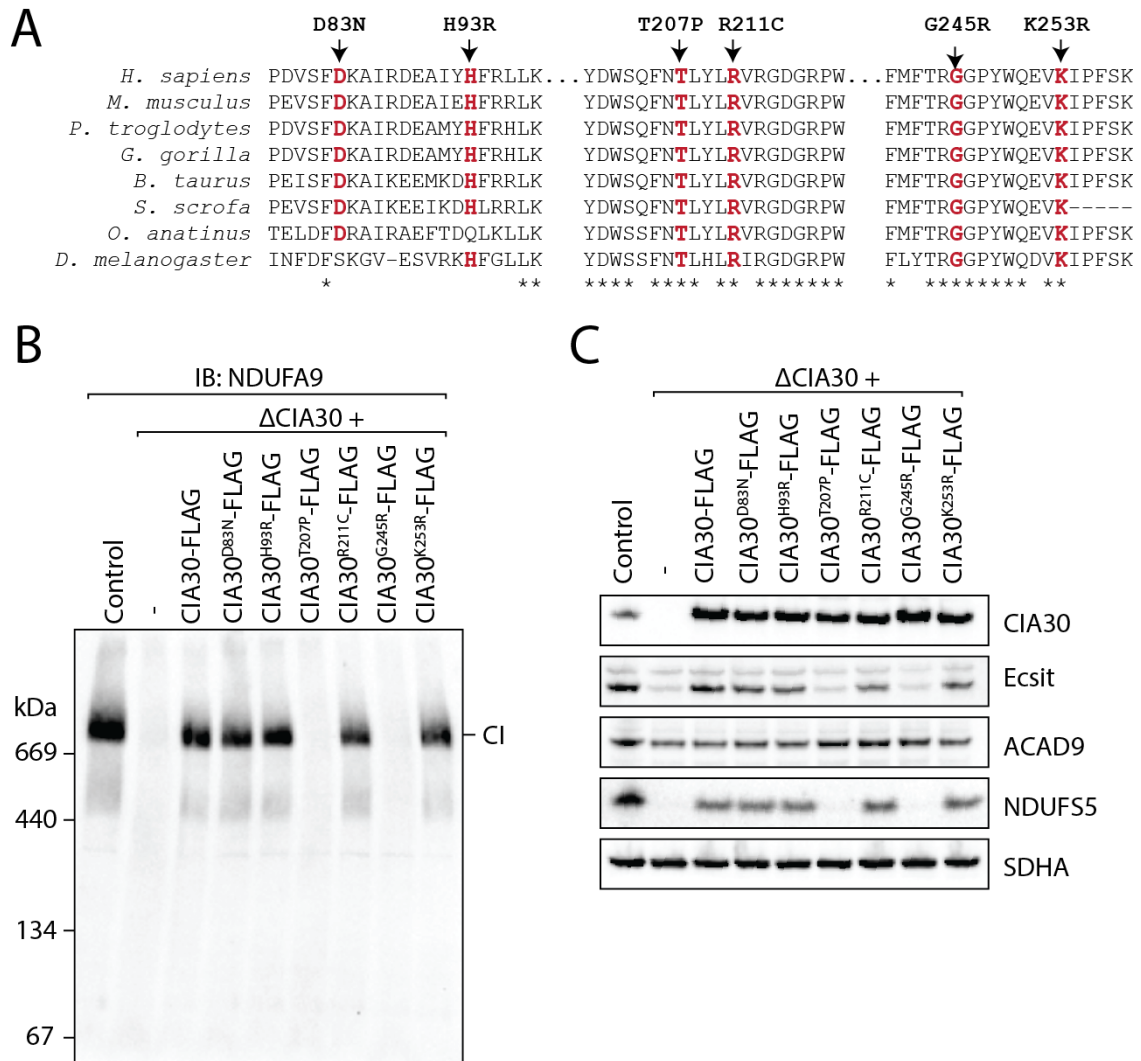


Figure 4.8: CIA30 patient mutation analysis in the Δ CIA30 background. (A) Sequence alignment of CIA30 from various species as indicated. The arrows indicate the position of the mutation present in the patient and the resulting amino acid substitution. Residues highlighted in red indicate the conservation of the mutated residue in CIA30. The asterisk indicates perfect conservation of the residue in the species shown. **(B)** Control or Δ CIA30 cells that were untreated or transfected with wild-type or mutant CIA30 were solubilised in 1% (v/v) TX100 and subjected to BN-PAGE and immunodecoration with NDUFA9 antibodies. **(C)** Cells were analysed by SDS-PAGE and immunodecorated with antibodies for various proteins as indicated.

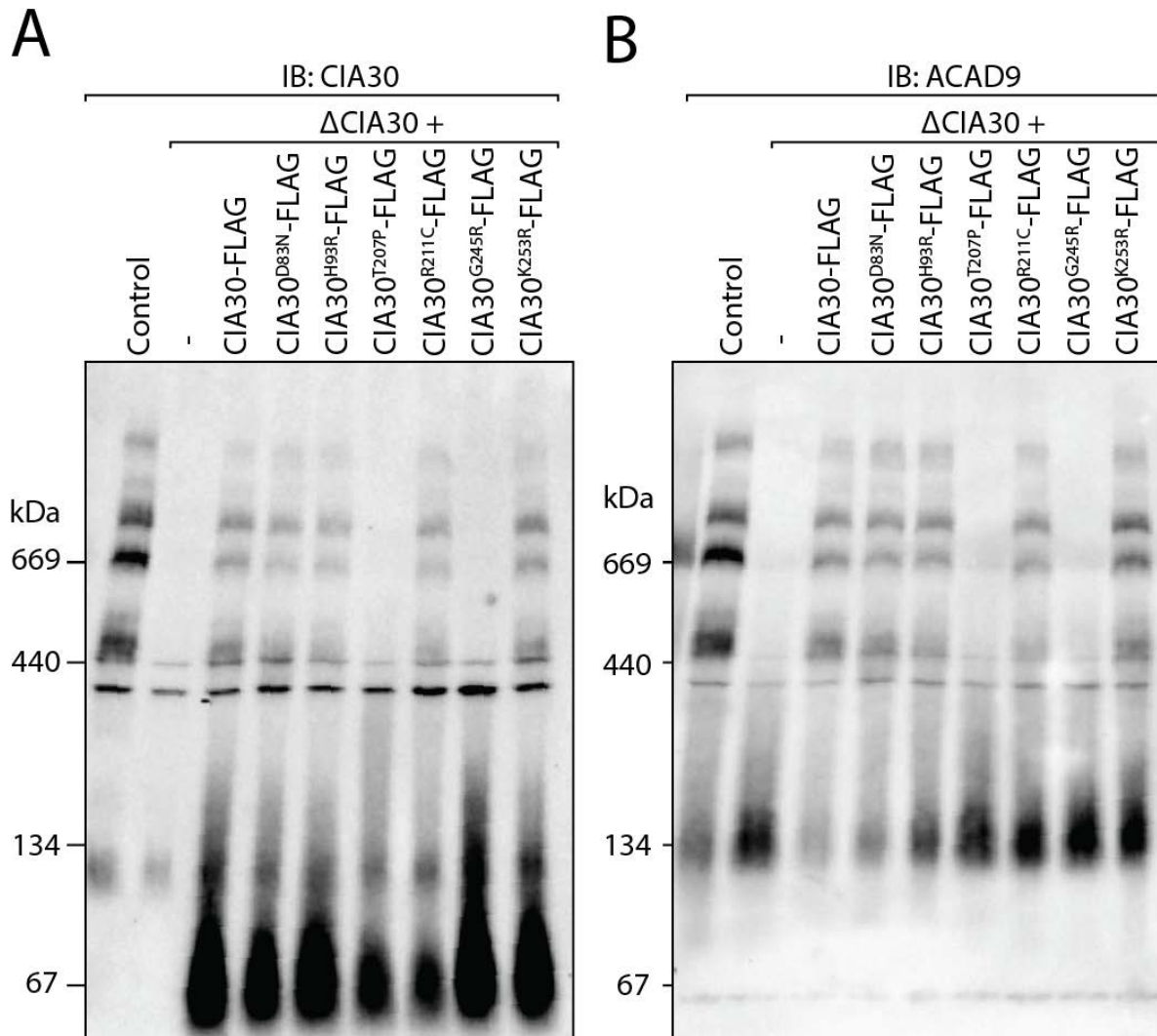


Figure 4.9: Inactive CIA30 fails to form higher molecular weight complexes. Control or Δ CIA30 cells that were untransfected or transfected with wildtype or mutant CIA30 were solubilised in 1% (w/v) digitonin and subjected to BN-PAGE and immunodecoration with antibodies against **(A)** CIA30 and **(B)** ACAD9.

4.9 TIMMDC1 accumulates in a ~440 kDa intermediate independent of other MCIA complex proteins

Next, the behaviour of TIMMDC1 in the absence of other MCIA complex proteins was assessed. BN-PAGE analysis of TIMMDC1 complexes in control mitochondria showed a similar profile to other MCIA complex proteins (Fig. 4.10A *cf.* Fig. 4.9). The similarity between TIMMDC1-containing complexes and complexes containing CIA30 and ACAD9 further demonstrates these proteins may be functionally related in the Complex I assembly pathway. Further analysis of TIMMDC1 in the absence of CIA30, Ecsit, ACAD9 or TMEM126B showed an accumulation of TIMMDC1 in a doublet complex of ~440 kDa (Fig. 4.10B-E, labelled "#"). These complexes appeared more abundant relative to the control mitochondria in all cases and may represent stalled intermediates of the Complex I assembly pathway due to the loss of other components of the MCIA complex. A high molecular weight complex containing TIMMDC1 was also observed in the Δ CIA30, Δ Ecsit, Δ ACAD9 and Δ TMEM126B cell lines that was not observed in the control mitochondria (Fig. 4.10B-E, labelled "+"). This complex may represent an aberrant assembly complex upon disruption to the assembly pathway in the absence of CIA30, Ecsit, ACAD9 or TMEM126B. These data suggest that upon loss of the other MCIA components, the progression of TIMMDC1 along the Complex I assembly pathway is halted at a ~440 kDa sub-complex.

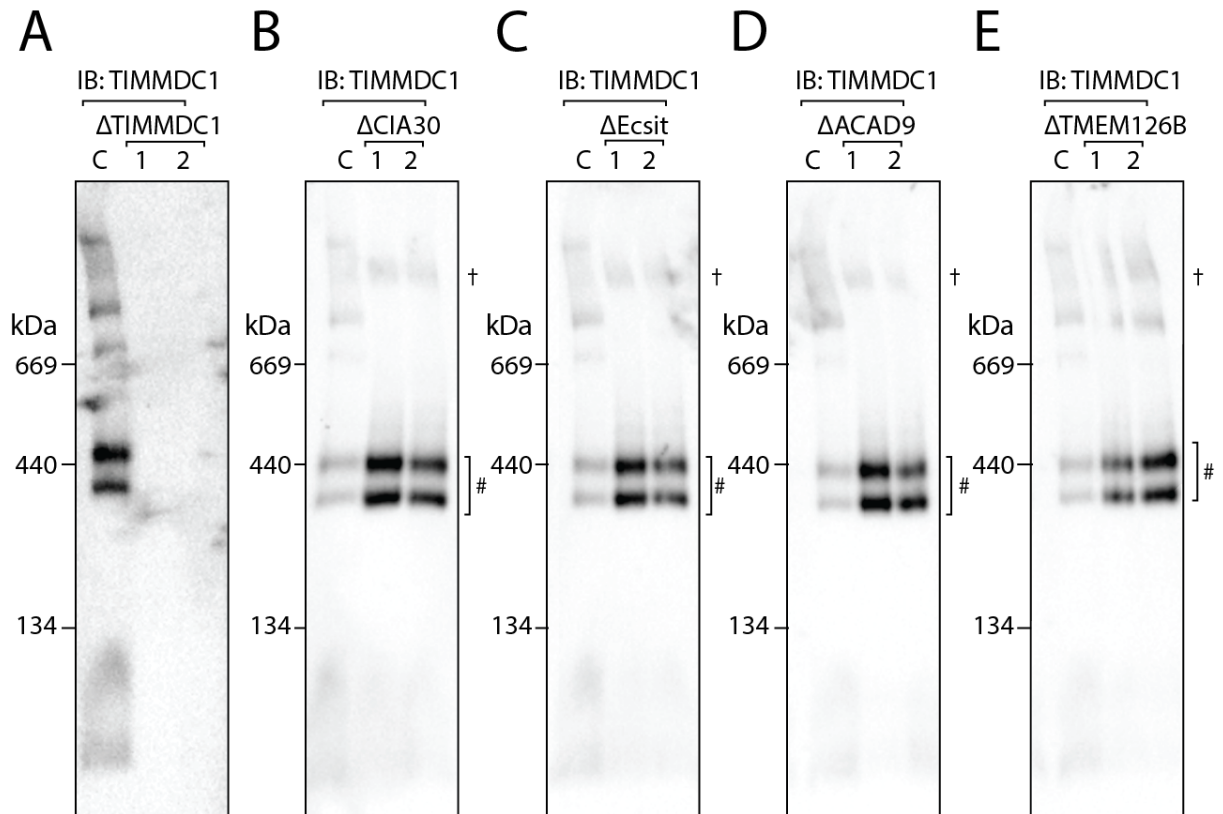


Figure 4.10: TIMMDC1 predominantly accumulates in a ~440 kDa complex in the absence of other MCIA complex proteins. Mitochondria were isolated from control and (A) Δ TIMMDC1, (B) Δ CIA30, (C) Δ Ecsit, (D) Δ ACAD9, and (E) Δ TMEM126B cell lines and analysed by BN-PAGE following solubilisation in 1% (w/v) digitonin and immunodecoration using TIMMDC1 antibodies. # represents the accumulated TIMMDC1 complex present in the absence of CIA30, Ecsit, ACAD9 and TMEM126B, also present in control mitochondria. † represents a TIMMDC1-containing complex present only in the absence of other MCIA complex proteins.

4.10 NDUF3 also accumulates in a ~440 kDa intermediate in the absence of MCIA complex proteins

The Complex I subunit NDUF3 assembles early in the Complex I pathway and resides in a number of Complex I intermediates (Vogel et al, 2007a). To determine if the assembly of NDUF3 was affected by the loss of MCIA complex proteins, isolated mitochondria were subjected to BN-PAGE and immunodecoration with NDUF3 antibodies (Fig. 4.11). In control mitochondria, it was observed that the majority of NDUF3 assembled into mature Complex I located in the super-complex together with Complexes III and IV (Fig. 4.11A-E, SC). Analysis of NDUF3 in the absence of the MCIA complex proteins CIA30, Ecsit, ACAD9 and TMEM126B revealed that NDUF3 accumulated in a complex of ~440 kDa (Fig. 4.11A-D, #). This complex is also observed in control mitochondria, however to a much lower extent. This suggests that the loss of CIA30, Ecsit, ACAD9 or TMEM126B results in a stalled complex harbouring NDUF3 that accumulates if biogenesis is disrupted. Lower molecular weight complexes were also detected in these cell lines, however these were similar to those observed in the control mitochondria (Fig. 4.11A-D).

Analysis of the mitochondria isolated from Δ TIMMDC1 cells showed that the NDUF3-containing complexes observed in the Δ CIA30, Δ Ecsit, Δ ACAD9 or Δ TMEM126B mitochondria were absent, suggesting that the observed complexes are dependent on TIMMDC1. Rather, the NDUF3 accumulated in a lower molecular weight complex of ~130-170 kDa (Fig. 4.11E, **). The complexes containing NDUF3 in the Δ TIMMDC1 mitochondria are also present in control mitochondria, and represent an early stage of the Complex I biogenesis pathway. These data suggests that loss of TIMMDC1 may disrupt the Complex I assembly pathway at an earlier stage than the loss of CIA30, Ecsit, ACAD9 or TMEM126B.

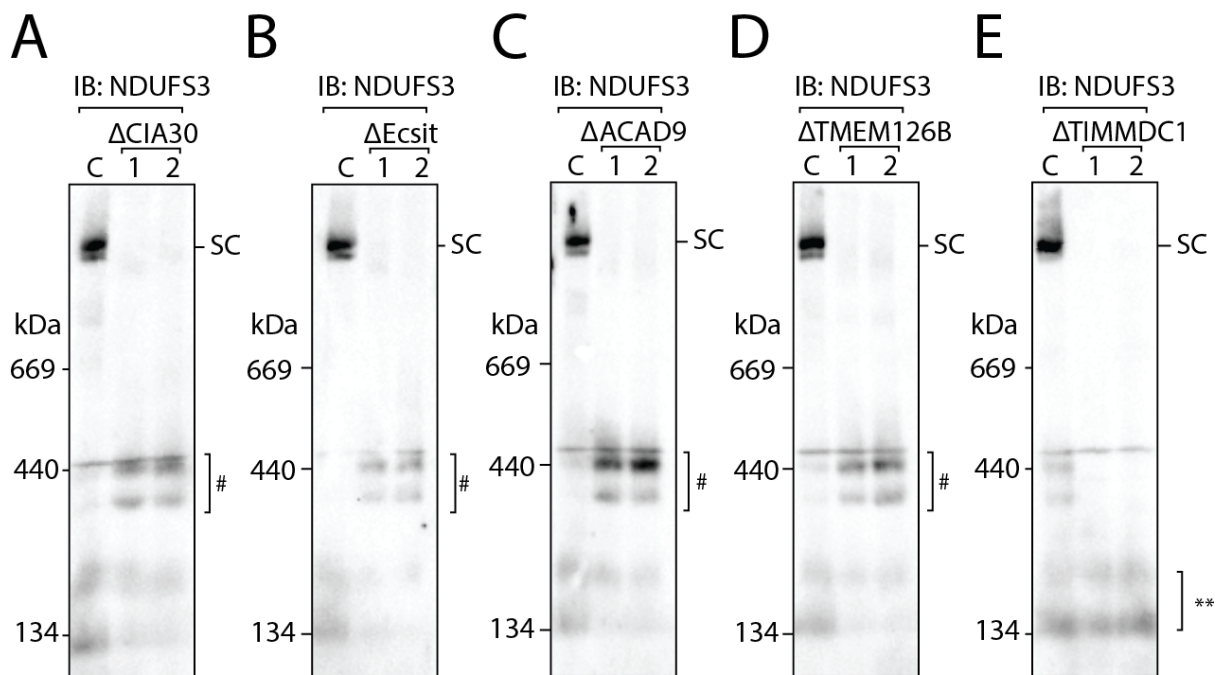


Figure 4.11: Loss of the MCIA complex results in NDUF53 accumulating in a ~440 kDa complex that is dependent on TIMMDC1. Mitochondria were isolated from control and MCIA disrupted cell lines as indicated, solubilised in 1% (w/v) digitonin and complexes analysed by BN-PAGE and immunodecoration using NDUF53 antibodies.

4.11 Identification of a unique loop in TIMMDC1 important for function in Complex I assembly

Sequence alignments of various TIM family protein translocases performed by Guarani et al (2014) showed that TIMMDC1 contained a hydrophilic region that is absent in the human or yeast TIM23 (TIMM23, TIMM23B and TIM23P), TIMM17 (TIMM17A, TIMM17B and TIM17P) and human TIMM22 proteins (Fig 4.12A). Sequence alignment of TIMMDC1 from various species showed that the chemico-physical properties of the residues in the unique region are highly conserved (Fig. 4.12B). This region is located between the first two predicted transmembrane domains of TIMMDC1, located in the conserved Tim17/22/23/PMP24 domain and so may be important for the unique function of TIMMDC1 in Complex I biogenesis. In order to determine if these residues were important for TIMMDC1 function, the residues 'YIEQS' were mutated to Alanine residues (Fig 4.12C, TIMMDC1^{A5}-FLAG). In addition, exome analysis of a cohort of patients with Leigh syndrome identified one patient with a homozygous mutation in the *TIMMDC1* gene resulting in the mutation R225* (David Thorburn, personal communication). This mutation results in a premature stop codon and the loss of the final 60 residues of the TIMMDC1 protein, which does not disrupt the conserved TIMM17/22/23 domain. In order to test the pathogenicity of this mutation and determine if the C-terminal domain was also required for TIMMDC1 function, the final 60 residues were removed deleting the C-terminal domain while maintaining the conserved TIM domain intact (Fig. 4.12C, TIMMDC1^{ΔC60}-FLAG).

The TIMMDC1-FLAG and TIMMDC1^{A5}-FLAG proteins were expressed in Δ TIMMDC1 cells and then analysed by BN-PAGE and SDS-PAGE (Fig. 4.12D). Immunodecoration with antibodies against the Complex I subunit NDUFA9 showed the presence of respiratory super-complexes in control cells, which were absent in the Δ TIMMDC1 cells (Fig. 4.12D). Analysis of the Δ TIMMDC1 cells expressing wildtype TIMMDC1-FLAG showed a partial recovery in super-complex restoration while the TIMMDC1^{A5}-FLAG mutant protein showed reduced capacity (Fig. 4.12D). SDS-PAGE and immunoblot analysis showed that both the wildtype and mutant protein were expressed, albeit at lower levels to endogenous TIMMDC1 (Fig. 4.12D). Interestingly, while the levels of the respiratory chain super-complex were reduced in the TIMMDC1^{A5}-FLAG rescued cells, the levels of the NDUFS5 subunit were restored to the same level as the rescue with wildtype TIMMDC1-FLAG. This suggests that the TIMMDC1^{A5} mutation may be partially functional in the ability to restore the levels of NDUFS5 and the role of the loop in TIMMDC1 performs in Complex I assembly occurs downstream of this. In a similar way, the TIMMDC1^{ΔC60}-FLAG was expressed in Δ TIMMDC1 cells (Fig 4.12E). Following immunodetection of Complex I subunit NDUFA9, it was observed that the both the wild-type TIMMDC1 and TIMMDC1^{ΔC60} mutant were able to partially recover Complex I levels to the same extent (Fig 4.12E). Comparable levels of expression were confirmed by detection of the FLAG epitope using SDS-PAGE, while SDHA was used as a loading control (Fig

4.12E). This suggests that the C-terminal domain of TIMMDC1 is dispensable in Complex I biogenesis.

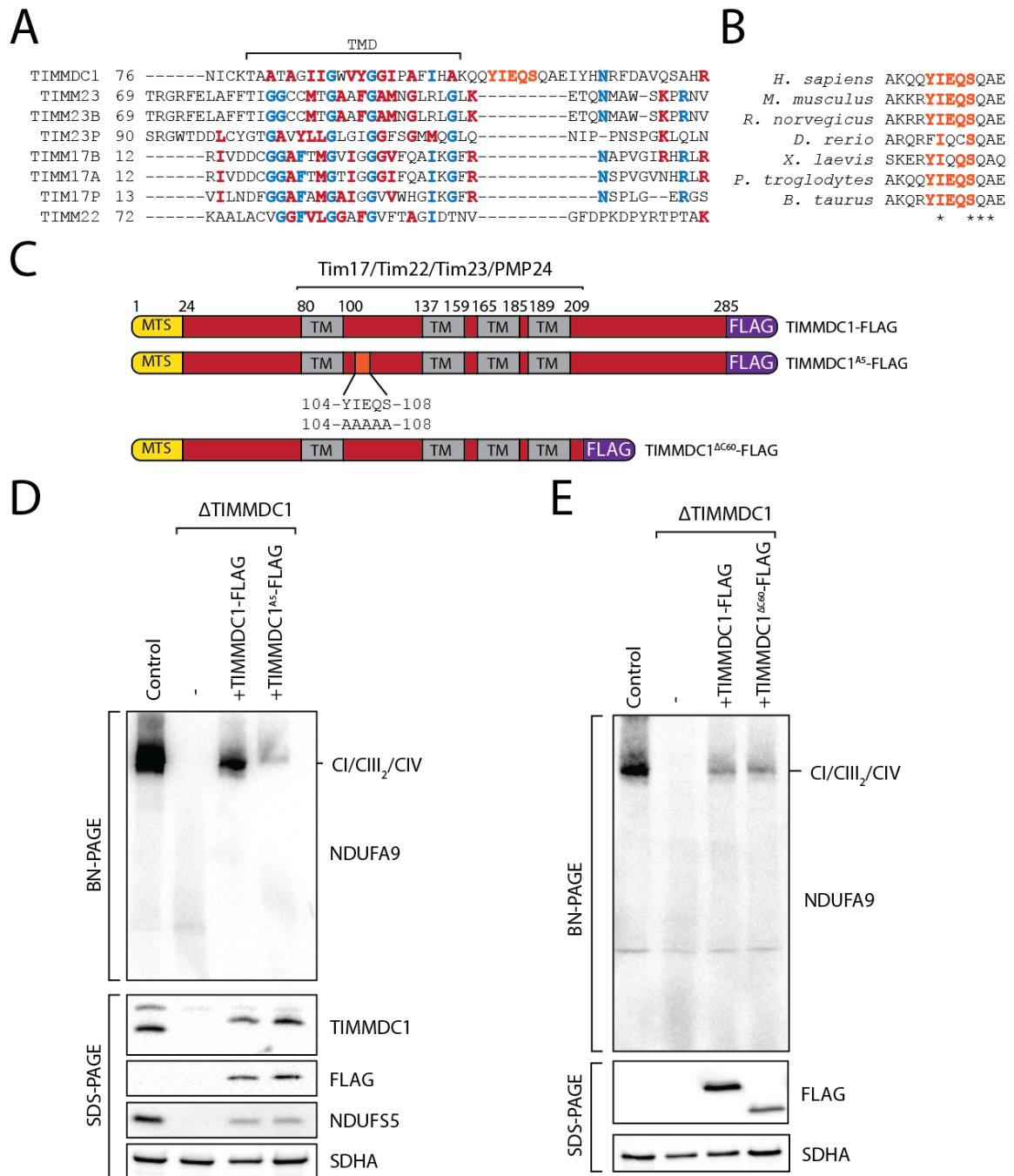


Figure 4.12: A loop in TIMMDC1 is important for Complex I biogenesis. (A) Sequence alignment of various TIM family proteins, with the first transmembrane domain (TMD) shown. Residues shown in red indicate similar chemico-physical properties. Residues shown in blue are identical in at least 50% of the sequences shown. The mutated residues are indicated in orange. **(B)** Sequence alignment showing the conservation of the hydrophilic region amongst TIMMDC1 from various species. Residues similar to the *H. sapiens* TIMMDC1 that mutated in TIMMDC1^{A5} are indicated in orange. **(C)** Schematic representation of TIMMDC1-FLAG, TIMMDC1^{A5}-FLAG and TIMMDC1^{ΔC60}-FLAG constructs generated. The mutations for the TIMMDC1^{A5} are indicated. BN-PAGE, SDS-PAGE analysis and immunodecoration with the indicated antibodies for complementation of **(D)** TIMMDC1^{A5}-FLAG and **(E)** TIMMDC1^{ΔC60}-FLAG.

4.12 The loss of TIMMDC1 affects the translation/stability of mt-ND1, while the loss of CIA30 affects the mt-ND2 protein

The components of the MCIA complexes have been implicated in the biogenesis of the membrane arm of Complex I (Andrews et al, 2013; Dunning et al, 2007). In order to investigate the effect of losing the MCIA complex on the translation and stability of mitochondrial encoded proteins, control, Δ CIA30 and Δ TIMMDC1 were subjected to pulse-chase analysis by radiolabelling of mtDNA-encoded subunits (Fig. 4.13). Following the pulse-chase of cells using [³⁵S]-Methionine, mitochondria were isolated and subjected to SDS-PAGE and phosphorimaging. Analysis of the mtDNA encoded proteins showed translation of all 13 subunits in the control mitochondria (Fig. 4.13B). Analysis of the Δ CIA30 mitochondria showed the translation of all 13 proteins at the 0h post-chase, however by 3h post-chase the signal of mt-ND2 was absent, while the levels of mt-ND1 were reduced (Fig. 4.13B) in agreement with Dunning et al (2007). Analysis of the mtDNA-encoded protein signals demonstrated that the absence of TIMMDC1 resulted in no detectable mt-ND1 signal at any time point analysed (Fig. 4.13B). In addition, the loss of TIMMDC1 did not affect the levels of the mt-ND2 protein signal as observed in the Δ CIA30 mitochondria and rather showed a reduced signal that decayed over time as seen in the control mitochondria (Fig. 4.13B). Western blot analysis was used to confirm the absence of CIA30 and TIMMDC1, while SDHA served as a loading control (Fig. 4.13C). These data suggest that while CIA30 is required for mt-ND2 translation and/or stability, the loss of TIMMDC1 appears to harbour a specific mt-ND1 defect, consistent with the steady state levels determined by immunoblotting. Therefore, while functionally related, CIA30 and TIMMDC1 appear to play different roles in the Complex I assembly pathway.

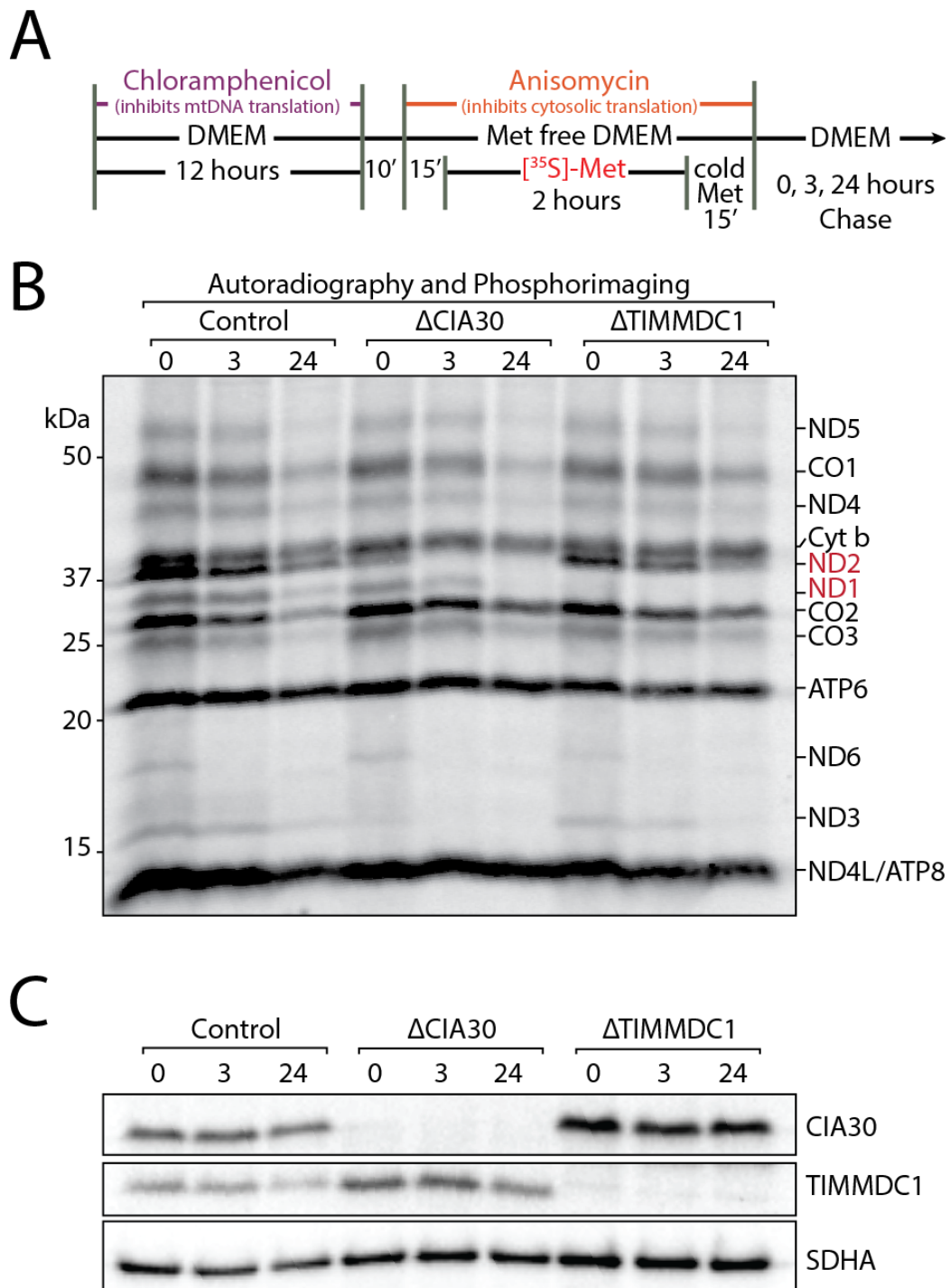


Figure 4.13: Δ CIA30 mitochondria have an mt-ND2-defect, while Δ TIMMDC1 mitochondria harbour an mt-ND1 defect. (A) The radiolabelling procedure used. Following inhibition of the mitoribosome by chloramphenicol, cells were incubated with the cytosolic ribosome inhibitor. Following this, cells were incubated with $[^{35}\text{S}]$ -Met to label mtDNA-encoded proteins and subsequently chased for 0, 3 or 24 hours. **(B)** Following pulse-chase treatment, mitochondria were isolated and subjected to SDS-PAGE and autoradiography. Complex I: mt-ND1, mt-ND2, mt-ND3, mt-ND4, mt-ND4L, mt-ND5, mt-ND6. Complex III: Cyt *b*. Complex IV: CO1, CO2, CO3. Complex V: ATP6, ATP8. **(C)** Western blot analysis of samples using antibodies directed to CIA30, TIMMDC1 and the loading control SDHA.

4.13 TIMMDC1 interacts with newly synthesised mt-ND1, while CIA30 interacts with mt-ND2

To determine if CIA30 or TIMMDC1 interact with newly synthesised mtDNA encoded proteins, CIA30-FLAG and TIMMDC1-FLAG were transfected into their respective cell line, radiolabelling pulse and chase was performed, followed by co-immunoprecipitation of FLAG-tagged proteins (Fig. 4.14A). Control cells that were not transfected and hence lacking the FLAG epitope were treated in the same manner. Analysis of the CIA30-FLAG elutions showed that a species that corresponded to the size of mt-ND2 was present at the 0h time point, which then reduced over time (Fig. 4.14B, CIA30-FLAG). By the 24h time-point, there was very little signal suggesting that by this time, any protein that was engaged with the CIA30-FLAG early in the biogenesis pathway had been released. A similar observation was made following analysis of the TIMMDC1-FLAG elutions, however, the observed species migrated faster than that observed for CIA30-FLAG indicating that TIMMDC1 may initially be in a complex containing mt-ND1 (Fig. 4.14B, TIMMDC1-FLAG). To a lesser extent, it appeared that TIMMDC1-FLAG may also be in association with mt-ND4 and mt-ND5, however, the enrichment of mt-ND1 was much stronger. In a similar way to the CIA30-FLAG elutions, the signal from TIMMDC1-FLAG elutions decreased over time relative to the input, suggesting over this time period the labelled protein is maturing and no longer associated with the TIMMDC1 protein. The signal from the control elution showed very little non-specific binding except for a signal that may correspond to the proteins mt-ND4L or ATP8. In order to confirm specific enrichment of the FLAG proteins, the samples were subject to immunoblot analysis using antibodies against the FLAG epitope and the SDHA protein (Fig. 4.14C). Analysis showed that the FLAG protein was present in the input samples and enriched in the FLAG elution samples (Fig. 4.14C, FLAG). On the contrary, the protein SDHA was present in the input samples, but was absent in the elutions, suggesting specific binding of the FLAG and associated proteins (Fig. 4.14C, SDHA). From this data, it can be concluded that CIA30 and TIMMDC1 engage different subsets of Complex I intermediates early in the biogenesis pathway and the loss of these proteins affect different stages of Complex I assembly.

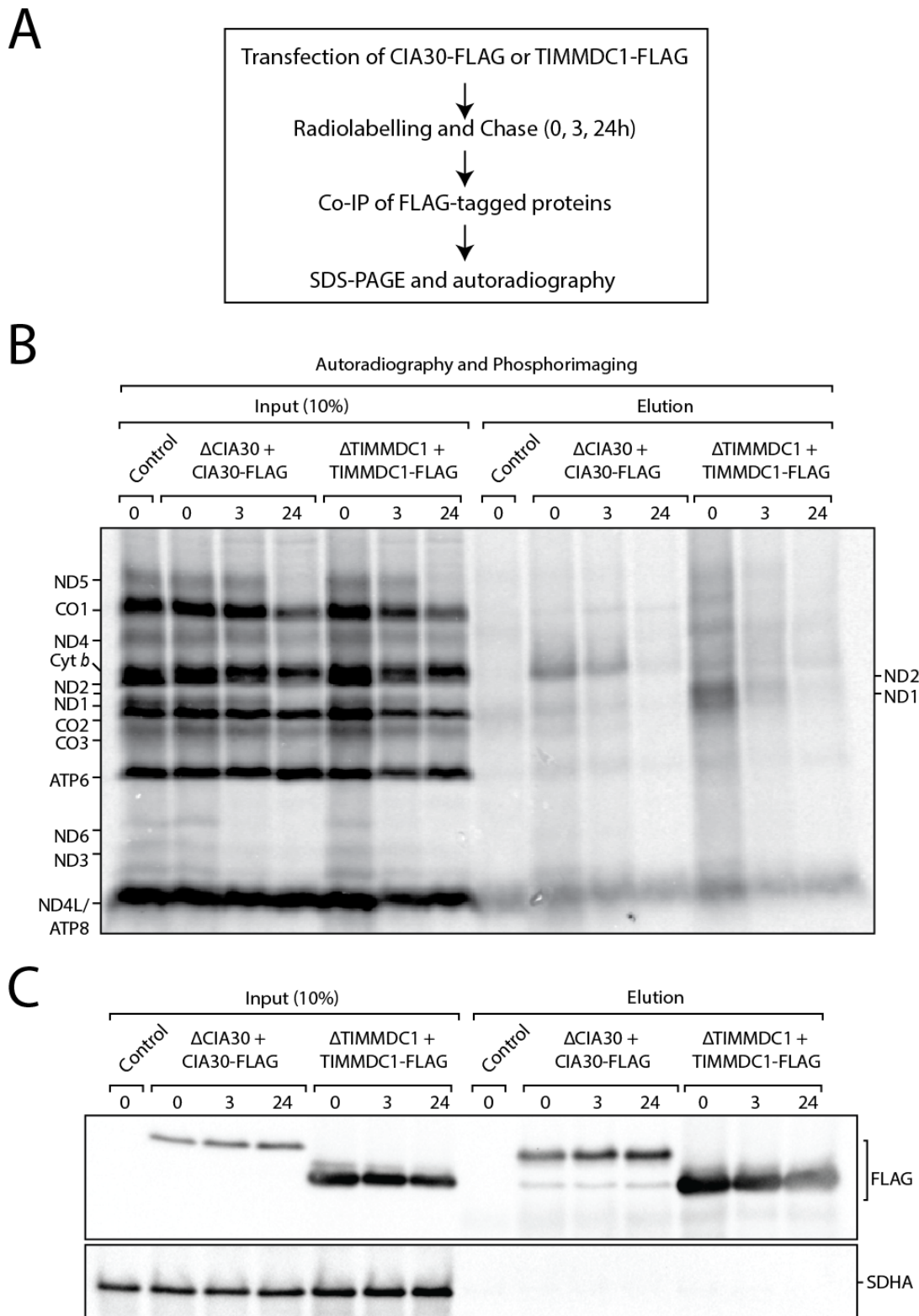


Figure 4.14: CIA30 and TIMMDC1 associate with mtDNA-encoded proteins early in the assembly pathway. (A) Transfection, radiolabelling and Co-IP procedure used. **(B)** Following transfection and pulse-chase treatment, mitochondria were isolated and subjected to FLAG co-immunoprecipitation using TX-100 followed by SDS-PAGE and autoradiography. Complex I: mt-ND1, mt-ND2, mt-ND3, mt-ND4, mt-ND4L, mt-ND5, mt-ND6. Complex III: Cyt b. Complex IV: CO1, CO2, CO3. Complex V: ATP6, ATP8. **(C)** Western blot analysis of samples using antibodies directed to the FLAG epitope and the control SDHA.

4.14 Loss of TIMMDC1 more closely resembles the disruption of Complex I assembly at an early stage

The absence of TIMMDC1 resulted in a loss of mt-ND1, which differed to the disruption of CIA30. Other assembly factors that have been identified have also been shown to harbour defects in the levels of mt-ND1, and function at an early stage of the Complex I assembly pathway (McKenzie et al, 2011; Rendón et al, 2014; Rendón & Shoubridge, 2012). To investigate the relationship of TIMMDC1 with other cell lines harbouring defects in early stage Complex I biogenesis further, *NDUFAF4* and *NDUFAF6* were targeted for gene disruption (Rendón & Shoubridge, 2012). TALEN pairs were designed to target the region encoding the mitochondrial targeting signal in both the *NDUFAF4* and *NDUFAF6* genes. Analysis of clones showed the presence of 2 alleles harbouring indels (Fig. 4.15A). The Δ *NDUFAF4* cell line harboured a 208 nucleotide deletion that spanned the 5' UTR, exon 1 and a region of intron 1. The other allele contained a 14 nucleotide deletion and resulted in a frame-shift that caused premature termination after 10 codons (Fig. 4.15A, Δ *NDUFAF4*). The Δ *NDUFAF6* cell line contained two separate deletions of a 17 and 20 nucleotides, both disrupting the reading frame (Fig. 4.15A, Δ *NDUFAF6*).

In order to compare the effects of the loss of TIMMDC1 with defects in other stages of Complex I assembly, the Δ TIMMDC1 cell line was compared against cell lines with disruption to the early- (Δ *NDUFAF4* and Δ *NDUFAF6*), mid- (Δ *CIA30*) or late- (Δ *FOXRED1*) stages of assembly. SDS-PAGE analysis of *CIA30*, *TIMMDC1* and *NDUFAF4* in the selected cell lines confirmed the loss of each protein in their respective disruption cell line (Fig. 4.15B). Antibodies against *NDUFAF6* were unavailable and so protein levels could not be assessed. Interestingly, the levels of *NDUFAF4* were decreased in the absence of *NDUFAF6*, suggesting that the stability of a portion of *NDUFAF4* was dependent on the presence of *NDUFAF6* (Fig 4.15C). Analysis of the Complex I subunits mt-ND1 and *NDUFA13* in these cell lines showed that the loss of TIMMDC1 behaved much like the cell lines with disruptions to the *NDUFAF4* and *NDUFAF6* genes with no detectable mt-ND1 and a reduction the levels of *NDUFA13* (Fig. 4.15B). The loss of *CIA30* or *FOXRED1* also reduced the levels of these proteins, however, not to the same extent as TIMMDC1, *NDUFAF4* and *NDUFAF6*. Analysis of the levels of *NDUFS5* across these cell lines showed a similar level of reduction in the absence of *CIA30*, *TIMMDC1*, *NDUFAF4* and *NDUFAF6*, while the levels of *NDUFS3* were more variable suggesting this protein was more responsive to the individual function of each assembly factor (Fig. 4.15B).

The steady-state level patterns of the cell lines is consistent with TIMMDC1 acting as an early stage assembly factor. To investigate this further, analysis of *ACAD9* in these cell lines was performed by solubilisation of mitochondria in digitonin followed by BN-PAGE and immunoblotting (Fig. 4.15C). Analysis of the *ACAD9*-containing complexes showed that the loss

of CIA30 inhibited the assembly of ACAD9 into its native higher order complexes as shown previously. Interestingly, the complexes of ACAD9 in the absence of TIMMDC1, NDUFAF4 and NDUFAF6 were comparable to each other, however, different to the control mitochondria. This suggests that the absence of TIMMDC1, NDUFAF4 and NDUFAF6 results in the same overall effect on ACAD9, and that these proteins act at the same stage of Complex I assembly. Interestingly, the profile of ACAD9 complexes in the Δ FOXRED1 cell line was similar to the control cells, with some changes in the abundance of various complexes (Fig. 4.15C). This may indicate that FOXRED1 functions downstream of ACAD9 as the loss of FOXRED1 leaves ACAD9-containing complexes the least perturbed relative to the other assembly factor disruptions analysed.

To assess the behaviour of the membrane arm subunit NDUF6 upon disruption of Complex I biogenesis at various stages of assembly, isolated mitochondria were solubilised in Triton X-100 and subjected to BN-PAGE and immunoblotting using NDUF6 antibodies. Analysis showed that in control cells NDUF6 accumulated in mature Complex I, while the absence of CIA30, TIMMDC1, NDUFAF4 or NDUFAF6 resulted in NDUF6 accumulating in a complex of ~400 kDa. In the absence of FOXRED1, the ~400 kDa complex was present, however, a low level of mature Complex I was also observed, suggesting the biogenesis pathway may not be efficient in the absence of FOXRED1 and the ~400 kDa intermediate containing NDUF6 complex may accumulate. These data suggest that Complex I defects relating to various assembly factors display trends common to proteins that act at the same stage. This can help elucidate the role these proteins play and the stage of Complex I biogenesis the assembly factors are important in.

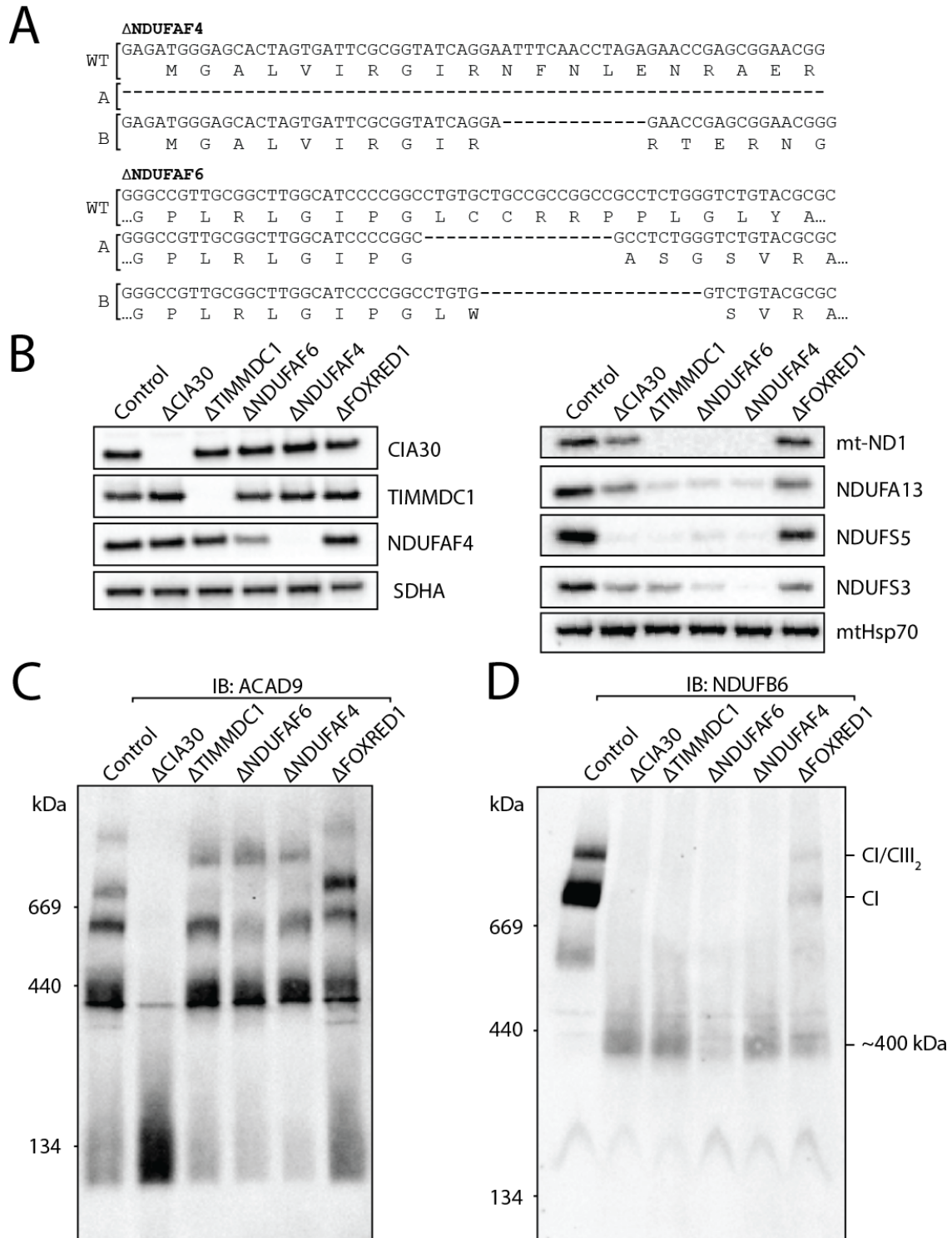


Figure 4.15: Loss of TIMMDC1 resembles the ΔNDUFAF4 and ΔNDUFAF6 disruption cell lines. (A) Genomic validation of the *NDUFAF4* and *NDUFAF6* gene disruptions performed by Sanger sequencing. The generated deletions are indicated as A and B with the corresponding translation shown. **(B)** Isolated mitochondria from the indicated cell lines were subjected to SDS-PAGE and immunoblotting. SDHA and mtHsp70 were used as loading controls. **(C)** Isolated mitochondria from the indicated cell lines were solubilised in 1% (w/v) digitonin, subjected to BN-PAGE and immunoblotted with ACAD9 antibodies **(D)** Isolated mitochondria from the indicated cell lines were solubilised in 1% (w/v) TX-100, subjected to BN-PAGE and immunoblotted with NDUFB6 antibodies.

4.15 Global Complex I levels suggest TIMMDC1 behaves in a similar fashion to the other MCIA complex proteins.

To determine the relationship of the MCIA complex with other stages of the Complex I biogenesis pathway, quantitative proteomics using SILAC mass spectrometry was performed with the assistance of Dr David Stroud (Ryan Lab, Monash University). Unbiased hierarchical clustering of cell lines containing similar Complex I defects placed the components of the MCIA complex together, suggesting the various gene disruptions harbour similar outcomes for Complex I subunits (Fig. 4.16). Interestingly, TIMMDC1 clusters with the other MCIA complex disruption cells lines and the early assembly factor NDUFAF6, highlighting an intermediate role for TIMMDC1 between the two stages of assembly (Fig. 4.16). In a similar way, individual subunits were clustered based on similar proteomic profiles in the various cell lines analysed (Fig. 4.16). Subunits comprising different regions of Complex I generally grouped together, consistent with different modules that make up the enzyme. Analysis showed that upon disruption of any stage of Complex I biogenesis, subunits comprising the N-module were destabilised, consistent with their latter stage of incorporation into the enzyme (Mimaki et al, 2012). The loss of NDUFAF4 and NDUFAF6 resulted in a loss of Complex I subunits comprising the Q-module including the matrix arm subunits NDUFS2, NDUFS3 and NDUFS7 and the membrane subunits mt-ND1 and NDUFA13 (Fig. 4.16). The loss of the MCIA complex resulted in a defect of the proximal P-module, consistent with a role in the biogenesis of the mt-ND2 containing intermediate.

Proteomic analysis of mitochondria derived from Δ TIMMDC1 cells additionally showed a decreased amount of mt-ND1 and NDUFA13 proteins relative to other MCIA complex disruptions, consistent with immunoblotting, immunoprecipitation and radiolabelling data. Additionally, the loss of TIMMDC1 did not affect the Q-module to the same extent as the loss of NDUFAF4 or NDUFAF6, suggesting that this part of the biogenesis pathway is less affected by the loss of TIMMDC1. These data confirm that while TIMMDC1 is required for the early stages of Complex I biogenesis, this protein is tightly connected with the MCIA complex and may act as a link between the early and mid-stages of the assembly pathway.

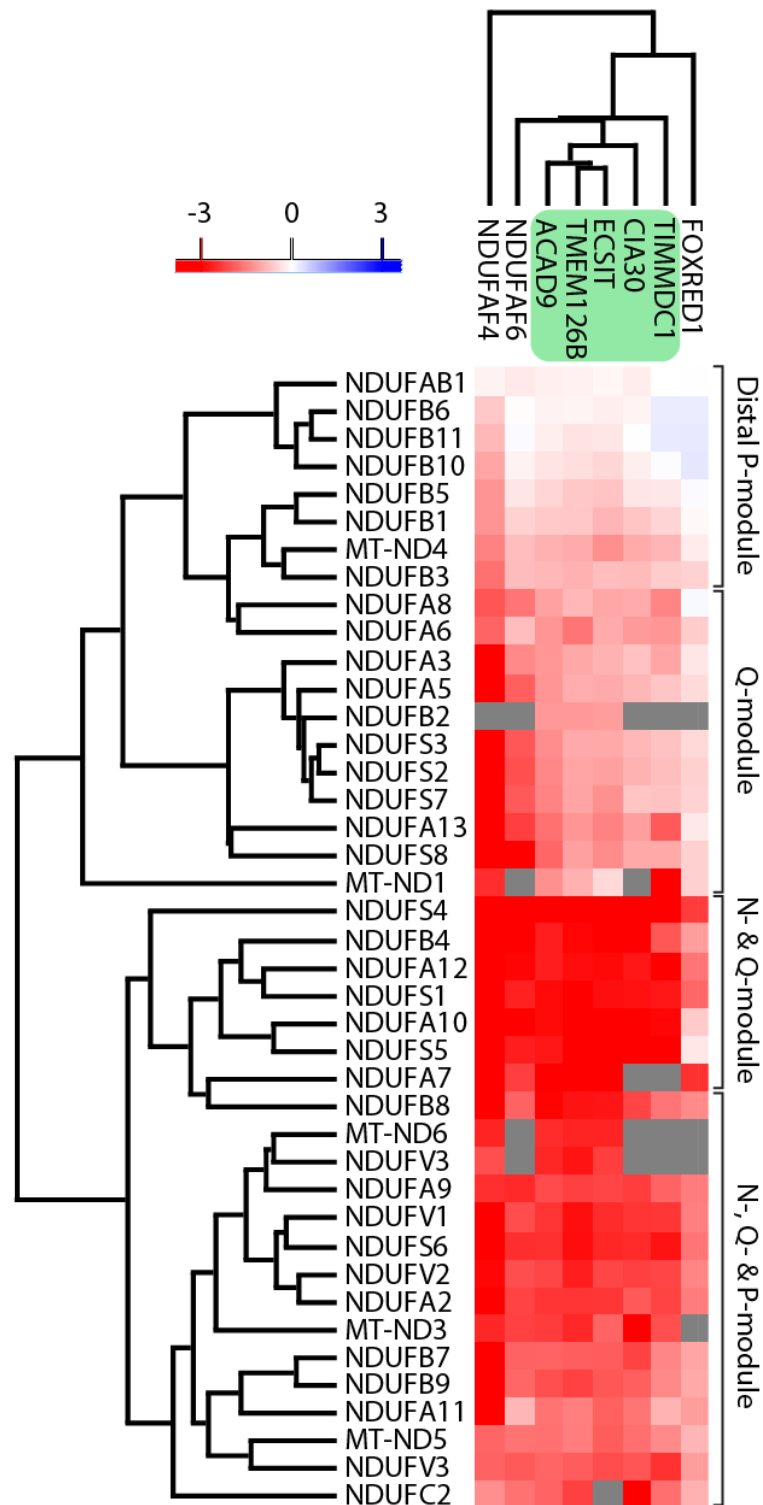


Figure 4.16: Quantitative proteomics and hierarchical clustering shows that TIMMDC1 behaves as a component of the MCIA complex. Quantitative mass spectrometry analysis of the generated Complex I assembly factor disruption cell lines. Each row represents one Complex I subunit, while each column represents the behaviour of Complex I in a particular cell line. Both Complex I subunits and cell lines are clustered based on similarity. The MCIA complex gene disruption cell lines are indicated in green. Regions of Complex I that cluster are shown on the right. The scale bar indicates the fold change of a protein. Grey boxes indicated the protein was not detected.

4.16 Discussion

4.16.1 TIMMDC1 functions at the nexus of the mt-ND1 and mt-ND2 assembly modules

Analysis of the MCIA complex disruptions strongly suggests that while TIMMDC1 is found in association with CIA30, Ecsit, ACAD9 and TMEM126B, the primary role of this protein is to assemble or stabilise the mt-ND1 subunit and an early Complex I intermediate. The loss of mt-ND1 has been observed upon loss or knockdown of a number of early stage assembly factors including NDUFAF3-7, but not the late stage assembly factor NDUFAF2 (McKenzie et al, 2011; Rendón et al, 2014; Rendón & Shoubridge, 2012). Similar defects observed in the absence of TIMMDC1 would suggest that TIMMDC1 acts together with these proteins to assemble and stabilise this early intermediate. Quantitative proteomic analysis suggests however, that the absence of TIMMDC1 clusters more closely to the other MCIA complex components rather than the other early stage assembly factors. This is likely due to the stability of the Q-module subunits in the absence of TIMMDC1, while in the absence of the other early stage assembly factors NDUFAF4 and NDUFAF6, the levels of Q-module subunits are reduced. This observation suggests that while the initial soluble components of the Q-module are relatively stable in the absence of the mt-ND1 intermediate as seen in the Δ TIMMDC1 mitochondria, the initial Q-module assembly is critical for the stability of newly translated mt-ND1. In support of this, the assembly factor NDUFAF7 has been shown to methylate the subunit NDUFS2, and the loss of NDUFAF7 results in depletion of NDUFS2 (Rendón et al, 2014; Rhein et al, 2013). The loss of NDUFAF7 also results in rapid turnover of mt-ND1 in an AFG3L2-dependent manner (Rendón et al, 2014). So while the primary role of NDUFAF7 is as a methyltransferase for the subunit NDUFS2, secondary effects in the absence of NDUFAF7 result in the loss of mt-ND1. In accordance with the proteomic data presented, it is likely that the loss of either NDUFAF4 or NDUFAF6 results in a loss of stability and assembly of the Q-module sub-complex, with the observed mt-ND1 defects seen by immunoblotting are secondary to this. This suggests that while NDUFAF4, NDUFAF6 and NDUFAF7 are required for the assembly of the Q-module, TIMMDC1 is not required for this stage, but rather required for biogenesis of the initial seed of the membrane arm consisting of mt-ND1 and other subunits. Further to this, the loss of CIA30, Ecsit, ACAD9 or TMEM126B resulted in the accumulation of a ~440kDa sub-complex that contained at least the assembly factor TIMMDC1 and the subunit NDUFS3. The rapid loss of mt-ND1 in the absence of TIMMDC1, and the association mt-ND1 with TIMMDC1-FLAG early in the assembly pathway would also suggest that the TIMMDC1-containing complex harbours mt-ND1. Based on the structure of bovine Complex I other subunits including NDUFS2 may also a part of this complex (Vinothkumar et al, 2014).

In contrast to this, the interplay between CIA30, Ecsit, ACAD9 and TMEM126B was evident through biochemical and proteomic analysis and disruption to this assembly complex likely hinders the biogenesis of the mt-ND2 containing intermediate of Complex I. The interdependence of these proteins was most clear upon steady-state analysis of these proteins, as well as the similar Complex I defects observed. Interestingly, the loss of TMEM126B resulted in a severe Complex I defect as observed for all MCIA complex disruptions, however, the levels of other MCIA components were unchanged relative to the control mitochondria. Further to this, in the absence of TMEM126B, the protein ACAD9, and presumably CIA30 and Ecsit, are still capable of assembly into higher molecular weight complexes with slight differences relative to the control. This was also observed upon knockdown of TMEM126B in 143B osteosarcoma cells (Heide et al, 2012). This was relatively unexpected as TMEM126B was thought to act as a membrane anchor for the other MCIA complex proteins. This suggests that the TMEM126B is dispensable for the remaining MCIA complex proteins to interact with at least a subset of other Complex I proteins or the mitochondrial inner membrane, while still resulting in an overall severe Complex I deficiency. Given that TMEM126B harbours 4 predicted transmembrane domains, it may be possible that this protein may function in the integration of proteins that form the mt-ND2 containing complex. The relationship between these proteins is not uniform, and the loss of any of CIA30, Ecsit or ACAD9 greatly reduces the amount of TMEM126B observed. It may be possible that CIA30, Ecsit and ACAD9 are required to maintain stability of the putative translocon that TMEM126B forms to function in the assembly of Complex I. The loss of any protein then compromises the stability of TMEM126B resulting in the Complex I deficiency. How CIA30, Ecsit and ACAD9 individually contribute to the stability of TMEM126B and whether they perform additional functions in Complex I biogenesis still remains to be determined. A model depicting the possible role of the MCIA complex in the biogenesis of Complex I is present in figure 4.17.

While this work has uncovered much about the assembly pathway upon disruption of the early or mid-stage of Complex I biogenesis further work into how these proteins perform these vital roles needs to be investigated. The mechanism is clearly different, as the loss of different assembly factors at the same stage can have different outcomes for the assembly pathway. Understanding the role of assembly factors at the molecular levels will lead to greater insights into how they perform this vital function and how defects lead to diseases.

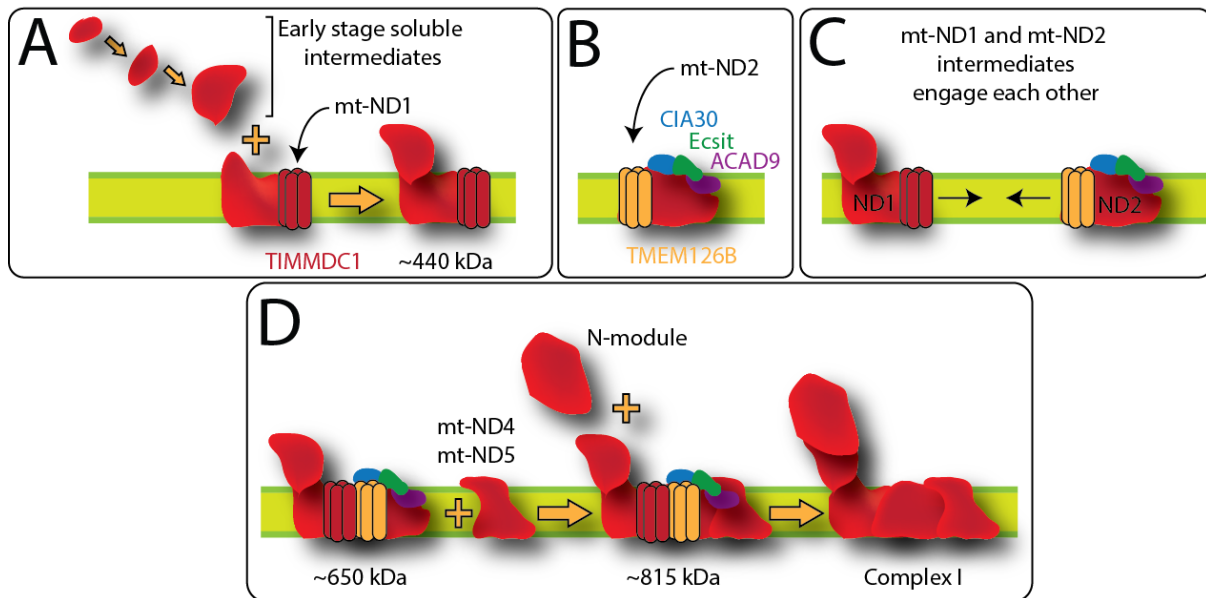


Figure 4.17: The MCIA complex may mediate the assembly of the mt-ND1 and mt-ND2 intermediates during the assembly of Complex I. (A) Early in Complex I assembly, a soluble intermediate and a membrane-bound intermediate is formed. This intermediate of ~440 kDa is composed of at least mt-ND1, NDUFS3 and TIMMDC1. **(B)** During the mid-stage of Complex I assembly, the mt-ND2 complex is formed with CIA30, Ecsit, ACAD9 and TMEM126B. **(C)** Upon completion of the individual intermediates, the mt-ND1 and mt-ND2 modules engage each other and to form the ~650 kDa intermediate. **(D)** This intermediate can then form the ~815kDa intermediate upon assembly with the distal part of the membrane arm containing mt-ND4, mt-ND5 and other subunits, which then assembles with the N-module to form the mature Complex I.

4.16.2 The subunits NDUFS5 and NDUF6 behave in a similar fashion if early or mid-stage assembly is disrupted

Analysis of the various assembly disruption cell lines showed that defects in the early or mid-stage of Complex I biogenesis resulted in the absence of the Complex I subunit NDUFS5. The NDUFS5 protein is ~15 kDa and harbours a twin CX₉C motif that directs NDUFS5 to the mitochondrial intermembrane space via the Mia40/CHCHD4 import and oxidative folding pathway (Szklarczyk et al, 2011). The assembly of NDUFS5 is thought to assemble late in the process as no detectable intermediates contain this protein (Antonicka et al, 2003; Ugalde et al, 2004), nor was CIA30 able to co-immunoprecipitate NDUFS5 (Dunning et al, 2007). Also, patient fibroblasts deficient of CIA30 also lacked detectable NDUFS5 (Dunning et al, 2007). This suggests that the incorporation of NDUFS5 occurs downstream of the MCIA complex function. In the absence of an intermediate for NDUFS5 to integrate into, degradation of this protein may be mediated by the *i*-AAA protease Yme1L present in the mitochondrial intermembrane space (Fig. 4.18)(Stiburek et al, 2012). It has been shown that defects in the folding or stability of small TIM proteins such as TIM9 and TIM10 (which have a similar fold to NDUFS5) are turned over in a Yme1 dependent manner in yeast (Baker et al, 2012). Interestingly, the subunit NDUF8, which harbours 4 CX₉C motifs appears more stable than NDUFS5 and follows a pattern of degradation akin to mt-ND1 and NDUF13 (Szklarczyk et al, 2011). This suggests that while the NDUFS5 subunit requires both the mt-ND1 and mt-ND2 intermediates to be incorporated into Complex I, the subunit NDUF8 only requires the mt-ND1 containing complex for partial stability. Indeed, the most recent structural analysis of bovine Complex I reveals that the bovine homologue of NDUF8 (PGIV) is located at the 'heel' of the complex (in vicinity of mt-ND1 and NDUF13) while NDUFS5 (15 kDa in *B. taurus*) is located close to both the mt-ND1 and mt-ND2 intermediates (Zhu et al, 2015), suggesting successful integration of NDUFS5 requires both the mt-ND1 and mt-ND2 containing modules to be present and assembled.

Previous studies indicate that the NDUF6 subunit of the membrane are assembles into an ~400 kDa intermediate (Ugalde et al, 2004). The observation of a NDUF6-containing complex in mitochondria lacking early or mid-stage assembly factors strongly suggests that the complex is stalled and further assembly into intermediates and finally Complex I is not possible. Because the NDUF6-containing complex is present in both the Δ TIMMDC1 and Δ CIA30 mitochondria, it would be expected that this complex lacks mt-ND1 or mt-ND2 proteins. This complex may instead consist of the distal tip of the membrane arm of Complex I containing mt-ND4 as well as NDUF6. Proteomic analysis of mitochondria isolated from various cell lines suggests that both NDUF6 and mt-ND4 protein levels are relatively stable. Furthermore, the protein subunits NDUF1, NDUF3, NDUF5, NDUF10, NDUF11 and NDUFAB1 cluster closely with NDUF6, suggesting

that these proteins may also be stabilised in this complex (Fig. 4.18). A recent study has elucidated further structural features of the membrane arm of Complex I by x-ray crystallography and has demonstrated that NDUFB10, NDUFB11 and NDUFAB1 are present in proximity to the mt-ND4 protein (Zhu et al, 2015). Further studies to identify the components of this sub-complex will provide greater insights into the biogenesis of the membrane arm of Complex I and how defects in these subunits can lead to Complex I deficiency.

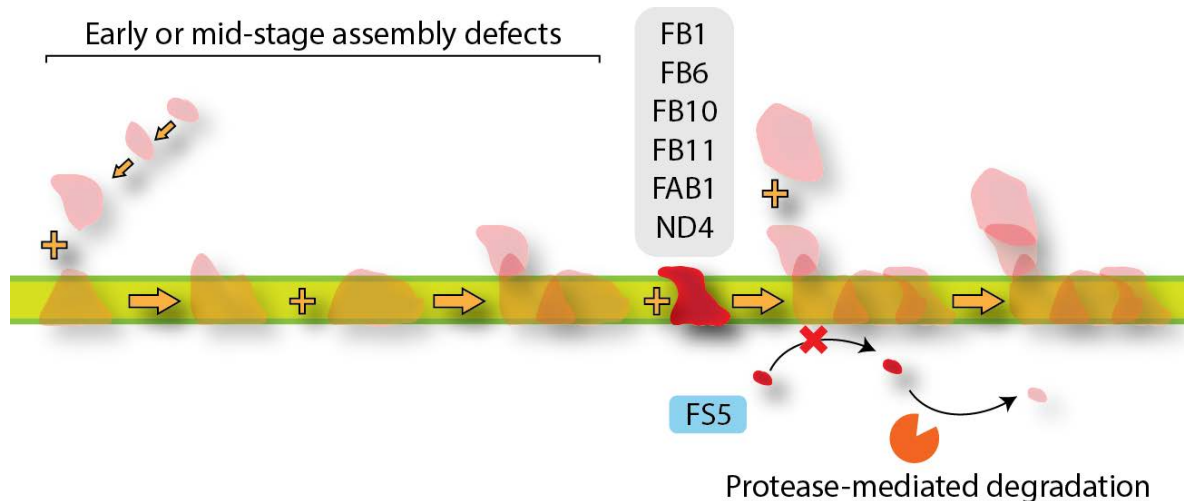


Figure 4.18: Early or mid-stage defects result in the accumulation of an NDUFB6 containing complex and turnover of NDUFS5. The loss of early or mid-stage assembly factors results in the accumulation of an ~400 kDa complex containing NDUFB6 and possibly mt-ND4, NDUFB1, NDUFB10, NDUFB11 and NDUFAB1 that likely comprise part of the distal region of the Complex I membrane arm. In the absence of a stable Complex I intermediate for the incorporation of the intermembrane space subunit NDUFS5, this protein is unable to assemble and is degraded.

4.16.3 Mutagenesis of CIA30 and TIMMDC1 provides insights into their role in Complex I biogenesis and disease

Complementation analysis using the CIA30 mutations identified in patients with Complex I deficiency revealed insights into the behaviour of these mutant proteins. Of these mutations, four were shown to be hypomorphic in nature (D83N, H93R, R211C and K253R) where analysis has shown that overexpression of mutant CIA30 proteins in Δ CIA30 cells was capable of restoring the Complex I defect observed. Interestingly, expression of CIA30 harbouring T207P or G245R mutations were unable to restore Complex I suggesting that these mutations are loss-of-function mutations observed in the patients. The introduction of a proline residue likely results in the disruption of local secondary structure, destabilising the hydrogen bond network in a probable α -helix, causing the protein to become destabilised and non-functional. The substitution of the simple hydrogen side chain of a glycine residue to the sterically large and positively charged side-chain of arginine appears to have detrimental effects on CIA30 function. To fully understand the pathogenicity of these changes, the structural determination of CIA30 and interacting proteins such as Ecsit and ACAD9 would provide further insights into why changes to these residues results in Complex I deficiency.

Analysis of a potential TIMMDC1 mutation identified in a cohort of patients with Leigh syndrome demonstrated that the loss of the final 60 residues of the protein did not affect the ability of this protein to assemble Complex I upon expression in HEK293T cells lacking TIMMDC1. Indeed, preliminary analysis of patient-derived fibroblasts do not suggest a Complex I deficiency, suggesting this mutation may not be the cause of Leigh syndrome observed. In contrast, the substitution of five residues unique to TIMMDC1 in the conserved TIM domain, and not present in other TIM family proteins reduced the ability of Complex I to assemble. Based on homology to the TIM family proteins, this region likely resides in the matrix side of the membrane (Guarani et al, 2014; Pudelski et al, 2010) and may be important in mediating interactions with Complex I subunits, other Complex I assembly factors or other proteins/complexes such as the mito-ribosome. Upon expression of the TIMMDC1^{A5} mutant, the levels of the Complex I subunit NDUFS5 detected by western blotting were restored to the same extent as the complementation with wild-type TIMMDC1. The significance of this requires further analysis, however this would suggest these residues may play a role downstream of the incorporation of NDUFS5 in the Complex I assembly pathway. These results suggest that the C-terminal domain is not required for Complex I assembly, and further work is necessary to determine what this region of the protein may be required for.

Chapter 5

*Identification of CIA30-
interacting proteins using
proximity based biotin labelling*

5.1 Introduction

Numerous approaches have been used to identify new components of the Complex I assembly machinery. These methods include analysis of components within assembly intermediates (Kuffner et al, 1998), identification of genes following whole genome subtraction of fermentative and aerobic yeast (Ogilvie et al, 2005) and in patients with Complex I deficiency (Calvo et al, 2010; Sugiana et al, 2008), and analysis of interactions with known Complex I assembly factors (Nouws et al, 2010). In addition, proteomic approaches including analysis of the evolutionary relationship of proteins with Complex I (Pagliarini et al, 2008), complexome profiling (Heide et al, 2012) and systems-based co-immunoprecipitation (Guarani et al, 2014) have been used. This has greatly increased the knowledge about the assembly factors required for Complex I biogenesis.

Approximately 50% of patients with a Complex I deficiency are yet to have a molecular diagnosis as no pathogenic mutations have been identified in Complex I subunits or known assembly factors (Hoefs et al, 2012). Furthermore, in comparison to the biogenesis of mitochondrial Complex IV, which requires at least 14 assembly factors for the biogenesis of an 11-subunit enzyme (Soto et al, 2012), it is expected that a number of proteins involved in the biogenesis of Complex I remain to be identified. In order to identify novel components of the Complex I assembly machinery, proximity-dependent biotin labelling of proteins was performed (Roux et al, 2012). This method, known as BioID (proximity-dependent biotin identification), utilises the promiscuous bacterial biotin ligase BirA* to covalently modify proteins in close proximity of the protein of interest (Choi-Rhee et al, 2004). This is achieved by the generation of a chimeric protein consisting of the protein of interest and the biotin ligase BirA*. Upon expression of the fusion protein, the BirA* can generate active biotin in the form of biotinyl-5'-AMP, which can readily react with primary amines close to the site of generation, and therefore, labelling proteins in close proximity (Choi-Rhee et al, 2004). Because the labelling occurs in a covalent manner, transient spatial and temporal interactions are maintained, providing a powerful tool for the analysis of interaction networks. In order to maximise the efficiency of incorporation and assembly of the fusion protein and minimise the effects of endogenous protein lacking a BirA* moiety, proteins were expressed in a cells that have undergone genome editing to disrupt expression of the endogenous protein. Furthermore, to avoid overexpression of the BirA* fusion protein that may lead to non-specific labelling, retroviral-mediated stable expression of the fusion protein was performed at levels similar to that of the endogenous protein.

To identify novel proteins that may be involved in Complex I assembly CIA30 was chosen as the bait protein, as this protein appears in multiple assembly intermediates (Fig. 5.1A). Since these intermediates incorporate different proteins at the various stages of the assembly process, it

would be expected that the CIA30-BirA* chimera could act to label proteins in these intermediates including potential novel assembly factors (Fig. 5.1B).

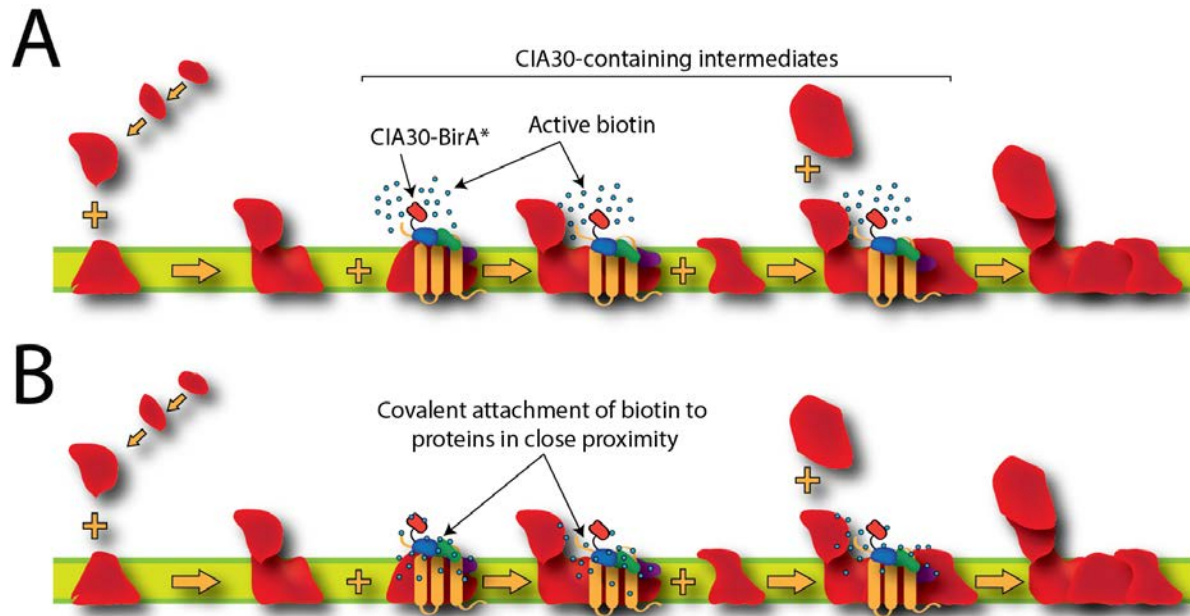


Figure 5.1: CIA30 can be used as a bait for the identification of potential new Complex I assembly factors using biotin-mediated proximity labelling of proteins. (A) Expression of CIA30-BirA*-HA can produce activated biotin in close proximity to intermediates that contain CIA30. **(B)** The active biotin can then covalently attach to proteins that can then be enriched and identified by mass spectrometry.

5.2 Generation of CIA30-BirA*-HA expressing cells in the Δ CIA30 cell line background

In order to investigate potential CIA30-binding partners involved in Complex I biogenesis, cell lines stably expressing CIA30-BirA*-HA or CIA30-HA were generated using pseudotyped pantropic retrovirus produced in HEK293T cells (Fig. 5.2A). To avoid competition of the transduced proteins with endogenous CIA30, viral particles with the ORF of interest were applied to Δ CIA30 cells for viral transduction and stable incorporation of the CIA30-BirA*-HA or CIA30-HA coding regions into the host genome. Following expression of the transduced proteins, selection of cells with functional Complex I was performed by incubation of cells in culture media containing galactose for 24 hours. Labelling of CIA30-BirA*-HA and CIA30-HA expressing cells was performed in the presence of 50 μ M Biotin, followed by pulldown using streptavidin beads, tryptic digest and proteomic analysis (Fig. 5.2A).

Expression of CIA30-BirA*-HA (~70 kDa) and CIA30-HA in the Δ CIA30 cell line was confirmed by subjecting mitochondrial proteins to SDS-PAGE analysis and immunodecoration using CIA30 and HA epitope reactive antibodies (Fig. 5.2B). In order to determine if the tagged CIA30 proteins were active in Complex I biogenesis pathway, mitochondria were solubilised in digitonin and subjected to BN-PAGE analysis and immunodecoration (Fig. 5.2C). Analysis of the NDUFA9 Complex I subunit showed the restoration of respiratory super-complex assembly in the Δ CIA30 cells transduced with CIA30-HA and CIA30-BirA*-HA. However the level of assembled super-complex was somewhat reduced following expression of CIA30-BirA*-HA, suggesting that the BirA* may reduce CIA30 activity.

Next, control cells, Δ CIA30 cells and Δ CIA30 cells expressing CIA30-HA or CIA30-BirA*-HA were incubated in the presence or absence of biotin prior to mitochondrial isolation, SDS-PAGE analysis and detection using streptavidin HRP (Fig. 5.2D). In the cell lines lacking the BirA* protein, endogenously biotinylated proteins were detected at ~75 kDa and ~140 kDa. This was also observed in mitochondria expressing CIA30-BirA*-HA without the addition of biotin. Upon addition of biotin to the culture media, an increased level of biotinylation was observed in cells expressing the CIA30-BirA*-HA compared to the other samples, indicating the BirA* was functional in the activation of biotin and covalent labelling of proteins in culture. Because these data suggest that CIA30-BirA*-HA and CIA30-HA were expressed and active in mitochondria, and the BirA* was capable of biotinylation of proteins, the cells were used for labelling and streptavidin mediated enrichment of biotinylated proteins and proteomic analysis.

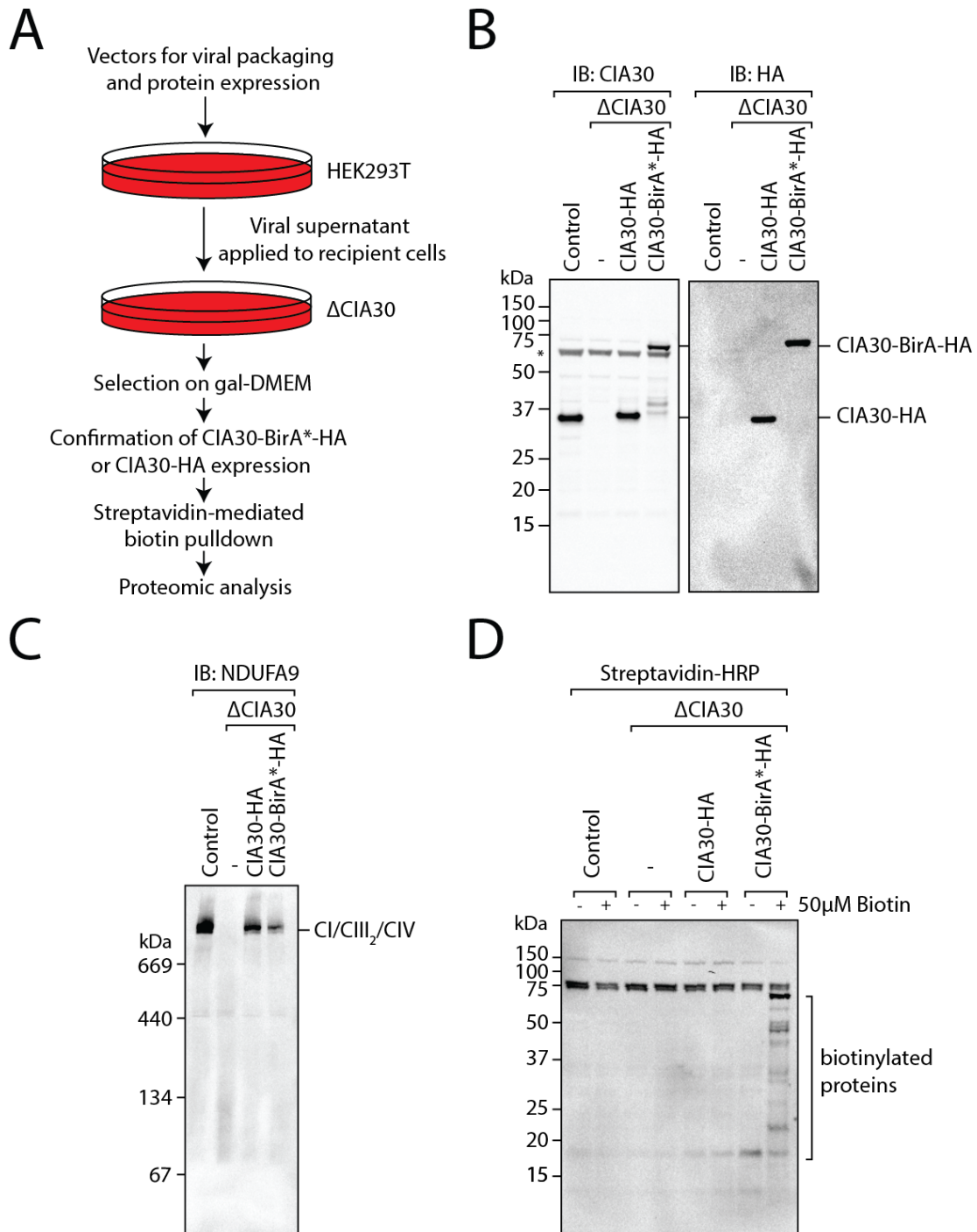


Figure 5.2: Generation and analysis of Δ CIA30 cells expressing CIA30-BirA*-HA and CIA30-HA. (A) Schematic outlining the general approach. HEK293T were transfected with vectors encoding the desired protein and viral helper vectors. Viral supernatant was applied to Δ CIA30 cells and transduced cells were selected by incubation with gal-DMEM. Following confirmation of expression, mitochondria were isolated and subjected to biotin pulldown using streptavidin beads and on-bead trypsin digestion. Peptides were then subjected to proteomic analysis. (B) Isolated mitochondria from the indicated cell lines were subjected to SDS-PAGE and immunoblotting against CIA30 and the HA-epitope. (C) Isolated mitochondria were solubilised in 1% (w/v) digitonin, subjected to BN-PAGE and immunoblotted with NDUFA9 antibodies. (D) Isolated mitochondria from the indicated cell lines were subject to SDS-PAGE and biotinylated proteins were detected using streptavidin HRP.

5.3 Identification of proteins enriched in proximity to CIA30

Following enrichment of biotinylated proteins, peptides were generated by on-bead tryptic digestion and analysed by mass spectrometry. Proteomics was performed by Dr David Stroud (Monash University). Of the proteins that were enriched in the CIA30-BirA*-HA pulldowns relative to the CIA30-HA pulldowns, 30 subunits of Complex I were detected, as well as 9 Complex I assembly factors, accounting for ~31% of the detected proteins (Fig. 5.3). A further 24 subunits of the mito-ribosome were also detected, accounting for 19% of enriched proteins. Also, subunits or assembly factors of Complexes III and IV including COX2 and COX5A also enriched. In addition, enriched proteins related to DNA, RNA and lipid metabolism, metabolic enzymes, proteins involved in protein translocation, proteins with chaperone activity and proteases were identified in proximity to CIA30, though to a lower extent.

Of note, a number of known binding partners of CIA30 were strongly enriched in the CIA30-BirA*-HA pull-downs, including the MCI complex proteins ACAD9, Ecsit and TMEM126B (Fig. 5.4A, indicated by arrows). Also, other Complex I assembly factors and subunits were enriched to different degrees (Fig. 5.4A, proteins labelled in red). Proteins significantly enriched by 1.5x or more relating to Complex I (Fig. 5.4B) or other non-Complex I functions (Fig. 5.4C) are also indicated.

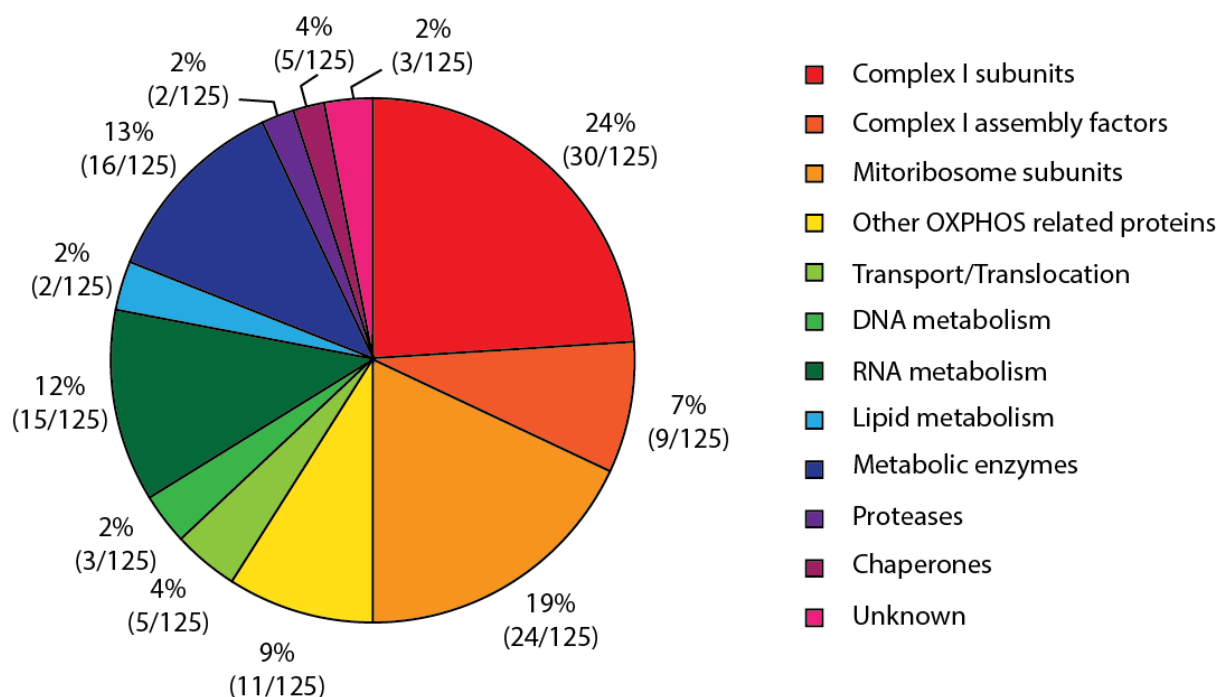


Figure 5.3: Analysis of the functional assignment of CIA30-BirA*-HA enriched proteins. Proportion of proteins belonging to different classes identified following proteomic analysis of peptides from CIA30-BirA*-HA and CIA30-HA streptavidin-mediated biotin enrichment. Analysis performed from 3 independent pull down experiments that had an enrichment in the CIA30-BirA*-HA samples.

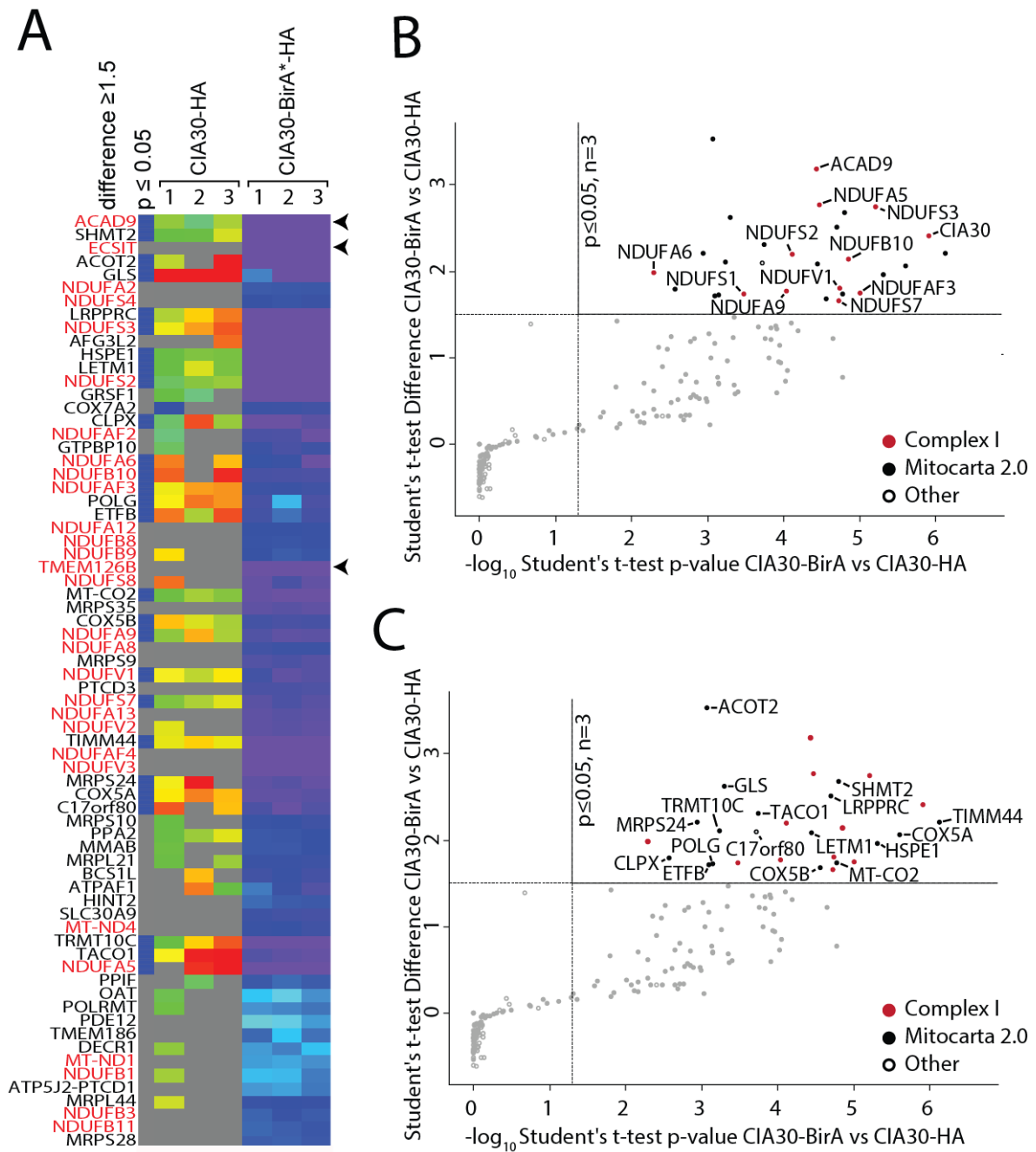


Figure 5.4: Proteins identified in proximity to CIA30 by BioID. (A) Heat-map indicating the enrichment of peptides following 3 independent streptavidin pull-down experiments. Arrows indicate CIA30-interacting assembly factors of the MCIA complex. Proteins listed in red represent other Complex I subunits or assembly factors. Proteins significantly enriched by 1.5x or more relative to CIA30-HA pull-down with a role in **(B)** Complex I (red circles) or **(C)** non-Complex I (black or white circles) function are also indicated as scatter plots.

5.4 Identification of TMEM186- A potential Complex I assembly factor

Given the significant number of additional proteins that were biotinylated by CIA30-BirA*, a bioinformatics approach was undertaken to select a subset of proteins that were not annotated to have a known function in mitochondria. In addition, we reasoned that the non-specific background proteins are likely to be large (containing many Lysine residues) and abundant within mitochondria, and were not selected for further analysis. Analysis of the proteins enriched in the CIA30-BirA*-HA pulldown without a known function identified TMEM186 as a potential candidate Complex I assembly factor. BLAST analysis of TMEM186 from *Homo sapiens* and *Drosophila melanogaster* against the proteome of *Saccharomyces cerevisiae* failed to identify any homologous proteins consistent with a role in Complex I assembly as *S. cerevisiae* lack this enzyme. Furthermore, systematic co-immunoprecipitation also identified TMEM186 to interact with Ecsit (Guarani et al, 2014). In light of these observations, TMEM186 was chosen as a candidate for further analysis.

The human *TMEM186* gene consists of two exons, the first consisting only of the initiation codon (Fig. 5.5A). The TMEM186 protein is 213 residues in length with an estimated size of 24.9 kDa, and is predicted to contain two transmembrane helices (Fig. 5.5B & C). The TMEM186 protein is highly conserved in a number of organisms including human (*H. sapiens*), mouse (*M. musculus*), rat (*R. norvegicus*), bovine (*B. taurus*), zebrafish (*D. rerio*) and flies (*D. melanogaster*) (Fig. 5.5C). Also, prediction of mitochondrial pre-sequences using the 'MitoFates' algorithm (Fukasawa et al, 2015) suggests that TMEM186 contains an N-terminal mitochondrial targeting signal. Furthermore, the presequence was predicted to be processed by the matrix processing peptidase (MPP) after 36 residues with probabilities of 0.86 and 0.92 respectively (Fukasawa et al, 2015) (Fig. 5.5B & C). Proteomic analysis using the MaxQuant database also indicates that the first TMEM186 peptide in the proteome starts at position 45 (Cox; & Mann, 2008). The predicted mitochondrial pre-sequence and membrane localisation of TMEM186 places this protein in the appropriate location to function in the assembly of Complex I.

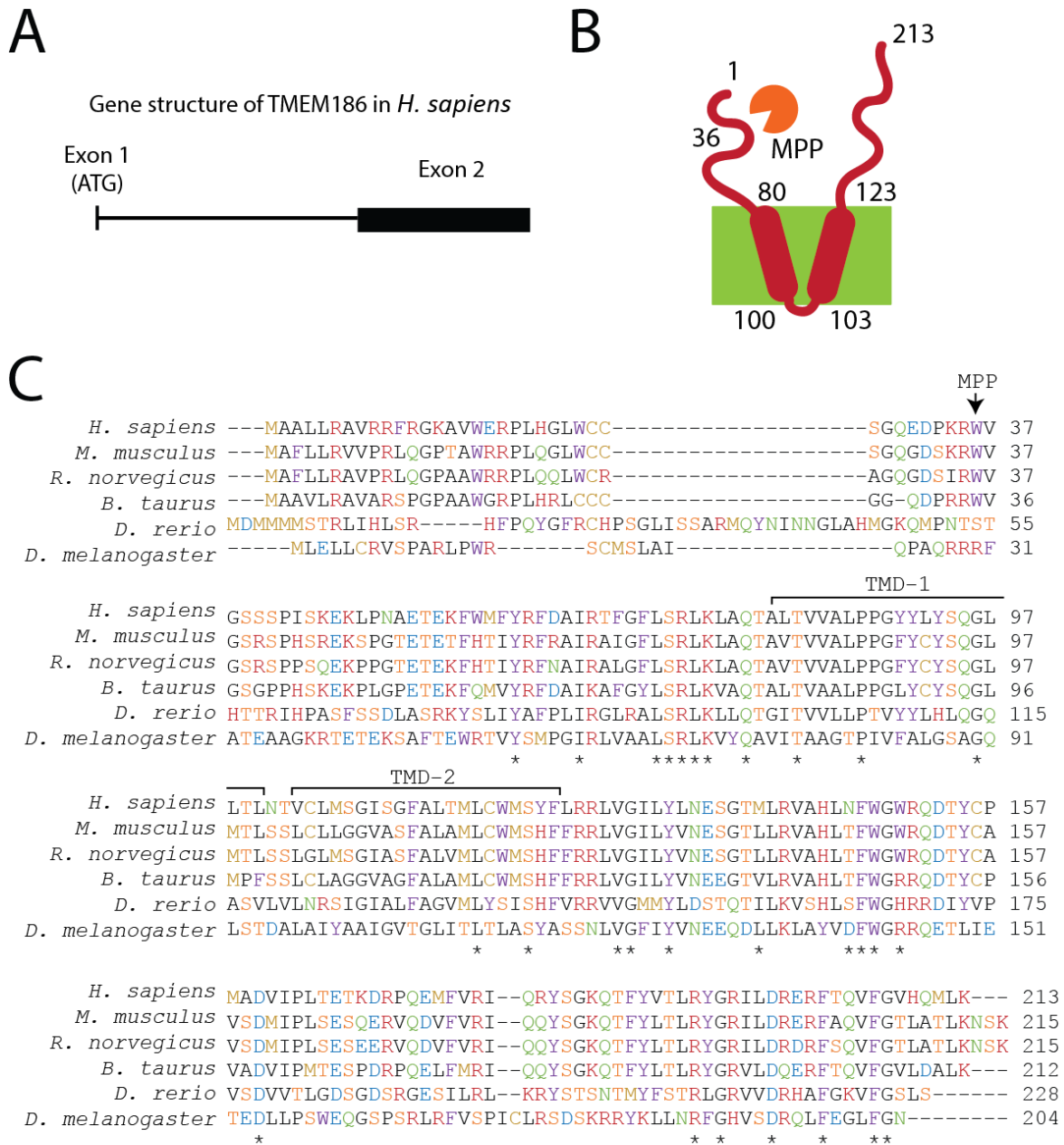


Figure 5.5: Bioinformatic analysis of TMEM186. (A) The *TMEM186* gene is annotated to contain two exons, the first only consisting of the initiation ATG codon. (B) Schematic representation of TMEM186 protein. This protein is predicted to contain two transmembrane domains with a processing site after 36 residues. (C) Multiple sequence alignment of TMEM186 from human (*H. sapiens*, UniProt ID: Q96B77), mouse (*M. musculus*, UniProt ID: Q9CR76), rat (*R. norvegicus*, UniProt ID: Q4KLZ1), bovine (*B. taurus*, UniProt ID: Q5EA03), zebrafish (*D. rerio*, UniProt ID: B3DI94) and flies (*D. melanogaster*, UniProt ID: Q059A4). Hydrophobic residues (G, A, L, I, V, P) are in black, basic residues (K, R, H) in red, acidic residues (D, E) in blue, amide-containing residues (N, Q) in green, hydroxyl containing residues (S, T) in orange, aromatic residues (F, W, Y) in purple and sulphur-containing residues (C, M) in gold. The position of the predicted MPP processing site and the transmembrane domains are indicated. Perfectly conserved residues are indicated by an asterisk (*).

5.5 TMEM186-FLAG localises to mitochondria

In order to determine the subcellular localisation of TMEM186, the coding region was amplified from a human cDNA library and cloned in frame with a C-terminal FLAG epitope for immunofluorescence analysis. The plasmid encoding TMEM186-FLAG was transiently transfected into HCT116 colorectal carcinoma cells, and immunostained for the FLAG epitope and the mitochondrial marker TOM20. Confocal microscopy was performed with the assistance of Mr Abeer Singh. Overlay of the acquired images showed co-localisation of TMEM186-FLAG and TOM20 signals confirmed localisation of TMEM186-FLAG to the mitochondria (Fig. 5.6).

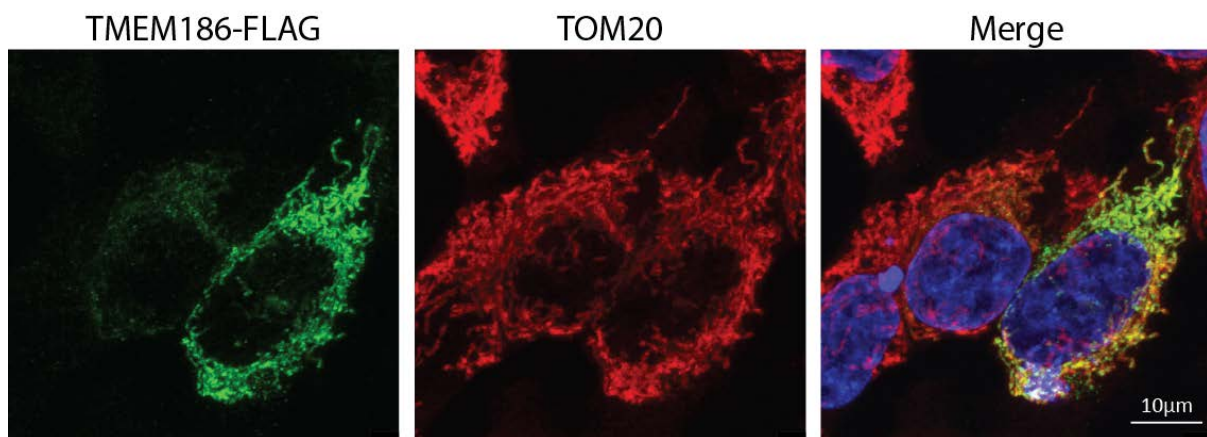


Figure 5.6: TMEM186 localises to the mitochondria. HCT116 cells were transiently transfected with TMEM186-FLAG. Immunofluorescence was performed using FLAG and TOM20 antibodies. The resulting images were merged using ImageJ software. The scale bar represents 10 μm.

5.6 Depletion of TMEM186 reduces the levels of mature Complex I

In order to determine if the loss of TMEM186 could impact Complex I biogenesis, gene disruption cell lines were generated using CRISPR-Cas9 gene editing. Following transfection, the HEK293T cells were sorted to generate individual clones, which were then screened by culturing in media containing galactose to determine if any clonal populations harboured an OXPHOS defect. No colonies harboured a growth defect on Gal-DMEM suggesting that if disruption to the *TMEM186* gene had occurred, the loss of TMEM186 may not result in a severe OXPHOS deficiency.

In order to determine if gene disruption had occurred, clonal populations were selected and screened for the presence of indels in the *TMEM186* gene. Analysis of two clones revealed the presence of indels that would result in loss of the TMEM186 protein (Fig. 5.7A). The Δ TMEM186-1 clone was found to harbour three different alleles, a single nucleotide deletion, a single nucleotide insertion and a 100 nucleotide deletion, all resulting in a change in reading frame. The Δ TMEM186-2 clone harboured two detectable alleles, a single nucleotide deletion and a 97 nucleotide deletion, both resulting in a frameshift mutation (Fig. 5.7A). Since the resulting alleles suggest loss of protein expression, these clones were used to further analyse the effect of TMEM186 deletion.

To determine the effect of TMEM186 depletion on Complex I biogenesis, mitochondria were isolated from control and Δ TMEM186 cells, subjected to BN-PAGE and immunoblotted for the Complex I subunit NDUFA9 (Fig. 5.7B). A reduced accumulation of respiratory super-complex (Fig. 5.7B, CI/CIII₂/CIV) and holo-Complex I (Fig. 5.7B, CI) was observed in the absence of TMEM186 relative to the control mitochondria. In-gel activity demonstrated that the Complex I present in both super-complex and holo-Complex I was enzymatically active in both Control and Δ TMEM186 mitochondria (Fig. 5.7C). These data suggest that the presence of TMEM186 is required for the efficient assembly of Complex I and loss of this protein results in impaired biogenesis, however, the assembly pathway can still proceed.

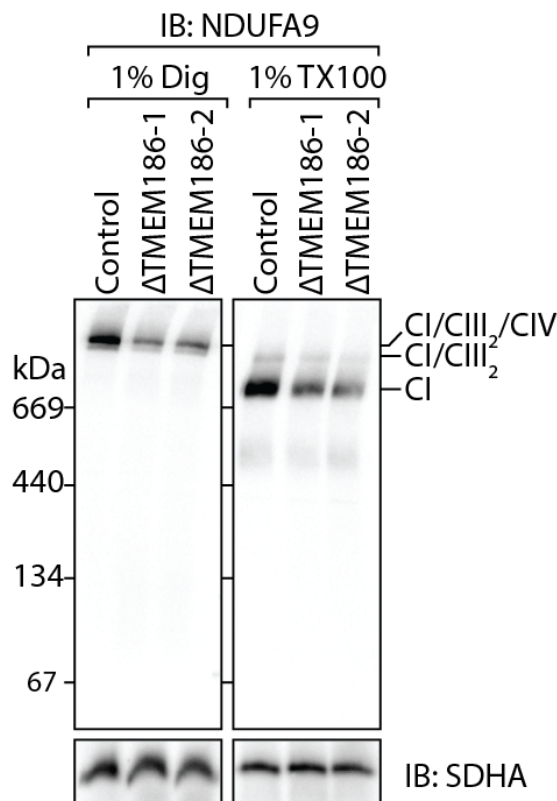
A

```

WT [ CAGGCTGCCCTTCTCCGAGCTGTGCGTAGGTTTCGGGGAAAAGCTGTGTGGGAAAGGCCTCTCCATGGGCTGTGGTGTCTG
      A A L L R A V R R F R G K A V W E R P L H G L W C
ΔTMEM186-1 [ CAGGCTGCCCTTCTCCGAGCTGTGCGTAGGTT-CGGGGAAAAGCTGTGTGGGAAAGGCCTCTCCATGGGCTGTGGTGTCTG
            A A L L R A V R R F G E K L C G K G L S M G C G A
            CAGGCTGCCCTTCTCCGAGCTGTGCGTAGGTTTCGGGGAAAAGCTGTGTGGGAAAGGCCTCTCCATGGGCTGTGGTGTCTG
            A A L L R A V R R F S G K S C V G K A S P W A V V L
            CAGGCTGCCCTTCTCCGAGCTGTGC-----
            A A L L R A V
ΔTMEM186-2 [ CAGGCTGCCCTTCTCCGAGCTGTGCGTAGGTT-CGGGGAAAAGCTGTGTGGGAAAGGCCTCTCCATGGGCTGTGGTGTCTG
            A A L L R A V R R F G E K L C G K G L S M G C G A
            CAGGCTGCCCTTCTCCGAGCTGTGC-----
            A A L L R A V

```

B



C

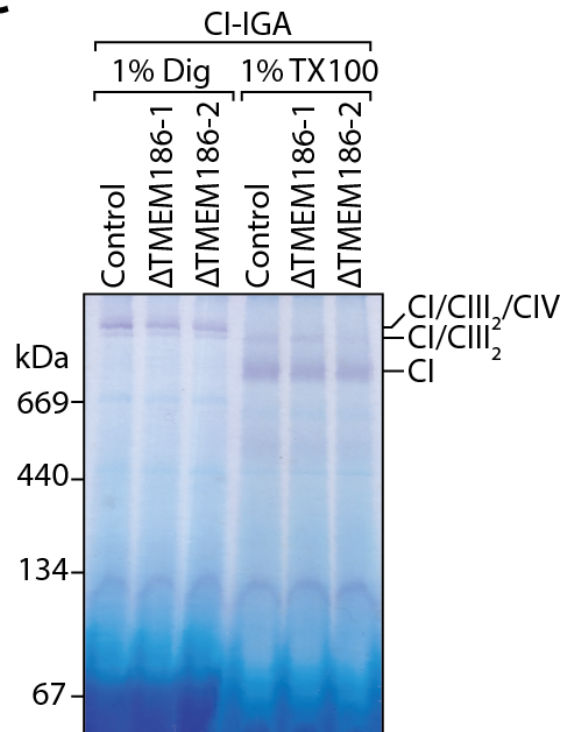


Figure 5.7: Generation and verification of Δ TMEM186 cell lines. (A) Genomic validation of the *TMEM186* gene disruptions performed by Sanger sequencing. The generated deletions are indicated with the corresponding translation. Translation shown from the start of exon 2 corresponding to the second residue of TMEM186 **(B)** Isolated mitochondria from the indicated cell lines were subjected to solubilisation in 1% (w/v) digitonin or 1% (v/v) TX100 and subjected to BN-PAGE and immunoblotting. SDHA was used as a loading control. **(C)** Isolated mitochondria were prepared as described in (B) and subjected to In-gel activity assay (IGA) for Complex I.

To further investigate the effects of *TMEM186* gene disruption, the Complex I subunits NDUFB6 and NDUF55 were analysed by immunoblotting following BN-PAGE. Analysis showed that NDUFB6 predominantly assembled into Complex I (Fig. 5.8A). Upon longer exposure, a sub-complex of ~400 kDa was evident in the Δ TMEM186 clones that was absent in control mitochondria (Fig. 5.8A, *). Analysis of the NDUF55 subunit by BN-PAGE showed a slight reduction of assembled Complex I consistent with a mild Complex I assembly defect (Fig. 5.8B). These data further suggest that in the absence of TMEM186, the ability Complex I to assemble is partially reduced.

Because TMEM186 was identified in proximity to CIA30 and an interaction with Ecsit had been documented (Guarani et al, 2014), the MCIA complex was next analysed to determine if the loss of TMEM186 had an impact at this stage. Mitochondria were isolated from control and Δ TMEM186 cells subjected to BN-PAGE and immunodecorated with ACAD9 antibodies (Fig. 5.8C). The loss of TMEM186 resulted in one ACAD9-containing complex to migrate faster than the equivalent complex in control mitochondria (Fig. 5.8C, #). Interestingly, two complexes of ~669 kDa did not alter migration, however the relative abundance of these complexes differed to control mitochondria. These data suggests that TMEM186 may influence the biogenesis of Complex I by interacting with a subset of intermediates containing the MCIA complex.

In order to investigate the steady state levels of Complex I subunits, mitochondria were isolated and analysed by SDS-PAGE and immunoblotting for various Complex I subunits (Fig. 5.8D). Immunodecoration for the Complex I N-module subunit, NDUFV2, was decreased relative to control levels. Other subunits analysed were generally unchanged relative to the control, indicating that these subunits are not altered in the absence of TMEM186. This is also consistent with the mild Complex I defect observed by BN-PAGE. Steady state levels of the assembly factor TIMMDC1 appeared reduced relative to control mitochondria (Fig. 5.8E). Levels of other Complex I assembly factors analysed did not show any changes relative to the control mitochondria, suggesting the loss of TMEM186 does not influence the stability of these proteins. Taken together, these data indicate that TMEM186 is required for efficient assembly of Complex I and that loss of this protein results in a mild Complex I defect.

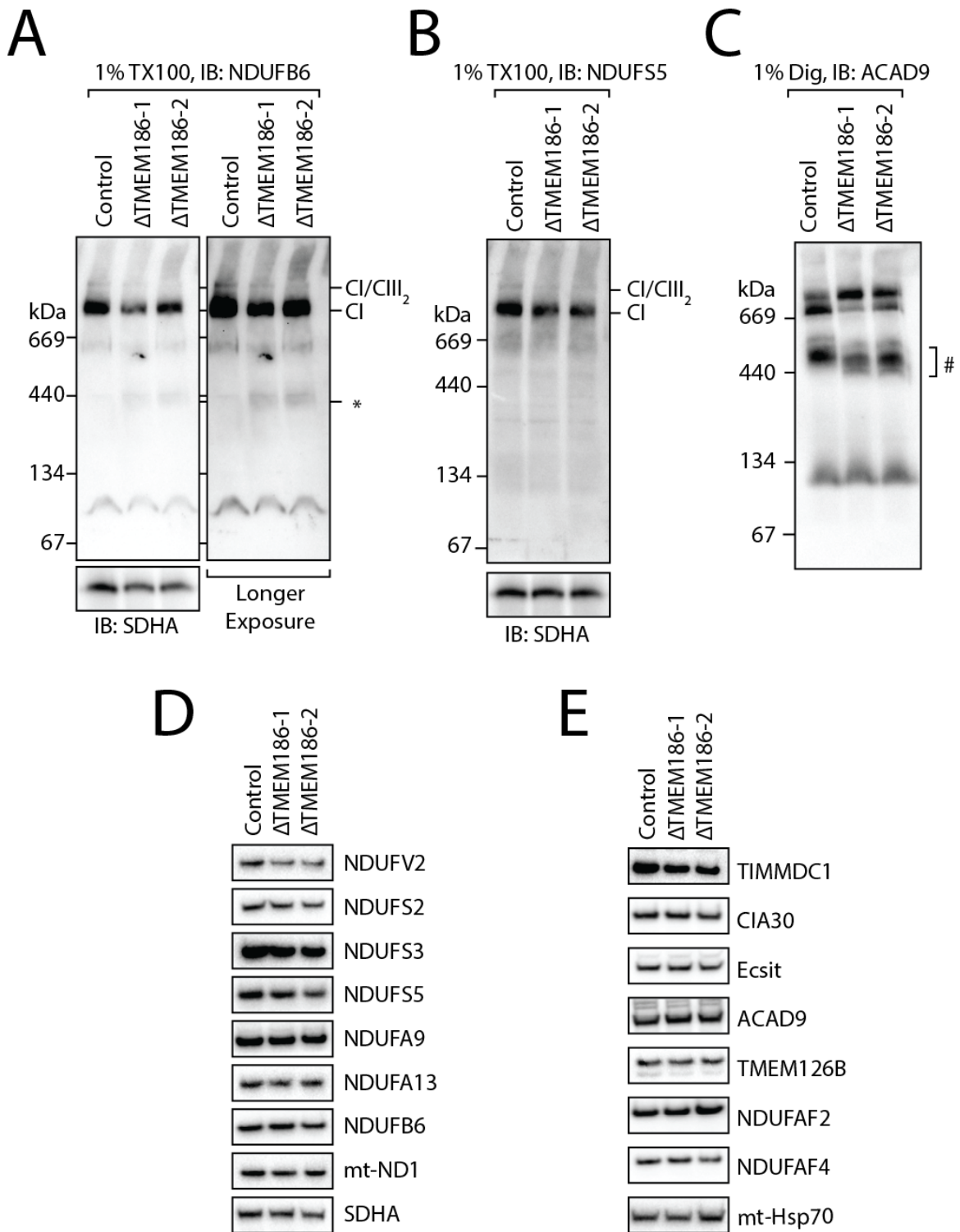


Figure 5.8: Loss of TMEM186 results in a minor Complex I deficiency. Mitochondria from control and Δ TMEM186 cells were isolated and subjected to BN-PAGE and immunoblotted using antibodies against **(A)** NDUFB6, **(B)** NDUFS5, and **(C)** ACAD9. Mitochondria were isolated from control and Δ TMEM186 cells and subjected to SDS-PAGE and immunodecorated with various **(D)** Complex I subunits and **(E)** Complex I assembly factors as indicated.

5.7 Discussion

5.7.1 CIA30 can act as a bait for the identification of new Complex I assembly factors

Various studies have thus far identified 13 assembly factors required for the biogenesis of Complex I (Andrews et al, 2013; Nouws et al, 2012). It is expected that more remain to be identified as the molecular defect in many patients with Complex I deficiency remains to be elucidated (Hoefs et al, 2012). This study aimed to identify novel components of the Complex I assembly machinery by determining proteins in close proximity to CIA30, a *bone fide* Complex I assembly factor. Expanding the repertoire of assembly factors used for BirA* mediated proximity labelling may help uncover protein interaction networks of assembly factors with Complex I subunits, other known Complex I assembly factors and potentially new Complex I assembly factors. This will aid in the identification of further proteins required for Complex I

5.7.2 Complex I intermediates that assemble into super-complexes may still contain CIA30

Analysis of the enriched proteins in the CIA30-BirA*-HA pulldown identified a number of subunits that belong to the respiratory chain Complexes III and IV that may come in close proximity to CIA30. It has also been shown that the ~815 kDa intermediate of Complex I associates with Complex III and IV subunits before biogenesis of Complex I is complete, suggesting that the ~815 kDa intermediate acts as a scaffold to assemble the respiratory super-complex (Moreno-Lastres et al, 2012). Both COX5A and COX2 are thought to assemble with a Complex I intermediate early in this process (Moreno-Lastres et al, 2012). Interestingly, both COX5A and COX2 proteins were significantly enriched in proximity to CIA30. This would suggest that CIA30, and the MCIA complex may still be in association with Complex I intermediates as super-complex assembly is initiated, suggesting that the MCIA complex may dissociate at a very late stage in Complex I assembly, following the incorporation of subunits from Complex IV.

5.7.3 TMEM186 plays a role in the biogenesis of Complex I

The identification of TMEM186 as a component of the Complex I assembly machinery has increased the understanding of the proteins required for efficient biogenesis of this enzyme. It is the third assembly factor to localise to mitochondria and integrate into the membrane by virtue of two predicted transmembrane helices, the others being TMEM126B and TIMMDC1 (Andrews et al, 2013; Guarani et al, 2014; Heide et al, 2012). Analysis of TMEM186 by immunofluorescence and the observed defect in Complex I biogenesis indicate mitochondrial localisation, however further biochemical analysis is required to determine the sub-mitochondrial location of this protein. The work presented in this chapter suggests the loss of TMEM186 does not result in a severe Complex I defect and so may act later in the assembly pathway, similar to what has been

observed upon loss of the late stage assembly factor FOXRED1 (Formosa et al, 2015). While this would be a likely conclusion, the changes to ACAD9-containing complexes and a decrease in the steady state levels of TIMMDC1 would suggest TMEM186 may play an earlier role in Complex I assembly, with a milder effect than the loss of other early- or mid-stage assembly factors (Fig. 5.9). Identifying how the mito-proteome responds to the loss of TMEM186 through quantitative proteomics and the identification of interacting partners will help to elucidate the role of TMEM186 in Complex I biogenesis. Nevertheless, the identification of a novel gene that may be involved in Complex I assembly may assist in the molecular diagnosis of patients with Complex I deficiency.

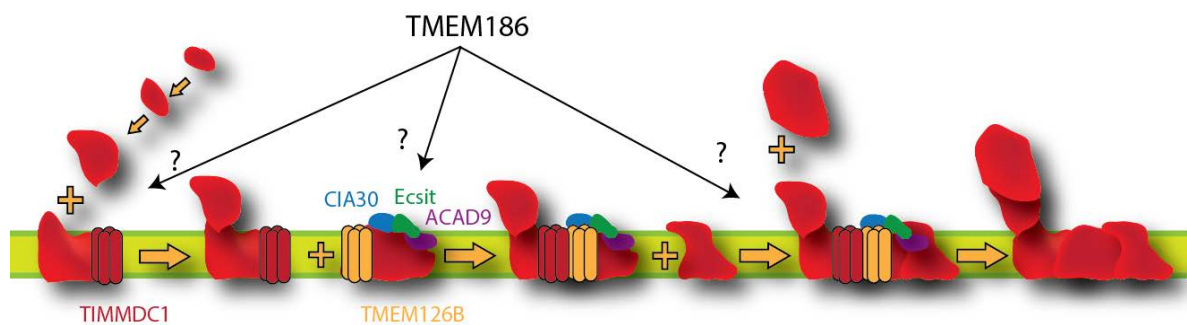


Figure 5.9: TMEM186 may function at different stages of Complex I assembly. Differences in TIMMDC1 steady state levels and ACAD9 containing complexes suggest TMEM186 may function early in Complex I assembly. The relatively mild Complex I deficiency suggests that TMEM186 may function later in Complex I biogenesis. Further work is required to understand the function of TMEM186 as a novel Complex I assembly factor.

Chapter 6

*Concluding remarks and
future directions*

6.1 Determining the molecular function of assembly factors will increase the understanding of Complex I biogenesis

While an increasing number of assembly factors required for the biogenesis of Complex I have been identified, surprisingly little is known about the molecular role they play. The exceptions to this are the assembly factor NDUFAF7, which is required for the dimethylation of NDUFS2 on Arg-85, and NUBPL, which is required for the delivery of Fe-S clusters to Complex I subunits of the N- and Q- module (Rendón et al, 2014; Sheftel et al, 2009). Of the remaining 11 known assembly factors, we have yet to understand their molecular mechanism of action. Much of the literature surrounding the biogenesis of Complex I, and in particular the role of assembly factors, has focussed on the identification of proteins and the characterisation of patient cells or knockdown/knockout studies where the protein of interest is absent or non-functional (Heide et al, 2012; McKenzie et al, 2011; Saada et al, 2008). This has provided important information in understanding how Complex I biogenesis is affected in the absence of various assembly factors, with patient cells being a useful tool to identify and confirm the causal gene responsible for the deficiency through complementation analysis (Calvo et al, 2010; Dunning et al, 2007). This however, has resulted in a lack of understanding of the molecular events these proteins perform. In order to extend the knowledge of the role of assembly factors in this process, the next logical step is to understand how these proteins act at the molecular level to promote Complex I biogenesis. This will assist in understanding how mutations in genes encoding Complex I assembly factors result in non-functional proteins that lead to Complex I deficiency, and may lead to the development of improved treatments by targeting the molecular functions specifically.

For some assembly factors the molecular function may be intrinsically related to other proteins with a common evolutionary history or by the sub-mitochondrial localisation of the protein. It is tempting to hypothesise that the transmembrane domain-containing assembly factors TMEM126B and TIMMDC1 may act as protein channels for the integration of Complex I subunits into the mitochondrial inner membrane. Indeed, TIMMDC1 belongs to the TIM17/22/23 protein family of translocases and may have retained this evolutionary function in Complex I assembly (Guarani et al, 2014). Furthermore, the data presented in this thesis demonstrated that the loss of TIMMDC1 results in a lack of the mt-ND1 protein, a highly hydrophobic protein that is inserted into the membrane early in the assembly of Complex I (Antonicka et al, 2003; Lazarou et al, 2007). The ability of these proteins to act as the translocation machinery needs to be investigated to determine if they actively incorporate proteins into the membrane or have evolved as scaffolds to stabilise intermediates during Complex I assembly and protect from premature turn-over.

Interestingly, the Complex I assembly machinery has evolved to use numerous scaffolds with traditionally different functions including, but not limited to, oxidoreductases, integral membrane proteins, methyltransferases and lipid synthesis or modification proteins (Andrews et al, 2013; Fassone et al, 2010; Pagliarini et al, 2008; Rendón et al, 2014). In some cases the enzymatic activity of the assembly factor is essential for activity in Complex I biogenesis (Rendón et al, 2014), while in other cases the enzyme activity is dispensable for the assembly process (Nouws et al, 2014a). Determining if the enzymatic activity of an assembly factor is important for function may provide insights into how these proteins act during the assembly process. For example, it is still to be determined if FOXRED1 possesses oxidoreductase activity *in vivo*, and if so to what extent this activity is required for Complex I biogenesis. The assembly factor NDUF5 has been shown to be important for Complex I assembly and the activity is dependent on a predicted methyltransferase fold (Carilla-Latorre et al, 2013; Sugiana et al, 2008). It is possible that this protein acts as a methyltransferase to modify NDUF3, which has been demonstrated to be highly methylated in mitochondria from bovine heart (Carroll et al, 2005). While NDUF5 has been postulated to be important for NDUF3 methylation by Sugiana et al (2008), this has not yet been determined experimentally.

6.2 Structural determination of components of the MCIA complex may uncover their molecular mechanism of action in the assembly of Complex I

The function of a protein is tightly connected with its amino acid sequence and the three-dimensional structure adopted after folding. Hence, elucidating the three-dimensional fold can provide insights into a protein's biological role. The identification of related proteins can also provide insights into the function of the protein of interest, however in many cases even highly similar proteins may perform quite different functions. This is indeed the case for ACAD9, which is highly similar to the β -oxidation enzyme VLCAD that is thought to have diverged from a duplication event at the root of vertebrate evolution (Nouws et al, 2010). In some cases a protein's sequence may not resemble any known protein, and so determining the molecular mechanism of a biological function may be more obscure. For example, analysis of the CIA30 and Ecsit amino acid sequences fails to identify any homologous human proteins, and so uncovering how these proteins function in Complex I biogenesis has been difficult.

The data presented in this thesis has suggested that the levels of CIA30 and Ecsit are dependent not only on one another but also on the presence of ACAD9, which has also been suggested based on knockdown studies (Nouws et al, 2010). Previous attempts to purify these proteins in isolation have met with little success, which may be due to their stability-dependent nature on other Complex I assembly factors. Future work in the expression and purification of a ternary complex comprising CIA30, Ecsit and ACAD9 may improve the purity and stability of these proteins for further structural characterisation. A structural understanding of these components of the Complex I assembly machinery would be expected to improve the understanding of the role these proteins perform during Complex I biogenesis, and how these proteins may be dependent on one another in the assembly pathway.

6.3 Assembling the mt-ND4/mt-ND5 module- Undiscovered assembly factors for the membrane arm of Complex I?

The Complex I assembly machinery orchestrates an intricate assembly process, bringing together subunits of dual genetic control. The assembly factors identified thus far can be categorised based on the stage they assist in Complex I biogenesis; either as early (mt-ND1-Q module assembly), mid (membrane arm biogenesis) or late (~815 kDa intermediate stability/N-module incorporation) stage assembly factors (McKenzie & Ryan, 2010; Mimaki et al, 2012). The models of Complex I assembly presented so far suggest the membrane arm forms from the mt-ND1 intermediate integrating with the mt-ND2 sub-complex, which may also contain the mtDNA encoded subunits mt-ND3, mt-ND6 and mt-ND4L, followed by the final addition of the mt-ND4/

mt-ND5 containing module to assemble the membrane arm of Complex I (Mimaki et al, 2012). Many of the assembly factors characterised to this point are involved in the biogenesis of the mt-ND1 or mt-ND2 containing intermediates or the late ~815 kDa intermediate (Dunning et al, 2007; Lazarou et al, 2007; Ogilvie et al, 2005; Rendón & Shoubridge, 2012). To date, no assembly factors have been identified for the biogenesis of the mt-ND4/mt-ND5 intermediate, which contains two of the three antiporter-like domains and represents approximately half of the membrane arm located at the distal tip of Complex I (Zhu et al, 2015). The requirement of such an extensive assembly machinery seems unlikely to be limited to the mt-ND1/mt-ND2 components of the membrane arm, and it would be expected that the mt-ND4/mt-ND5 module may require extrinsic factors for protein translocation and insertion into the mitochondrial membrane, stability and subsequent association with other Complex I assembly modules to build the final active enzyme. While a number of patients have been identified with mtDNA mutation in the mt-ND4 and mt-ND5 genes (Lertrit et al, 1992; Swalwell et al, 2011; Wallace et al, 1988), no patients have been identified with defects in assembly of these proteins. It may be possible that patients with assembly defects in mt-ND4 and mt-ND5 do exist, however they have yet to be diagnosed (Hoefs et al, 2012).

6.4 TMEM186- A novel assembly factor for Complex I

The identification and characterisation of novel assembly factors required for the biogenesis of Complex I will improve the diagnosis of patients with Complex I deficiency and may shed light into the intricacies required to build this molecular machine. The identification of TMEM186 as a possible assembly factor suggests that the *TMEM186* gene can now be used as a new candidate gene to be screened in patients with mitochondrial disease resulting from Complex I deficiency. While the loss of TMEM186 does not result in a total loss of Complex I, a reduction is observed suggesting a mild Complex I deficiency. Since TMEM186 has also been shown to co-immunoprecipitate with Ecsit (Guarani et al, 2014), further investigations into the behaviour of Ecsit-containing complexes in the absence of the TMEM186 protein would provide further insights into how TMEM186 may function in Complex I assembly. Interestingly, the other known Complex I assembly factors that harbour transmembrane domains, TMEM126B and TIMMDC1, function together in the assembly of two distinct modules of the membrane arm of Complex I, together with Ecsit, CIA30 and ACAD9 (Andrews et al, 2013; Guarani et al, 2014; Heide et al, 2012). Preliminary evidence suggests a role for TMEM186 with the MCIA complex, however this will need to be investigated further.

While the effects of TMEM186 depletion appear to affect the biogenesis of Complex I, whether the loss of this protein results in an isolated Complex I defect or a more general perturbation of respiratory chain complexes remains to be determined. The changes observed in ACAD9 assembly intermediates and TIMMDC1 steady state levels would suggest a role in the assembly of Complex I, however one cannot discount the possibility that TMEM186 may play an ancillary role in general maintenance of the OXPHOS system. Indeed, it has been shown that Complex I is important for the biogenesis of respiratory super-complexes and furthermore, defects in Complex III biogenesis can result in a secondary Complex I deficiency (Moreno-Lastres et al, 2012; Schägger et al, 2004). Further work to determine the effects of TMEM186 depletion on other respiratory chain complexes by BN-PAGE and quantitative mass spectrometry analysis of the Δ TMEM186 mitochondrial proteome will provide further insights into these questions. In addition, analysis of the TMEM186 interaction network may help to elucidate the role of this protein in mitochondria.

6.5 Assembly factors to the end- Required for the stability of the ~815 kDa intermediate?

The current model of Complex I assembly suggests that the ~815 kDa intermediate is composed of a number of subunits, encoded by both the nuclear and mitochondrial genomes as well as a number of assembly factors that have accumulated from early stages of the assembly pathway (Andrews et al, 2013; Mimaki et al, 2012). This stage appears to act as a nexus for Complex I biogenesis, with assembled Q- and P- modules before the final addition of the N-module (Antonicka et al, 2003). Furthermore, a number of assembly factors have been shown to be present in various assembly intermediates that somehow dissociate prior to the enzyme being fully assembled (Dunning et al, 2007; Heide et al, 2012; Lazarou et al, 2007; Saada et al, 2009). At first glance this may seem reasonable, however, why should a protein that has performed a function early in the assembly pathway remain associated almost to the very end? One hypothesis would be that these early and mid-stage assembly factors not only aid in the assembly of the individual modules that they associate with, but are also required for the stability of the late ~815 kDa intermediate. Indeed, the Δ NDUFA9 and Δ FOXRED1 cell lines harbour a stalled sub-complex that appears to be a breakdown product of the ~815 kDa intermediate that contains the late subunit NDUFS5 (Formosa et al, 2015; Stroud et al, 2013). This work has shown that in the absence of FOXRED1, ACAD9 was observed in Complex I intermediates similar to those observed in control mitochondria and not part of the stalled complex. Furthermore, analysis also showed that CIA30 was no longer associated with the ~475 kDa stalled complex present in patient fibroblast lacking FOXRED1 (Formosa et al, 2015). This would suggest that the breakdown occurs

after the assembly factors CIA30 and ACAD9 have dissociated from the ~815 kDa intermediate. Since the intermediate cannot progress to form mature Complex I, in the absence of the stabilising effects of the assembly factors, the ~815 kDa intermediate falls apart to form a stable complex. Further work to determine if this is indeed the case would provide evidence for the role of assembly factors during the entire assembly pathway and not simply at a single step where an initial defect may be observed.

6.6 Assembly factors, mtDNA translation, the membrane insertion machinery and protein quality control- functionally connected for functional mitochondria?

In the model organism *S. cerevisiae*, the Oxa1 protein has been shown to be involved in the biogenesis of mitochondrial inner membrane proteins acting as a general membrane insertase (Bohnert et al, 2010; Hell et al, 2001). Furthermore, Oxa1 has also been demonstrated to interact with the mitochondrial ribosome to co-translationally insert mitochondrial encoded subunits into the membrane (Jia et al, 2003; Szyrach et al, 2003). Indeed, depletion of the human homologue of yeast Oxa1 (Oxa1L) leads to a combined OXPHOS deficiency in Complex I and IV (Coenen et al, 2005), or impaired biogenesis of Complex I or V (Stiburek et al, 2007). With defects in mtDNA encoded subunits observed in both cells lacking Complex I assembly factors and Complex I patient fibroblasts (Dunning et al, 2007; McKenzie et al, 2011; Rendón & Shoubridge, 2012) could there be a functional relationship between assembly factors, Oxa1L and the mitochondrial ribosome to cooperate in Complex I assembly? With the proteins encoded by mtDNA being highly hydrophobic (Ott & Herrmann, 2010), minimising exposure to the aqueous environment of the mitochondrial matrix would be beneficial minimising protein aggregation, and so therefore an efficient means of membrane protein sorting and integration would be advantageous. How the process of translation through to membrane integration and finally assembly occurs in mammalian mitochondria is a poorly understood aspect of Complex I biology and requires further investigation. Given the defects observed in a number of mtDNA-encoded subunits of patients with defects in various assembly factors, these proteins may play a central role in the process.

If proteins are unable to be efficiently assembled, proteolytic mechanisms are activated to degrade the aberrant proteins (Rendón & Shoubridge, 2012). From the work presented in this thesis, it is interesting that some Complex I subunits such as NDUFS2 and NDUFS3 show variable levels of stability that are dependent on the particular gene that has been disrupted. In contrast to this, NDUFS5 was completely lost if early or mid-stage assembly was disrupted and only minor defects if late stage assembly was perturbed. Furthermore, N-module defects were observed

across all cell lines harbouring a Complex I defect, which suggest the biogenesis of this region of the enzyme is under strict control and surplus subunits that cannot be incorporated to form the mature enzyme are degraded. This may be to reduce ROS generation and oxidative stress that could potentially occur through the N-module via the redox active FMN moiety that is responsible for NADH oxidation, which is accessible to molecular oxygen (Esterházy et al, 2008; Koopman et al, 2010). Given the complexity of the assembly of Complex I and the differences observed in protein stability, understanding how the protein quality control machinery is activated in the event of an assembly defect would be of great interest. It has been shown that defects in the mitochondrial proteases AFG3L2 and Yme1L are associated with various OXPHOS defects and these proteins are important in the maturation and quality control of mitochondrial proteins that are involved oxidative phosphorylation (Coenen et al, 2005; Richter et al, 2015).

Further understanding into the mechanisms underlying these processes and how the assembly factors may interact with these processes will lead to a more holistic understanding of Complex I biogenesis is health and disease, and potential avenues for future treatment of mitochondrial disorders. Analysis of the role of assembly factors began with the study of *N. crassa* CIA30 and CIA84 by Kuffner et al (1998), and while the understanding of Complex I biogenesis has improved over the last two decades, the list of unanswered questions continues to grow. With the advent of genome editing and improved proteomics coupled to traditional biochemical analysis, and the constant development of new techniques to investigate biological systems, the biochemist has unprecedented power to tackle these questions in the years to come. Complex I biogenesis, though still mysterious, is a wonderfully intricate process that has withstood the test of evolution and still has many secrets yet to be uncovered.

References

Anderson S, Bankier AT, Barrell BG, de Bruijn MH, Coulson AR, Drouin J, Eperon IC, Nierlich DP, Roe BA, Sanger F, Schreier PH, Smith AJ, Staden R, Young IG (1981) Sequence and organization of the human mitochondrial genome. *Nature* **290**: 457-465

Andreazza AC, Shao L, Wang J-FF, Young LT (2010) Mitochondrial complex I activity and oxidative damage to mitochondrial proteins in the prefrontal cortex of patients with bipolar disorder. *Archives of General Psychiatry* **67**: 360-368

Andrews B, Carroll J, Ding S, Fearnley IM, Walker JE (2013) Assembly factors for the membrane arm of human complex I. *Proceedings of the National Academy of Sciences of the United States of America* **110**: 18934-18939

Angerer H (2013) The superfamily of mitochondrial Complex I LYR motif-containing (LYRM) proteins. *Biochemical Society Transactions* **41**: 1335-1341

Antonicka H, Ogilvie I, Taivassalo T, Anitori RP, Haller RG, Vissing J, Kennaway NG, Shoubridge EA (2003) Identification and characterization of a common set of complex I assembly intermediates in mitochondria from patients with complex I deficiency. *Journal of Biological Chemistry* **278**: 43081-43088

Arenas J, Campos Y, Ribacoba R, Martín MA, Rubio JC, Ablanado P, Cabello A (1998) Complex I defect in muscle from patients with Huntington's disease. *Annals of Neurology* **43**: 397-400

Baker MJ, Mooga VP, Guiard B, Langer T, Ryan MT, Stojanovski D (2012) Impaired folding of the mitochondrial small TIM chaperones induces clearance by the i-AAA protease. *Journal of Molecular Biology* **424**: 227-239

Baradaran R, Berrisford JM, Minhas GS, Sazanov LA (2013) Crystal structure of the entire respiratory complex I. *Nature* **494**: 443-448

Berrisford JM, Sazanov LA (2009) Structural basis for the mechanism of respiratory complex I. *The Journal of Biological Chemistry* **284**: 29773-29783

Betarbet R, Sherer TB, MacKenzie G, Garcia-Osuna M, Panov AV, Greenamyre JT (2000) Chronic systemic pesticide exposure reproduces features of Parkinson's disease. *Nature Neuroscience* **3**: 1301-1306

Bohnert M, Rehling P, Guiard B, Herrmann JM, Pfanner N, van der Laan M (2010) Cooperation of stop-transfer and conservative sorting mechanisms in mitochondrial protein transport. *Current Biology* **20**: 1227-1232

Branda SS, Isaya G (1995) Prediction and identification of new natural substrates of the yeast mitochondrial intermediate peptidase. *The Journal of Biological Chemistry* **270**: 27366-27373

Brandt U (2006) Energy Converting NADH:Quinone Oxidoreductase (Complex I). *Annual Review of Biochemistry* **75**: 69-92

Bych K, Kerscher S, Netz DJ, Pierik AJ, Zwicker K, Huynen MA, Lill R, Brandt U, Balk J (2008) The iron-sulphur protein Ind1 is required for effective complex I assembly. *EMBO Journal* **27**: 1736-1746

Calvo SE, Tucker EJ, Compton AG, Kirby DM, Crawford G, Burt NP, Rivas M, Guiducci C, Bruno DL, Goldberger OA, Redman MC, Wiltshire E, Wilson CJ, Altshuler D, Gabriel SB, Daly MJ, Thorburn DR, Mootha VK (2010) High-throughput, pooled sequencing identifies mutations in NUBPL and FOXRED1 in human complex I deficiency. *Nature Genetics* **42**: 851-858

Candé C, Cohen I, Daugas E, Ravagnan L, Larochette N, Zamzami N, Kroemer G (2002) Apoptosis-inducing factor (AIF): a novel caspase-independent death effector released from mitochondria. *Biochimie* **84**: 215-222

Carilla-Latorre S, Annesley SJ, Muñoz-Braceras S, Fisher PR, Escalante R (2013) Ndufa5 deficiency in the Dictyostelium model: new roles in autophagy and development. *Molecular Biology of the Cell* **24**: 1519-1528

Carilla-Latorre S, Gallardo ME, Annesley SJ, Calvo-Garrido J, Grana O, Accari SL, Smith PK, Valencia A, Garesse R, Fisher PR, Escalante R (2010) MidA is a putative methyltransferase that is required for mitochondrial complex I function. *Journal of Cell Science* **123**: 1674-1683

Carroll J, Fearnley IM, Shannon RJ, Hirst J, Walker JE (2003) Analysis of the Subunit Composition of Complex I from Bovine Heart Mitochondria. *Molecular and Cellular Proteomics* **2**: 117-126

Carroll J, Fearnley IM, Skehel JM, Runswick MJ, Shannon RJ, Hirst J, Walker JE (2005) The post-translational modifications of the nuclear encoded subunits of complex I from bovine heart mitochondria. *Molecular and Cellular Proteomics* **4**: 693-699

Chen Y, Zhu J, Lum PY, Yang X, Pinto S, MacNeil DJ, Zhang C, Lamb J, Edwards S, Sieberts SK, Leonardson A, Castellini LW, Wang S, Champy M-FF, Zhang B, Emilsson V, Doss S, Ghazalpour A, Horvath S, Drake TA, Lusk AJ, Schadt EE (2008) Variations in DNA elucidate molecular networks that cause disease. *Nature* **452**: 429-435

Chew A, Buck EA, Peretz S, Sirugo G, Rinaldo P, Isaya G (1997) Cloning, expression, and chromosomal assignment of the human mitochondrial intermediate peptidase gene (MIPEP). *Genomics* **40**: 493-496

Choi-Rhee E, Schulman H, Cronan JE (2004) Promiscuous protein biotinylation by Escherichia coli biotin protein ligase. *Protein science : a publication of the Protein Society* **13**: 3043-3050

Chomczynski P, Sacchi N (2006) The single-step method of RNA isolation by acid guanidinium thiocyanate-phenol-chloroform extraction: twenty-something years on. *Nature Protocols* **1**: 581-585

Chung CT, Niemela SL, Miller RH (1989) Once-step preparation of competent *Escherichia coli*: Transformation and storage of bacterial cells in the same solution. *Proceedings of the National Academy of Sciences, USA* **86**: 2172-2175

Coenen MJ, Smeitink JA, Smeets R, Trijbels FJ, van den Heuvel LP (2005) Mutation detection in four candidate genes (OXA1L, MRS2L, YME1L and MIPEP) for combined deficiencies in the oxidative phosphorylation system. *Journal of Inherited Metabolic Disease* **28**: 1091-1097

Cox; J, Mann M (2008) MaxQuant enables high peptide identification rates, individualized p.p.b.-range mass accuracies and proteome-wide protein quantification. *Nature Biotechnology* **26**: 1367-1372

Crofts AR (2004) The cytochrome bc1 complex: function in the context of structure. *Annual Review of Physiology* **66**: 689-733

Deltcheva E, Chylinski K, Sharma CM, Gonzales K, Chao Y, Pirzada ZA, Eckert MR, Vogel J, Charpentier E (2011) CRISPR RNA maturation by trans-encoded small RNA and host factor RNase III. *Nature* **471**: 602-607

DiMauro S, Rustin P (2009) A critical approach to the therapy of mitochondrial respiratory chain and oxidative phosphorylation diseases. *Biochimica et Biophysica Acta (BBA)-Molecular Basis of Disease* **1792**: 1159-1167

Dunning CJR, McKenzie M, Sugiana C, Lazarou M, Silke J, Connelly A, Fletcher JM, Kirby DM, Thorburn DR, Ryan MT (2007) Human CIA30 is involved in the early assembly of mitochondrial complex I and mutations in its gene cause disease. *The EMBO Journal* **26**: 3227-3237

Efremov RG, Baradaran R, Sazanov LA (2010) The architecture of respiratory complex I. *Nature* **465**: 441-445

Efremov RG, Sazanov LA (2011) Structure of the membrane domain of respiratory complex I. *Nature* **476**: 414-420

El-Hattab AW, Adesina AM, Jones J, Scaglia F (2015) MELAS syndrome: Clinical manifestations, pathogenesis, and treatment options. *Molecular Genetics and Metabolism* **116**: 4-12

Ensenauer R, He M, Willard J-MM, Goetzman ES, Corydon TJ, Vandahl BB, Mohsen A-WW, Isaya G, Vockley J (2005) Human acyl-CoA dehydrogenase-9 plays a novel role in the mitochondrial beta-oxidation of unsaturated fatty acids. *The Journal of Biological Chemistry* **280**: 32309-32316

Escarceller M, Pluvinet R, Sumoy L, Estivill X (2000) Identification and expression analysis of C3orf1, a novel human gene homologous to the Drosophila RP140-upstream gene. *DNA Sequence: the Journal of DNA Sequencing and Mapping* **11**: 335-338

Esterházy D, King MS, Yakovlev G, Hirst J (2008) Production of Reactive Oxygen Species by Complex I (NADH:Ubiquinone Oxidoreductase) from Escherichia coli and Comparison to the Enzyme from Mitochondria. *Biochemistry* **47**: 3964-3971

Fan W, Waymire KG, Narula N, Li P, Rocher C, Coskun PE, Vannan MA, Narula J, Macgregor GR, Wallace DC (2008) A mouse model of mitochondrial disease reveals germline selection against severe mtDNA mutations. *Science (New York, NY)* **319**: 958-962

Fassone E, Duncan AJ, Taanman JW, Pagnamenta AT, Sadowski MI, Holand T, Qasim W, Rutland P, Calvo SE, Mootha VK, Bitner-Glindzicz M, Rahman S (2010) FOXRED1, encoding an FAD-dependent oxidoreductase complex-I-specific molecular chaperone, is mutated in infantile-onset mitochondrial encephalopathy. *Human Molecular Genetics* **19**: 4837-4847

Fassone E, Taanman J-WW, Hargreaves IP, Sebire NJ, Cleary MA, Burch M, Rahman S (2011) Mutations in the mitochondrial complex I assembly factor NDUFAF1 cause fatal infantile hypertrophic cardiomyopathy. *Journal of Medical Genetics* **48**: 691-697

Fearnley IM (2001) GRIM-19, a Cell Death Regulatory Gene Product, Is a Subunit of Bovine Mitochondrial NADH:Ubiquinone Oxidoreductase (Complex I). *Journal of Biological Chemistry* **276**: 38345-38348

Finsterer J (2008) Leigh and Leigh-like syndrome in children and adults. *Pediatric Neurology* **39**: 223-235

Flinn L, Mortiboys H, Volkmann K, Köster RW, Ingham PW, Bandmann O (2009) Complex I deficiency and dopaminergic neuronal cell loss in parkin-deficient zebrafish (Danio rerio). *Brain : a Journal of Neurology* **132**: 1613-1623

Formosa LE, Hofer A, Tischner C, Wenz T, Ryan MT (2016) Translation and Assembly of Radiolabeled Mitochondrial DNA-Encoded Protein Subunits from Cultured Cells and Isolated Mitochondria. *Methods in Molecular Biology (Clifton, NJ)* **1351**: 115-129

Formosa LE, Mimaki M, Frazier AE, McKenzie M, Stait TL, Thorburn DR, Stroud DA, Ryan MT (2015) Characterization of mitochondrial FOXRED1 in the assembly of respiratory chain complex I. *Human Molecular Genetics* **24**: 2952-2965

Frazier AE, Thorburn DR (2012) Biochemical analyses of the electron transport chain complexes by spectrophotometry. *Methods in Molecular Biology (Clifton, NJ)* **837**: 49-62

- Fukasawa Y, Tsuji J, Fu S-CC, Tomii K, Horton P, Imai K (2015) MitoFates: improved prediction of mitochondrial targeting sequences and their cleavage sites. *Molecular & Cellular Proteomics* **14**: 1113-1126
- Gaj T, Gersbach CA, Barbas CF (2013) ZFN, TALEN, and CRISPR/Cas-based methods for genome engineering. *Trends in Biotechnology* **31**: 397-405
- Garone C, Donati MA, Sacchini M, Garcia-Diaz B, Bruno C, Calvo S, Mootha VK, Dimauro S (2013) Mitochondrial encephalomyopathy due to a novel mutation in ACAD9. *JAMA Neurology* **70**: 1177-1179
- Gerards M, Sluiter W, van den Bosch BJ, de Wit LE, Calis CM, Frentzen M, Akbari H, Schoonderwoerd K, Scholte HR, Jongbloed RJ, Hendrickx AT, de Coo IF, Smeets HJ (2010a) Defective complex I assembly due to C20orf7 mutations as a new cause of Leigh syndrome. *Journal of Medical Genetics* **47**: 507-512
- Gerards M, van den Bosch BJC, Danhauser K, Serre V, van Weeghel M, Wanders RJA, Nicolaes GAF, Sluiter W, Schoonderwoerd K, Scholte HR, Prokisch H, Rotig A, de Coo IFM, Smeets HJM (2010b) Riboflavin-responsive oxidative phosphorylation complex I deficiency caused by defective ACAD9: new function for an old gene. *Brain* **134**: 210-219
- Guarani V, Paulo J, Zhai B, Huttlin EL, Gygi SP, Harper JW (2014) TIMMDC1/C3orf1 functions as a membrane-embedded mitochondrial complex I assembly factor through association with the MCIA complex. *Molecular and Cellular Biology* **34**: 847-861
- Haack TB, Danhauser K, Haberberger B, Hoser J, Strecker V, Boehm D, Uziel G, Lamantea E, Invernizzi F, Poulton J, Rolinski B, Iuso A, Biskup S, Schmidt T, Mewes HW, Wittig I, Meitinger T, Zeviani M, Prokisch H (2010) Exome sequencing identifies ACAD9 mutations as a cause of complex I deficiency. *Nature Genetics* **42**: 1131-1134
- Hangen E, Féraud O, Lachkar S, Mou H, Doti N, Fimia GM, Lam N-VV, Zhu C, Godin I, Muller K, Chatzi A, Nuebel E, Ciccosanti F, Flamant S, Bénit P, Perfettini J-LL, Sauvat A, Bennaceur-Griscelli A, Ser-Le Roux K, Gonin P, Tokatlidis K, Rustin P, Piacentini M, Ruvo M, Blomgren K, Kroemer G, Modjtahedi N (2015) Interaction between AIF and CHCHD4 Regulates Respiratory Chain Biogenesis. *Molecular Cell* **58**: 1001-1014
- Harlow E, Lane D (1999) *Using antibodies: A laboratory manual*: Cold Spring Harbour Laboratory Press.
- He M, Rutledge SL, Kelly DR, Palmer CA, Murdoch G, Majumder N, Nicholls RD, Pei Z, Watkins PA, Vockley J (2007) A new genetic disorder in mitochondrial fatty acid beta-oxidation: ACAD9 deficiency. *American Journal of Human Genetics* **81**: 87-103
- Hedderich R (2004) Energy-converting [NiFe] hydrogenases from archaea and extremophiles: ancestors of complex I. *Journal of Bioenergetics and Biomembranes* **36**: 65-75

- Heide H, Bleier L, Steger M, Ackermann J, Dröse S, Schwamb B, Zörnig M, Reichert AS, Koch I, Wittig I, Brandt U (2012) Complexome profiling identifies TMEM126B as a component of the mitochondrial complex I assembly complex. *Cell Metabolism* **16**: 538-549
- Hell K, Neupert W, Stuart RA (2001) Oxa1p acts as a general membrane insertion machinery for proteins encoded by mitochondrial DNA. *The EMBO Journal* **20**: 1281-1288
- Hoedt E, Zhang G, Neubert TA (2014) Stable isotope labeling by amino acids in cell culture (SILAC) for quantitative proteomics. *Advances in Experimental Medicine and Biology* **806**: 93-106
- Hoefs SJ, Rodenburg RJ, Smeitink JA, van den Heuvel LP (2012) Molecular base of biochemical complex I deficiency. *Mitochondrion* **12**: 520-532
- Hoogenraad NJ, Ward LA, Ryan MT (2002) Import and assembly of proteins into mitochondria of mammalian cells. *Biochimica Biophysica Acta* **1592**: 97-105
- Hunte C, Zickermann V, Brandt U (2010) Functional Modules and Structural Basis of Conformational Coupling in Mitochondrial Complex I. *Science* **329**: 448-451
- Iwata S, Lee JW, Okada K, Lee JK, Iwata M, Rasmussen B, Link TA, Ramaswamy S, Jap BK (1998) Complete structure of the 11-subunit bovine mitochondrial cytochrome bc1 complex. *Science (New York, NY)* **281**: 64-71
- Janssen R, Smeitink J, Smeets R, van Den Heuvel L (2002) CIA30 complex I assembly factor: a candidate for human complex I deficiency? *Human Genetics* **110**: 264-270
- Janssen RJ, Nijtmans LG, Heuvel LPvd, Smeitink JAM (2006) Mitochondrial complex I: Structure, function and pathology. *Journal of Inherited Metabolic Disease* **29**: 499-515
- Janssen RJ, Distelmaier F, Smeets R, Wijnhoven T, Østergaard E, Jaspers NG, Raams A, Kemp S, Rodenburg RJ, Willems PH, van den Heuvel LP, Smeitink JA, Nijtmans LG (2009) Contiguous gene deletion of ELOVL7, ERCC8 and NDUFAF2 in a patient with a fatal multisystem disorder. *Human Molecular Genetics* **18**: 3365-3374
- Jia L, Dienhart M, Schrap M, McCauley M (2003) Yeast Oxa1 interacts with mitochondrial ribosomes: the importance of the C-terminal region of Oxa1. *The EMBO Journal* **22**: 6438-6447
- Jinek M, Chylinski K, Fonfara I, Hauer M, Doudna JA, Charpentier E (2012) A programmable dual-RNA-guided DNA endonuclease in adaptive bacterial immunity. *Science* **337**: 816-821
- Johnston AJ, Hoogenraad J, Dougan DA, Truscott KN, Yano M, Mori M, Hoogenraad NJ, Ryan MT (2002) Insertion and assembly of human tom7 into the preprotein translocase complex of the outer mitochondrial membrane. *The Journal of Biological Chemistry* **277**: 42197-42204

Karry R, Klein E, Ben Shachar D (2004) Mitochondrial complex I subunits expression is altered in schizophrenia: a postmortem study. *Biological Psychiatry* **55**: 676-684

Kerr DS (2010) Treatment of mitochondrial electron transport chain disorders: a review of clinical trials over the past decade. *Molecular genetics and metabolism* **99**: 246-255

Kim B, Simon E (2004) Mitochondrial β -oxidation. *European Journal of Biochemistry* **271**: 462-469

Kim SH, Vlkolinsky R, Cairns N, Fountoulakis M, Lubec G (2001) The reduction of NADH ubiquinone oxidoreductase 24- and 75-kDa subunits in brains of patients with Down syndrome and Alzheimer's disease. *Life Sciences* **68**: 2741-2750

Koopman WJH, Nijtmans LGJ, Dieteren CEJ, Roestenberg P, Valsecchi F, Smeitink JAM, Willems PHGM (2010) Mammalian mitochondrial complex I: biogenesis, regulation, and reactive oxygen species generation. *Antioxidants & Redox Signaling* **12**: 1431-1470

Kopp E, Medzhitov R, Carothers J, Xiao C, Douglas I, Janeway CA, Ghosh S (1999) ECSIT is an evolutionarily conserved intermediate in the Toll/IL-1 signal transduction pathway. *Genes & Development* **13**: 2059-2071

Kuffner R, Rohr A, Schmiede A, Krull C, Schulte U (1998) Involvement of two novel chaperones in the assembly of mitochondrial NADH:Ubiquinone oxidoreductase (complex I). *Journal of Molecular Biology* **283**: 409-417

Lake NJ, Compton AG, Rahman S, Thorburn DR (2015) Leigh Syndrome: One disorder, more than 75 monogenic causes. *Annals of Neurology* doi: 10.1002/ana.24551

Lang BF, Gray MW, Burger G (1999) Mitochondrial genome evolution and the origin of eukaryotes. *Annual Review of Genetics* **33**: 351-397

Lazarou M, McKenzie M, Ohtake A, Thorburn DR, Ryan MT (2007) Analysis of the assembly profiles for mitochondrial- and nuclear-DNA-encoded subunits into complex I. *Molecular and Cellular Biology* **27**: 4228-4237

Lazarou M, Thorburn D, Ryan M, McKenzie M (2009) Assembly of mitochondrial complex I and defects in disease. *Biochimica et Biophysica Acta - Molecular Cell Research* **1793**: 78-88

Lemire BD (2015a) Evolution of FOXRED1, an FAD-dependent oxidoreductase necessary for NADH:ubiquinone oxidoreductase (Complex I) assembly. *Biochimica et Biophysica Acta* **1847**: 451-457

Lemire BD (2015b) A structural model for FOXRED1, an FAD-dependent oxidoreductase necessary for NADH: Ubiquinone oxidoreductase (complex I) assembly. *Mitochondrion* **22**: 9-16

Lertrit P, Noer AS, Jean-Francois MJ, Kapsa R, Dennett X, Thyagarajan D, Lethlean K, Byrne E, Marzuki S (1992) A new disease-related mutation for mitochondrial encephalopathy lactic acidosis and strokelike episodes (MELAS) syndrome affects the ND4 subunit of the respiratory complex I. *American Journal of Human Genetics* **51**: 457-468

Liu S, Lee Y-FF, Chou S, Uno H, Li G, Brookes P, Massett MP, Wu Q, Chen L-MM, Chang C (2011) Mice lacking TR4 nuclear receptor develop mitochondrial myopathy with deficiency in complex I. *Molecular Endocrinology (Baltimore, Md)* **25**: 1301-1310

Liu X, Kim CN, Yang J, Jemmerson R, Wang X (1996) Induction of apoptotic program in cell-free extracts: requirement for dATP and cytochrome c. *Cell* **86**: 147-157

Loeffen J, Smeitink JAM, Trijbels JMF, Janssen AJM, Triepels RH, Sengers RCA, Heuvel VLP (2000) Isolated complex I deficiency in children: clinical, biochemical and genetic aspects. *Human Mutation* **15**: 123-134

Ma J, Ito A (2002) Tyrosine residues near the FAD binding site are critical for FAD binding and for the maintenance of the stable and active conformation of rat monoamine oxidase A. *Journal of Biochemistry* **131**: 107-111

Man PY, Griffiths PG, Brown DT, Howell N, Turnbull DM, Chinnery PF (2003) The epidemiology of Leber hereditary optic neuropathy in the North East of England. *American Journal of Human Genetics* **72**: 333-339

Marraffini LA (2015) CRISPR-Cas immunity in prokaryotes. *Nature* **526**: 55-61

Mathiesen C, Hägerhäll C (2002) Transmembrane topology of the NuoL, M and N subunits of NADH: quinone oxidoreductase and their homologues among membrane-bound hydrogenases and bona fide antiporters. *Biochimica et Biophysica Acta (BBA)- Bioenergetics* **1556**: 121-132

McKenzie M, Lazarou M, Thorburn D, Ryan M (2007) Analysis of mitochondrial subunit assembly into respiratory chain complexes using Blue Native polyacrylamide gel electrophoresis. *Analytical Biochemistry* **364**: 128-137

McKenzie M, Ryan MT (2010) Assembly factors of human mitochondrial complex I and their defects in disease. *IUBMB Life* **62**: 497-502

McKenzie M, Tucker EJ, Compton AG, Lazarou M, George C, Thorburn DR, Ryan MT (2011) Mutations in the Gene Encoding C8orf38 Block Complex I Assembly by Inhibiting Production of the Mitochondria-Encoded Subunit ND1. *Journal of Molecular Biology* **414**: 413-426

Mewies M, McIntire WS, Scrutton NS (1998) Covalent attachment of flavin adenine dinucleotide (FAD) and flavin mononucleotide (FMN) to enzymes: the current state of affairs. *Protein Science : a publication of the Protein Society* **7**: 7-20

Meyer K, Buettner S, Ghezzi D, Zeviani M, Bano D, Nicotera P (2015) Loss of apoptosis-inducing factor critically affects MIA40 function. *Cell Death & Disease* **6**, e1814; doi:10.1038/cddis.2015.170

Mimaki M, Wang X, McKenzie M, Thorburn DR, Ryan MT (2012) Understanding mitochondrial complex I assembly in health and disease. *Biochim et Biophys Acta* **1817**: 851-862

Mitchell P (2011) Chemiosmotic coupling in oxidative and photosynthetic phosphorylation. 1966. *Biochimica et Biophysica Acta* **1807**: 1507-1538

Montague TG, Cruz JMM, Gagnon JA, Church GM, Valen E (2014) CHOPCHOP: a CRISPR/Cas9 and TALEN web tool for genome editing. *Nucleic Acids Research* **42**: W401-W407

Moreno-Lastres D, Fontanesi F, García-Consuegra I, Martín MA, Arenas J, Barrientos A, Ugalde C (2012) Mitochondrial complex I plays an essential role in human respirasome assembly. *Cell Metabolism* **15**: 324-335

Morgenstern JP, Land H (1990) Advanced mammalian gene transfer: high titre retroviral vectors with multiple drug selection markers and a complementary helper-free packaging cell line. *Nucleic Acids Research* **18**: 3587-3596

Nouws J, Nijtmans L, Houten SM, van den Brand M, Huynen M, Venselaar H, Hoefs S, Gloerich J, Kronick J, Hutchin T, Willems P, Rodenburg R, Wanders R, van den Heuvel L, Smeitink J, Vogel RO (2010) Acyl-CoA dehydrogenase 9 is required for the biogenesis of oxidative phosphorylation complex I. *Cell Metabolism* **12**: 283-294

Nouws J, Nijtmans LG, Smeitink JA, Vogel RO (2012) Assembly factors as a new class of disease genes for mitochondrial complex I deficiency: cause, pathology and treatment options. *Brain : a Journal of Neurology* **135**: 12-22

Nouws J, Te Brinke H, Nijtmans LG, Houten SM (2014a) ACAD9, a complex I assembly factor with a moonlighting function in fatty acid oxidation deficiencies. *Human Molecular Genetics* **23**: 1311-1319

Nouws J, Wibrand F, van den Brand M, Venselaar H, Duno M, Lund AM, Trautner S, Nijtmans L, Ostergard E (2014b) A Patient with Complex I Deficiency Caused by a Novel ACAD9 Mutation Not Responding to Riboflavin Treatment. *JIMD Reports* **12**: 37-45

Oeljeklaus S, Schummer A, Suppanz I, Warscheid B (2014) SILAC labeling of yeast for the study of membrane protein complexes. *Methods in Molecular Biology (Clifton, NJ)* **1188**: 23-46

Oey NA, Ruiten JP, Ijlst L, Attie-Bitach T, Vekemans M, Wanders RJ, Wijburg FA (2006) Acyl-CoA dehydrogenase 9 (ACAD 9) is the long-chain acyl-CoA dehydrogenase in human embryonic and fetal brain. *Biochemical and Biophysical Research Communications* **346**: 33-37

Ogilvie I, Kennaway NG, Shoubridge EA (2005) A molecular chaperone for mitochondrial complex I assembly is mutated in a progressive encephalopathy. *The Journal of Clinical Investigation* **115**: 2784-2792

Ong S-EE, Blagoev B, Kratchmarova I, Kristensen DB, Steen H, Pandey A, Mann M (2002) Stable isotope labeling by amino acids in cell culture, SILAC, as a simple and accurate approach to expression proteomics. *Molecular & cellular proteomics* **1**: 376-386

Ott M, Herrmann JM (2010) Co-translational membrane insertion of mitochondrially encoded proteins. *Biochimica et Biophysica Acta* **1803**: 767-775

Pagliarini DJ, Calvo SE, Chang B, Sheth SA, Vafai SB, Ong SE, Walford GA, Sugiana C, Boneh A, Chen WK, Hill DE, Vidal M, Evans JG, Thorburn DR, Carr SA, Mootha VK (2008) A mitochondrial protein compendium elucidates complex I disease biology. *Cell* **134**: 112-123

Palade GE (1952) The fine structure of mitochondria. *The Anatomical Record* **114**: 427-451

Polianskyte Z, Peitsaro N, Dapkunas A, Liobikas J, Soliymani R, Lalowski M, Speer O, Seitsonen J, Butcher S, Cereghetti GM, Linder MD, Merckel M, Thompson J, Eriksson O (2009) LACTB is a filament-forming protein localized in mitochondria. *Proceedings of the National Academy of Sciences of the United States of America* **106**: 18960-18965

Pospisilik JA, Knauf C, Joza N, Benit P, Orthofer M, Cani PD, Ebersberger I, Nakashima T, Sarao R, Neely G, Esterbauer H, Kozlov A, Kahn CR, Kroemer G, Rustin P, Burcelin R, Penninger JM (2007) Targeted deletion of AIF decreases mitochondrial oxidative phosphorylation and protects from obesity and diabetes. *Cell* **131**: 476-491

Pudelski B, Kraus S, Soll J, Philippar K (2010) The plant PRAT proteins - preprotein and amino acid transport in mitochondria and chloroplasts. *Plant Biology (Stuttgart, Germany)* **12**: 42-55

Ran FA, Hsu PD, Wright J, Agarwala V, Scott DA, Zhang F (2013) Genome engineering using the CRISPR-Cas9 system. *Nature Protocols* **8**: 2281-2308

Rendón OZ, Neiva LS, Sasarman F, Shoubridge EA (2014) The arginine methyltransferase NDUFAF7 is essential for complex I assembly and early vertebrate embryogenesis. *Human Molecular Genetics* **23**: 5159-5170

Rendón OZ, Shoubridge EA (2012) Early complex I assembly defects result in rapid turnover of the ND1 subunit. *Human Molecular Genetics* **21**: 3815-3824

Reyon D, Tsai S, Khayter C, Foden J, Sander J, Joung J (2012) FLASH assembly of TALENs for high-throughput genome editing. *Nature Biotechnology* **30**: 460-465

Rhein VF, Carroll J, Ding S, Fearnley IM, Walker JE (2013) NDUFAF7 methylates arginine 85 in the NDUFS2 subunit of human complex I. *The Journal of Biological Chemistry* **288**: 33016-33026

Rich P (2003) Chemiosmotic coupling: The cost of living. *Nature* **421**: 583

Richter U, Lahtinen T, Marttinen P, Suomi F, Battersby BJ (2015) Quality control of mitochondrial protein synthesis is required for membrane integrity and cell fitness. *The Journal of Cell Biology* **211**: 373-389

Robinson BH, Petrova-Benedict R, Buncic JR, Wallace DC (1992) Nonviability of cells with oxidative defects in galactose medium: a screening test for affected patient fibroblasts. *Biochemical Medicine and Metabolic Biology* **48**: 122-126

Rosenberg I (1996) *Protein Analysis and Purification: Benchtop Techniques*, Birkhouser: Boston.

Rouault TA, Tong W-HH (2005) Iron-sulphur cluster biogenesis and mitochondrial iron homeostasis. *Nature Reviews Molecular Cell Biology* **6**: 345-351

Roux KJ, Kim DI, Raida M, Burke B (2012) A promiscuous biotin ligase fusion protein identifies proximal and interacting proteins in mammalian cells. *The Journal of Cell Biology* **196**: 801-810

Rubio-Gozalbo ME, Dijkman KP, van den Heuvel LP, Sengers RC, Wendel U, Smeitink JA (2000) Clinical differences in patients with mitochondriocytopathies due to nuclear versus mitochondrial DNA mutations. *Human Mutation* **15**: 522-532

Ruhoy IS, Saneto RP (2014) The genetics of Leigh syndrome and its implications for clinical practice and risk management. *The Application of Clinical Genetics* **7**: 221-234

Saada A, Edvardson S, Rapoport M, Shaag A, Amry K, Miller C, Lorberboum-Galski H, Elpeleg O (2008) C6ORF66 is an assembly factor of mitochondrial complex I. *American Journal of Human Genetics* **82**: 32-38

Saada A, Edvardson S, Shaag A, Chung WK, Segel R, Miller C, J alas C, Elpeleg O (2012) Combined OXPHOS complex I and IV defect, due to mutated complex I assembly factor C20ORF7. *Journal of Inherited Metabolic Disease* **35**: 125-131

Saada A, Vogel RO, Hoefs SJ, van den Brand MA, Wessels HJ, Willems PH, Venselaar H, Shaag A, Barghuti F, Reish O, Shohat M, Huynen MA, Smeitink JA, van den Heuvel LP, Nijtmans LG (2009) Mutations in NDUFAF3 (C3ORF60), encoding an NDUFAF4 (C6ORF66)-interacting complex I assembly protein, cause fatal neonatal mitochondrial disease. *American Journal of Human Genetics* **84**: 718-727

Sambrook J, Russell DW (2001) *Molecular Cloning: A laboratory manual*, 3 edn. New York: Cold Spring Harbour Laboratory Press.

- Sander JD, Maeder ML, Reyon D, Voytas DF, Joung JK, Dobbs D (2010) ZiFiT (Zinc Finger Targeter): an updated zinc finger engineering tool. *Nucleic Acids Research* **38**: W462-W468
- Sander JD, Zaback P, Joung JK, Voytas DF, Dobbs D (2007) Zinc Finger Targeter (ZiFiT): an engineered zinc finger/target site design tool. *Nucleic Acids Research* **35**: W599-W605
- Sazanov LA (2015) A giant molecular proton pump: structure and mechanism of respiratory complex I. *Nature Reviews Molecular Cell Biology* **16**: 375-388
- Sazanov LA, Peak-Chew SY, Fearnley IM, Walker JE (2000) Resolution of the Membrane Domain of Bovine Complex I into Subcomplexes: Implications for the Structural Organization of the Enzyme. *Biochemistry* **39**: 7229-7235
- Schägger H, de Coo R, Bauer MF, Hofmann S, Godinot C, Brandt U (2004) Significance of Respirasomes for the Assembly/Stability of Human Respiratory Chain Complex I. *Journal of Biological Chemistry* **279**: 36349-36353
- Schagger H, von Jagow G (1987) Tricine-Sodium Dodecyl Sulfate-Polyacrylamide Gel Electrophoresis for the Separation of Proteins in the Range from 1 to 100 kDa. *Analytical Biochemistry* **166**: 368-379
- Schagger H, von Jagow G (1991) Blue Native Electrophoresis for Isolation of Membrane Protein Complexes in Enzymatically Active Form. *Analytical Biochemistry* **199**: 223-231
- Schapira AH, Cooper JM, Dexter D, Jenner P, Clark JB, Marsden CD (1989) Mitochondrial complex I deficiency in Parkinson's disease. *Lancet (London, England)* **1**: 1269
- Schapira AH, Mann VM, Cooper JM, Dexter D, Daniel SE, Jenner P, Clark JB, Marsden CD (1990) Anatomic and disease specificity of NADH CoQ1 reductase (complex I) deficiency in Parkinson's disease. *Journal of Neurochemistry* **55**: 2142-2145
- Schiff M, Haberberger B, Xia C, Mohsen A-WW, Goetzman ES, Wang Y, Uppala R, Zhang Y, Karunanidhi A, Prabhu D, Alharbi H, Prochownik EV, Haack T, Häberle J, Munnich A, Rötig A, Taylor RW, Nicholls RD, Kim J-JJ, Prokisch H, Vockley J (2015) Complex I assembly function and fatty acid oxidation enzyme activity of ACAD9 both contribute to disease severity in ACAD9 deficiency. *Human Molecular Genetics* **24**: 3238-3247
- Schneider CA, Rasband WS, Eliceiri KW (2012) NIH Image to ImageJ: 25 years of image analysis. *Nature Methods* **9**: 671-675
- Scholte HR, Busch HF, Bakker HD, Bogaard JM, Luyt-Houwen IE, Kuyt LP (1995) Riboflavin-responsive complex I deficiency. *Biochimica et Biophysica Acta* **1271**: 75-83

Schultz BE, Chan SI (2001) Structures and proton-pumping strategies of mitochondrial respiratory enzymes. *Annual Reviews of Biophysics and Biomolecular Structure* **30**: 23-65

Seth RB, Sun L, Ea C-KK, Chen ZJ (2005) Identification and characterization of MAVS, a mitochondrial antiviral signaling protein that activates NF-kappaB and IRF 3. *Cell* **122**: 669-682

Sheftel AD, Stehling O, Pierik AJ, Netz DJ, Kerscher S, Elsässer H-PP, Wittig I, Balk J, Brandt U, Lill R (2009) Human ind1, an iron-sulfur cluster assembly factor for respiratory complex I. *Molecular and Cellular Biology* **29**: 6059-6073

Sherer TB, Richardson JR, Testa CM, Seo BB, Panov AV, Yagi T, Matsuno-Yagi A, Miller GW, Greenamyre JT (2007) Mechanism of toxicity of pesticides acting at complex I: relevance to environmental etiologies of Parkinson's disease. *Journal of Neurochemistry* **100**: 1469-1479

Skladal D, Halliday J, Thorburn DR (2003) Minimum birth prevalence of mitochondrial respiratory chain disorders in children. *Brain : a Journal of Neurology* **126**: 1905-1912

Smeitink J, van den Heuvel L, DiMauro S (2001) The genetics and pathology of oxidative phosphorylation. *Nature Reviews Genetics* **2**: 342-352

Soto IC, Fontanesi F, Liu J, Barrientos A (2012) Biogenesis and assembly of eukaryotic cytochrome c oxidase catalytic core. *Biochimica et Biophysica Acta* **1817**: 883-897

Stewart JB, Chinnery PF (2015) The dynamics of mitochondrial DNA heteroplasmy: implications for human health and disease. *Nature Reviews Genetics* **16**: 530-542

Stiburek L, Cesnekova J, Kostkova O, Fornuskova D, Vinsova K, Wenchich L, Houstek J, Zeman J (2012) YME1L controls the accumulation of respiratory chain subunits and is required for apoptotic resistance, cristae morphogenesis, and cell proliferation. *Molecular Biology of the Cell* **23**: 1010-1023

Stiburek L, Fornuskova D, Wenchich L, Pejznochova M, Hansikova H, Zeman J (2007) Knockdown of human Oxa1l impairs the biogenesis of F1Fo-ATP synthase and NADH:ubiquinone oxidoreductase. *Journal of Molecular Biology* **374**: 506-516

Stroud DA, Formosa LE, Wijeyeratne XW, Nguyen TN, Ryan MT (2013) Gene knockout using transcription activator-like effector nucleases (TALENs) reveals that human NDUFA9 protein is essential for stabilizing the junction between membrane and matrix arms of complex I. *Journal of Biological Chemistry* **288**: 1685-1690

Stroud DA, Maher MJ, Lindau C, Vögtle FNN, Frazier AE, Surgenor E, Mountford H, Singh AP, Bonas M, Oeljeklaus S, Warscheid B, Meisinger C, Thorburn DR, Ryan MT (2015) COA6 is a mitochondrial complex IV assembly factor critical for biogenesis of mtDNA-encoded COX2. *Human Molecular Genetics* **24**: 5404-5415

Sugiana C, Pagliarini DJ, McKenzie M, Kirby DM, Salemi R, Abu-Amero KK, Dahl HH, Hutchison WM, Vascotto KA, Smith SM, Newbold RF, Christodoulou J, Calvo S, Mootha VK, Ryan MT, Thorburn DR (2008) Mutation of C20orf7 disrupts complex I assembly and causes lethal neonatal mitochondrial disease. *American Journal of Human Genetics* **83**: 468-478

Sugio A, Yang B, Zhu T, White FF (2007) Two type III effector genes of *Xanthomonas oryzae* pv. *oryzae* control the induction of the host genes OsTFIIAgamma1 and OsTFX1 during bacterial blight of rice. *Proceedings of the National Academy of Sciences of the United States of America* **104**: 10720-10725

Sun X, Wang J-FF, Tseng M, Young LT (2006) Downregulation in components of the mitochondrial electron transport chain in the postmortem frontal cortex of subjects with bipolar disorder. *Journal of Psychiatry & Neuroscience* **31**: 189-196

Swalwell H, Kirby DM, Blakely EL, Mitchell A, Salemi R, Sugiana C, Compton AG, Tucker EJ, Ke B-XX, Lamont PJ, Turnbull DM, McFarland R, Taylor RW, Thorburn DR (2011) Respiratory chain complex I deficiency caused by mitochondrial DNA mutations. *European Journal of Human Genetics* **19**: 769-775

Szklarczyk R, Wanschers BFJ, Nabuurs SB, Nouws J (2011) NDUFB7 and NDUF8 are located at the intermembrane surface of complex I. *FEBS Letters* **585**: 737-743

Szyrach G, Ott M, Bonnefoy N, Neupert W (2003) Ribosome binding to the Oxa1 complex facilitates co-translational protein insertion in mitochondria. *The EMBO Journal* **22**: 6448-6457

Taylor RW, Turnbull DM (2005) Mitochondrial DNA mutations in human disease. *Nature Reviews Genetics* **6**: 389-402

Thorburn DR, Chow CW, Kirby DM (2004) Respiratory chain enzyme analysis in muscle and liver. *Mitochondrion* **4**: 363-375

Torija P, Vicente JJ, Rodrigues TB, Robles A, Cerdán S, Sastre L, Calvo RM, Escalante R (2006) Functional genomics in *Dictyostelium*: MidA, a new conserved protein, is required for mitochondrial function and development. *Journal of Cell Science* **119**: 1154-1164

Trickey P, Wagner MA, Jorns MS, Mathews FS (1999) Monomeric sarcosine oxidase: structure of a covalently flavinylated amine oxidizing enzyme. *Structure (London, England : 1993)* **7**: 331-345

Tucker EJ, Mimaki M, Compton AG, McKenzie M, Ryan MT, Thorburn DR (2012) Next-generation sequencing in molecular diagnosis: NUBPL mutations highlight the challenges of variant detection and interpretation. *Human Mutation* **33**: 411-418

Ugalde C, Vogel R, Huijbens R, Van Den Heuvel B, Smeitink J, Nijtmans L (2004) Human mitochondrial complex I assembles through the combination of evolutionary conserved modules: a framework to interpret complex I deficiencies. *Human Molecular Genetics* **13**: 2461-2472

Vahsen N, Cande C, Briere JJ, Benit P, Joza N, Larochette N, Mastroberardino PG, Pequignot MO, Casares N, Lazar V, Feraud O, Debili N, Wissing S, Engelhardt S, Madeo F, Piacentini M, Penninger JM, Schagger H, Rustin P, Kroemer G (2004) AIF deficiency compromises oxidative phosphorylation. *EMBO Journal* **23**: 4679-4689

Vinothkumar KR, Zhu J, Hirst J (2014) Architecture of mammalian respiratory complex I. *Nature* **515**: 80-84

Vogel RO, Dieteren CE, van den Heuvel LP, Willems PH, Smeitink JA, Koopman WJ, Nijtmans LG (2007a) Identification of mitochondrial complex I assembly intermediates by tracing tagged NDUFS3 demonstrates the entry point of mitochondrial subunits. *Journal of Biological Chemistry* **282**: 7582-7590

Vogel RO, Janssen RJ, van den Brand MA, Dieteren CE, Verkaart S, Koopman WJ, Willems PH, Pluk W, van den Heuvel LP, Smeitink JA, Nijtmans LG (2007b) Cytosolic signaling protein Ecsit also localizes to mitochondria where it interacts with chaperone NDUFAF1 and functions in complex I assembly. *Genes and Development* **21**: 615-624

Vogel RO, Janssen RJ, Ugalde C, Grovenstein M, Huijbens RJ, Visch H-JJ, van den Heuvel LP, Willems PH, Zeviani M, Smeitink JA, Nijtmans LG (2005) Human mitochondrial complex I assembly is mediated by NDUFAF1. *The FEBS Journal* **272**: 5317-5326

Vogel RO, Smeitink J, Nijtmans L (2007c) Human mitochondrial complex I assembly: A dynamic and versatile process. *Biochimica et Biophysica Acta - Bioenergetics* **1767**: 1215-1227

Vogel RO, van den Brand MAA, Rodenburg RJ, van den Heuvel LP, Tsuneoka M, Smeitink JA, Nijtmans LG (2007d) Investigation of the complex I assembly chaperones B17.2L and NDUFAF1 in a cohort of CI deficient patients. *Molecular Genetics and Metabolism* **91**: 176-182

Walker JE (2013) The ATP synthase: the understood, the uncertain and the unknown. *Biochemical Society Transactions* **41**: 1-16

Wallace DC, Singh G, Lott MT, Hodge JA, Schurr TG, Lezza AM, Elsas LJ, Nikoskelainen EK (1988) Mitochondrial DNA mutation associated with Leber's hereditary optic neuropathy. *Science* **242**: 1427-1430

Wessels HJ, Vogel RO, van den Heuvel L, Smeitink JA, Rodenburg RJ, Nijtmans LG, Farhoud MH (2009) LC-MS/MS as an alternative for SDS-PAGE in blue native analysis of protein complexes. *Proteomics* **9**: 4221-4228

West AP, Brodsky IE, Rahner C, Woo DK, Erdjument-Bromage H, Tempst P, Walsh MC, Choi Y, Shadel GS, Ghosh S (2011) TLR signalling augments macrophage bactericidal activity through mitochondrial ROS. *Nature* **472**: 476-480

White DJ, Wolff JN, Pierson M, Gemmell NJ (2008) Revealing the hidden complexities of mtDNA inheritance. *Molecular Ecology* **17**: 4925-4942

Wu L, Peng J, Ma Y, He F, Deng X, Wang G, Lifan Y, Yin F (2014) Leukodystrophy associated with mitochondrial complex I deficiency due to a novel mutation in the NDUFAF1 gene. *Mitochondrial DNA* **doi**: 10.3109/19401736.2014.926543

Xiao C, Shim J-hH, Klüppel M, Zhang SS, Dong C, Flavell RA, Fu X-YY, Wrana JL, Hogan BL, Ghosh S (2003) Ecsit is required for Bmp signaling and mesoderm formation during mouse embryogenesis. *Genes & Development* **17**: 2933-2949

Yoshikawa S, Muramoto K, Shinzawa-Itoh K (2011) Proton-pumping mechanism of cytochrome C oxidase. *Annual Review of Biophysics* **40**: 205-223

Zhang J, Zhang W, Zou D, Chen G, Wan T, Zhang M, Cao X (2002) Cloning and functional characterization of ACAD-9, a novel member of human acyl-CoA dehydrogenase family. *Biochemical and Biophysical Research Communications* **297**: 1033-1042

Zhang K, Li Z, Jaiswal M, Bayat V, Xiong B, Sandoval H, Charng W-LL, David G, Haueter C, Yamamoto S, Graham BH, Bellen HJ (2013) The C8ORF38 homologue Sicily is a cytosolic chaperone for a mitochondrial complex I subunit. *The Journal of Cell Biology* **200**: 807-820

Zhou BP, Wu B, Kwan S-W, Abell CW (1998) Characterization of a Highly Conserved FAD-binding Site in Human Monoamine Oxidase B. *Journal of Biological Chemistry* **273**: 14862-14868

Zhu J, King MS, Yu M, Klipcan L, Leslie AG, Hirst J (2015) Structure of subcomplex I β of mammalian respiratory complex I leads to new supernumerary subunit assignments. *Proceedings of the National Academy of Sciences of the United States of America* **112**: 12087-12092

Zhu S, Vik SB (2015) Constraining the Lateral Helix of Respiratory Complex I by Cross-linking Does Not Impair Enzyme Activity or Proton Translocation. *The Journal of Biological Chemistry* **290**: 20761-20773